

LIBHARY Michigan State University

This is to certify that the dissertation entitled

THERMODYNAMIC AND KINETIC INVESTIGATION OF CHIRAL SEPARATIONS USING POLYSACCHARIDE STATIONARY PHASES

presented by

Kahsay Gebreyohannes

has been accepted towards fulfillment of the requirements for the

Ph.D.	degree in _	Chemistry
ĵ(Victoria n	Muffen jessor's Signature
	Major Prof	essor's Signature
	5/1.	4/2010
		Date

PLACE IN RETURN BOX to remove this checkout from your record. **TO AVOID FINES** return on or before date due. **MAY BE RECALLED** with earlier due date if requested.

DATE DUE	DATE DUE	DATE DUE

5/08 K:/Proj/Acc&Pres/CIRC/DateDue.indd

THERMODYNAMIC AND KINETIC INVESTIGATION OF CHIRAL SEPARATIONS USING POLYSACCHARIDE STATIONARY PHASES

Ву

Kahsay Gebreyohannes

A DISSERTATION

Submitted to
Michigan State University
in partial fulfillment of the requirements
for the degree of

DOCTOR OF PHILOSOPHY

Chemistry

2010

ABSTRACT

THERMODYNAMIC AND KINETIC INVESTIGATION OF CHIRAL SEPARATIONS USING POLYSACCHARIDE STATIONARY PHASES

By

Kahsay Gebreyohannes

Chiral separation continues to be one of the most challenging problems in the development of pharmaceutical compounds. The success of any chiral separation is mainly determined by the selection of an appropriate chiral stationary phase. In this regard, β -cyclodextrin (native and derivatized) and derivatized amylose and cellulose are the most popular chiral stationary phases.

The separation of coumarin-based anticoagulants (warfarin, coumachlor, coumafuryl, coumatetralyl, and 4-hydroxycoumarin) on 2,6-dinitro-4-trifluoromethyl phenyl ether (DNP) and tris-(3,5-dimethylphenyl carbamate) (DMPC) derivatized β -cyclodextrin is compared. Using polar-organic or reversed-phase eluents, the chiral selectivities (α) are adequate in the DNP derivatized phase, but non-existent in the DMPC derivatized β -cyclodextrin.

Amylose and cellulose derivatized with DMPC are compared using polarorganic eluents and the same coumarin-based solutes. Different mobile phase modifiers (methanol, acetone, and tetrahydrofuran) at 5 and 10 % concentration are used to investigate retention, chiral selectivity and kinetic rate constants of the separation. Methanol and acetone decreased the selectivity in both phases, but tetrahydrofuran increased the selectivity of coumafuryl and coumatetralyl on the DMPC-amylose phase. The rate constants for the second-eluted enantiomer of coumatetralyl decreased on DMPC-amylose, but increased on DMPC-cellulose.

Detailed thermodynamic and kinetic studies are performed on amylose derivatized with tris-(3,5-dimethylphenyl carbamate) stationary phase. Polarorganic eluents that contain acetonitrile as bulk solvent with modifiers such as methanol, *i*-butanol, *t*-butanol, and tetrahydrofuran are used in the study. Temperature studies are conducted from 5 to 45 °C at constant pressure of 1500 psi. The van't Hoff plots showed both linear and nonlinear behavior. From the van't Hoff plots, thermodynamic changes in molar enthalpy and entropy and kinetic rate constants and activation energies are estimated. The change in enthalpy and entropy induced by each mobile phase modifier varies greatly. The kinetic data indicate that the rate of sorption is always greater than the rate of desorption.

Computational studies can also provide thermodynamic and kinetic information. The effect of torsion angle flexibility on sampling of warfarin conformers is studied using umbrella sampling in water and acetonitrile solvents. The results revealed the presence of a thermodynamic barrier between each structure with positive and negative torsion angle (α) for the different R- and S-warfarin conformers. In a related study, R- and S-warfarin structures are docked with β -cyclodextrin. R-Warfarin structures interacted more strongly than S-warfarin. In addition, R- and S-warfarin structures show evidence of cyclodextrin.

TABLE OF CONTENTS

LIST	T OF TABLES	хi
LIST	r of figures	xiii
CHA	APTER 1. INTRODUCTION AND BACKGROUND	1
1.1.	Significance of chiral separation	1
	Methods of chiral separations using liquid chromatography	2
	1.2.1. Indirect methods	2
	1.2.2. Direct methods	3
	1.2.2.1. Chiral mobile phase additives	3
	1.2.2.2. Chiral stationary phases	4
1.3.	Types of chiral stationary phases	5
	1.3.1. Donor-acceptor CSPs	
	1.3.2. Protein-type stationary phases	
	1.3.3. Inclusion-type stationary phases	7
	1.3.4. Polysaccharide-type phases	9
1.4.	Thermodynamics and kinetic theories	11
	1.4.1. Thermodynamics	11
	1.4.1.1. Enthalpy-entropy compensations	14
	1.4.2. Kinetics	16
1.5.	· · · · · · · · · · · · · · · · · · ·	18
		18
		21
		28
1.7.	References	30
	APTER 2. COMPARISON OF DERIVATIZED β -CYCLODEXTE	
		34
		34
2.2.	— · · · · · · · · · · · · · · · · · · ·	36
	2.2.1. Chemicals	36
	2.2.2. Column preparation and packing	38
	2.2.3. Chromatographic system	38
	2.2.4. Data analysis	39
2.3.		41
		41
		41
		43
	2.3.1.3. Comparison of native, DMPC- and DNP-CD stationary	47
0.4	• • • • • • • • • • • • • • • • • • • •	47
	Conclusions	50
2.5.	References	53

CHA	PTER	3.	COMP	ARISON	OF DERIVA	ATIZED	POLYSA	CCHAR	DE
PHA	SES F	OR SEF	PARATI	ON OF W	ARFARIN AN	ID RELAT	TED DRUG	GS	55
3.1.	Introd	uction		•••••				•••••	55
									57
	3.2.1.	Chemic	als		• • • • • • • • • • • • • • • • • • • •			*******	57
									57
					• • • • • • • • • • • • • • • • • • • •				59
3.3	Resul	ts and d	iscussio	n	• • • • • • • • • • • • • • • • • • • •				60
									61
									66
	3 3 3	Effect of	of modifie	ers	• • • • • • • • • • • • • • • • • • • •				
									76
									82
									84
J.J.	I VEIEI	CIICES	••••••	••••••	•••••	••••••	•••••	••••••	0-
CHA	DTED		THEDM		IC AND KI	JETIC 6	TUDY O		AI
					IC AND KII RIN-BASED				ON
					NARY PHASE				86
									86
4.1.	Evno	iuciion	mothode			••••••	•••••	• • • • • • •	89
									89
					•••••				
									89
4.0	4.2.3.	Data Ai	naiysis .		••••••	•••••	• • • • • • • • • • • • • • • • • • • •	•••••	91
					• • • • • • • • • • • • • • • • • • • •				95
•	4.3.1.	Inermo	odynami	c eπects.					95
		4.3.1.1.			type and con				00
									98
		4.3.1.2.			ture on molar				
					etonitrile				103
		4.3.1.3.			ture and mod				
					bs free energy				109
					y compensation				123
4								•••••	127
		4.3.2.1.			type and con	centration	n on rate		
				nts		•••••	• • • • • • • • • • • • • • • • • • • •		129
		4.3.2.2.	Effect of	of tempera	iture on the ra	ite consta	ints and a		
			energy	• • • • • • • • • • • • • • • • • • • •			• • • • • • • • • • • • • • • • • • • •		133
4.4.	Conc	lusions .	••••••		• • • • • • • • • • • • • • • • • • • •	• • • • • • • • • • • • • • • • • • • •			138
4.5.	Refer	ences	•••••	••••••		•••••		•••••	140
CHA	PTER	5. CO	MPUTA		STUDIES ON				RIN
ENA	NTIO	MERS	AND	THEIR	DOCKING	INTER/	ACTION	WITH	β-
CYC	LODE	EXTRIN		•••••			•••••	•••••	143
					ers				143
									143

	5.1.2. Simulated systems and parameters	144
	5.1.3. Umbrella sampling simulations	147
	5.1.4. Results and discussions	147
	5.1.5. Conclusions	144
5.2.	Docking of warfarin enantiomers with β-cyclodextrin	156
	5.2.1. Introduction	156
	5.2.2. Methods	157
	5.2.3. Results and discussion	160
	5.2.4. Conclusions	166
5.3.	References	168
CHA	APTER 6. CONCLUSIONS AND FUTURE DIRECTIONS	172
6.1.	Introduction	172
	Experimental studies on derivatized β-CD, amylose and cellulose	
	stationary phases	172
6.3.	Computational studies on warfarin sampling and docking	176
	References	179

LIST OF TABLES

Table 2.1.	Effect of acetic acid and triethylamine additives on the retention (k) and chiral selectivity (α) of warfarin using DNP-CD
Table 2.2.	Comparison of retention factor (k) and selectivity (α) of warfarin in native and derivatized cyclodextrins. 51
Table 3.1.	Effect of acetic acid and triethylamine concentration on retention and selectivity of warfarin enantiomers using DMPC-amylose phase. Mobile phase contains acetonitrile. Standard deviations in k and α are \pm 0.01
Table 3.2 .	Comparison of retention and selectivity of coumarins using DMPC-amylose and DMPC-cellulose phases. Mobile phase contains acetonitrile with 0.1 % acetic acid and 0.2 % triethylamine. Standard deviations in k and α are \pm 0.01
Table 3.3 .	Effect of modifier concentration on the separation of coumarins using DMPC-amylose phase. Mobile phase contains acetonitrile with 0.1 % acetic acid and 0.2 % triethylamine and varying concentrations of organic modifier (%). Standard deviations in k and α are \pm 0.01.
Table 3.4.	Comparison of sorption (k_{sm}) and desorption (k_{ms}) rate constants of coumatetralyl enantiomers using DMPC-amylose and DMPC-cellulose phases. Mobile phase contains acetonitrile with 0.1 % acetic acid and 0.2 % triethylamine and varying concentrations of THF $(\%)$.
Table 4.1 .	Retention factor (k) and chiral selectivity (α) for the coumarin-based solutes at 20 °C. Column: Chiralpak IA; mobile phase: acetonitrile with 0.1 % acetic acid and 0.2 % triethylamine additives; flow rate:1 μL/min
Table. 4.2.	Solvatochromic properties of modifiers used in the study. The α scale represents the ability of a solvent to donate a proton, while the β scale evaluates the ability of a solvent to accept a proton (donate an electron pair) in a solvent-to-solute hydrogen bond
Table. 4.3 .	Comparison of retention factor (k) and chiral selectivity (α) for warfarin enantiomers at 20 °C. Other experimental conditions as given in Table 4.1

Table 4.4.	Comparison of retention factor (k) and chiral selectivity (α) for coumatetralyl enantiomers at 20 °C. Other experimental conditions as given in Table 4.1
Table. 4.5 .	Thermodynamic quantities for coumarins in acetonitrile mobile phase. Other experimental conditions as given in Table 4.1 108
Table. 4.6 .	Thermodynamic parameters for warfarin in different modifier. Other experimental conditions as given in Table 4.1
Table. 4.7 .	Thermodynamic parameters for coumatetralyl in different modifiers. Other experimental conditions as given in Table 4 117
Table. 4.8.	Sorption (k _{sm}) and desorption (k _{ms}) rate constants for coumarin enantiomers at 10 °C. Other experimental conditions as given in Table 4.1
Table. 4.9 .	Effect of concentration of modifier on desorption rate constants (k _{ms}) of warfarin enantiomers at 10 °C. Other experimental conditions as given in Table 4.1
Table. 4.10 .	Effect of concentration of modifier on desorption rate constants (k _{ms}) of coumatetralyl enantiomers at 10 °C. Other experimental conditions as given in Table 4.1
Table. 4.11.	Comparison of activation energy for sorption ($\Delta E_{\ddagger m}$) and desorption ($\Delta E_{\ddagger s}$) processes of coumatetralyl enantiomers. Other experimental conditions as given in Table 4.1 137
Table 5.1.	Relative free energies ($\Delta\Delta G$) in kcal/mol between states I and II (ΔG_{II} - ΔG_{I}) obtained from umbrella sampling 151
Table 5.2.	Binding affinity for the energetically most favorable docking pose at 8 Å radius from the center of cyclodextrin cavity
Table 5.3.	Comparison of hydroxycoumarin group orientation of 50 randomly generated warfarin structures in β -CD. Radius of sphere is taken at 8 Å
Table 5.4.	Intermolecular hydrogen bond distance (Å) between docked warfarin functional groups and the secondary hydroxyl groups of β-CD. Radius of sphere used is 8 Å

LIST OF FIGURES

Figure 1.1.	Structure of β-cyclodextrin
Figure 1.2.	Structures of tris-(3,5-dimethylphenyl carbamate) a) amylose, b) cellulose
Figure 2.1.	The structures of coumarin anticoagulants
Figure 2.2.	Schematic diagram of the experimental system for capillary liquid chromatography with on-column laser-induced fluorescence detection. I: injection valve, T: splitting tee, S: splitting capillary, F: filter, PMT: photomultiplier tube, AMP: current to voltage amplifier.
Figure 2.3.	Separation of a) warfarin, b) coumachlor, and c) coumatetrally enantiomers in DMPC-CD stationary phase. Mobile phase contains acetonitrile with 1 % methanol, 0.1 % acetic acid, and 0.4 % triethylamine.
Figure 2.4.	The separation of a) warfarin, b) coumafuryl, and c) coumachlor in DNP-CD using acetonitrile mobile phase. Mobile phase also contains 0.1 % acetic acid and 0.2 % triethylamine.
Figure 2.5.	Effect of methanol concentration a) 5 %, b) 3 %, c) 1 %, and d) 0 % on the separation of warfarin enantiomers in DNP-CD. Mobile phase also contains acetonitrile with 0.1 % acetic acid and triethylamine.
Figure 2.6.	Separation of warfarin enantiomers in a) native β -CD, b) DNP-CD, and c) DMPC-CD. Mobile phase contains acetonitrile with 0.1 % acetic acid and 0.2 % triethylamine.
Figure 3.1.	Representative chromatograms showing the separation of warfaring enantiomers using DMPC-amylose phase and acetonitrile mobile phase that contains a) 0.2 % triethylamine; b) 0.1 % acetic acid; c) 0.1 % acetic acid and 0.2 % triethylamine
Figure 3.2.	Fluorescence spectrum of warfarin (25 μ M) in acetonitrile mobile phase that contains a) no additives; b) 0.1 % acetic acid; c) 0.2 % triethylamine; d) 0.1 % acetic acid and 0.2 % triethylamine 63
Figure 3.3.	Structures of warfarin isomers in cyclic, open, and deprotonated forms

rigure 3.4.	separation of coumarins using DMPC-amylose phase and acetonitrile mobile phase that contains 0.1 % acetic acid and 0.2 % triethylamine. Solutes: a) warfarin; b) coumachlor; c) coumafuryl; d) coumatetralyl
Figure 3.5.	Separation of coumarins using DMPC-cellulose phase and acetonitrile mobile phase that contains 0.1 % acetic acid and 0.2 % triethylamine. Solutes: a) warfarin; b) coumachlor; c) coumafuryl; d) coumatetralyl
Figure 3.6.	Effect of THF on the kinetics of coumatetralyl using DMPC-amylose phase and acetonitrile mobile phase that contains 0.1 % acetic acid and 0.2 % triethylamine with a) 10 % THF; b) 5 % THF; c) 0 % THF.
Figure 3.7.	Effect of THF on the kinetics of coumatetralyl using DMPC-cellulose phase and acetonitrile mobile phase that contains 0.1 % acetic acid and 0.2 % triethylamine additives with a) 10 % THF; b) 5 % THF; c) 0 % THF
Figure 4.1.	Chromatograms and structures of coumarin-based anticoagulants. Column: Chiralpak IA; mobile phase: acetonitrile with 0.1 % acetic acid and 0.2 % triethylamine additives; temperature: 20 °C; flow rate: 1 μ L/min.
Figure 4.2a	Natural logarithm of the retention factor of the second eluted enantiomer (k₂) versus inverse temperature (1/T) for all coumarins. Warfarin (•), coumachlor (△), coumafuryl (•), coumatetralyl (■), and 4-hydroxycoumarin (□). Other experimental conditions as given in Figure 4.1
Figure 4.2b.	Natural logarithm of selectivity (α) versus 1/T for all coumarins. Warfarin (\bullet) , coumachlor (\blacktriangle) , coumafuryl (\bullet) , and coumatetralyl (\blacksquare) . Other experimental conditions as given in Figure 4.1 106
Figure 4.3a	Natural logarithm of the retention factor of the second eluted enantiomer (k₂) versus inverse temperature (1/T) for warfarin enantiomers in the presence of 5 % modifiers. MeOH (•), <i>i</i> -BuOH (•), <i>t</i> -BuOH (▲), and THF (■). Other experimental conditions as given in Figure 4.1
Figure 4.3b	 Natural logarithm of selectivity (α) versus 1/T for warfaring enantiomers in the presence of 5 % modifiers. MeOH (●), i-BuOH (♦), t-BuOH (▲), and THF (■). Other experimental conditions as given in Figure 4.1

Figure 4.4a	enantiomer (k₂) versus inverse temperature (1/T) for coumatetralyl enantiomers in the presence of 5 % modifiers. MeOH (•), <i>i</i> -BuOH (•), <i>t</i> -BuOH (▲), and THF (■). Other experimental conditions as given in Figure 4.1
Figure 4.4b	. Natural logarithm of selectivity (α) versus 1/T for coumatetralylenantiomers in the presence of 5 % modifiers. MeOH (●), <i>i</i> -BuOH (♦), <i>t</i> -BuOH (▲), and THF (■). Other experimental conditions as given in Figure 4.1
Figure 4.5a	. Natural logarithm of the retention factor of the second eluted enantiomer (k₂) versus inverse temperature (1/T) for warfarin enantiomers in the presence of 10 % modifiers. MeOH (•), <i>i</i> -BuOH (•), <i>t</i> -BuOH (▲), and THF (■). Other experimental conditions as given in Figure 4.1
Figure 4.5b	 Natural logarithm of selectivity (α) versus 1/T for warfaring enantiomers in the presence of 10 % modifiers. MeOH (●), i-BuOH (♦), t-BuOH (▲), and THF (■). Other experimental conditions as given in Figure 4.1
Figure 4.6a	. Natural logarithm of the retention factor of the second eluted enantiomer (k₂) versus inverse temperature (1/T) for coumatetrally enantiomers. MeOH (•), <i>i</i> -BuOH (•), <i>t</i> -BuOH (▲), and THF (■). Other experimental conditions as given in Figure 4.1
Figure 4.6b	. Natural logarithm of selectivity (α) versus 1/T for coumatetrally enantiomers in the presence of 10 % modifiers. MeOH (●), <i>i</i> -BuOH (♦), <i>t</i> -BuOH (▲), and THF (■). Other experimental conditions as given in Figure 4.1
Figure 4.7.	Enthalpy–entropy compensation plot of the natural logarithm of the retention factor (k) versus change in molar enthalpy ($-\Delta H$) for all coumarin enantiomers in Figure 4.1. The equation of the line is y = $1 \times 10^{-4} \times - 1.2719$ ($r^2 = 0.971$). Other experimental conditions as given in Figure 4.1

Figure 4.8.	Enthalpy—entropy compensation plot of the natural logarithm of the retention factor (k) versus change in molar enthalpy ($-\Delta H$) for warfarin (\triangle) and coumatetralyl enantiomers (\blacksquare) with 5 % of MeOH, <i>i</i> -BuOH, <i>t</i> -BuOH, and THF. The equation of the lines are: y = 7x 10^{-5} x -0.503 ($r^2 = 0.889$) for warfarin and y = 1x10 ⁻⁴ x -0.538 ($r^2 = 0.889$) for coumatetralyl. Other experimental conditions as given in Figure 4.1
Figure 4.9	Natural logarithm of the desorption rate constant of the first eluted enantiomer (k _{ms1}) versus inverse temperature (1/T). Warfarin (●), coumachlor (▲), coumafuryl (♦), coumatetralyl (■), and 4-hydroxycoumarin (□). Other experimental conditions as given in Figure 4.1
Figure 4.10.	Arrhenius plots for coumatetralyl: natural logarithm of the desorption rate constant of the second eluted enantiomer (k_{ms2}) versus inverse temperature (1/T) in the presence of 5 % modifiers. MeOH (\bullet), i -BuOH (\bullet), t -BuOH (\bullet), and THF (\bullet). Other experimental conditions as given in Figure 4.1
Figure 5.1.	Structures of open side chain warfarin conformers 145
Figure 5.2.	Potentials of mean force as a function of dihedral angle α (C4-C3-C1'-C2') from umbrella sampling of R- and S-warfarin in water. R, depr (\blacksquare); R-2OH (\bullet); R-4OH (\triangle); S, depr (\square); S-2OH (\circ); S-4OH
Figure 5.3.	(Δ)
Figure 5.4.	Potentials of mean force from probability distributions of HO2-O3' distance in S/R-warfarin-2-OH. (A) in water and (B) in acetonitrile. Sampling for S-warfarin in state I (◆) and state II (■); for R-warfarin state I (△) and state II (○)
Figure 5.5.	Potentials of mean force from probability distributions of HO4-O3' distance in S/R-warfarin-4-OH. (A) in water and (B) in acetonitrile. Sampling for S-warfarin in state I (◆) and state II (■); for R-warfarin state I (△) and state II (○)

Figure 5.6.	Representative structures with hydrogen-bonded conformations. (A) R-warfarin-4-OH in state II and (B) S-warfarin-4-OH in state I
Figure 5.7.	Representative lowest energy conformation β-CD obtained from simulation
Figure 5.8.	Energetically most favorable docked A) R-warfarin-4-OH (state I) in the "Up" orientation, B) S-warfarin-4-OH (state I) in the "Down" orientation. Radius of sphere from the center of the cavity is 8 Å

CHAPTER 1

INTRODUCTION AND BACKGROUND

1.1. SIGNIFICANCE OF CHIRAL SEPARATION

Enantiomers are stereoisomers that are non-superimposable mirror images. They have the same chemical and physical properties and, as a result, their separation is very challenging. However, they differ in their interaction with other chiral molecules. Many biologically active substances such as enzymes, receptors, amino acids, and sugars have inherent chiral selectivity. Consequently, a pair of enantiomers in drugs, food additives, and agrochemicals is usually found to display different pharmacological and pharmacokinetic effects when they interact with chiral biomolecules. For instance, the β-blocker Spropranolol is 100 times more potent and has a longer half-life in plasma than Rpropranolol. For many classes of pharmaceuticals, only one of the enantiomers exhibits the desirable therapeutic activity, while the other enantiomer can often be inactive or cause harmful side effects.² In 1992, the U.S. Food and Drug Administration (FDA) issued guidelines for development of stereoisomeric drugs. These guidelines demand that pharmaceutical companies provide a full documentation of the separate pharmacological and pharmacokinetic profiles of the individual enantiomers, as well as the racemates of new drugs.³ Currently, a large number of the best-selling drugs around the globe are single enantiomers, with total annual sales greater than 200 billion dollars.4

The analysis of enantiomers also has important applications in the agrochemical and food industries. About a quarter of all pesticides used

commercially are chiral and most of these compounds are marketed as racemates.^{5,6} Hence, there is a strong interest in the development and mechanistic understanding of chiral separation methods.

1.2. METHODS OF CHIRAL SEPARATIONS USING LIQUID CHROMATOGRAPHY

During the last two decades, liquid chromatography (LC) has become an important tool for the separation of enantiomers in both analytical (small) and preparative (large) scales. In the analytical scale, components are identified and quantified, while in the preparative scale components of interest are isolated and collected for further use. In general, enantioseparations by HPLC involve direct methods (chiral mobile phase additives or chiral stationary phases) and indirect methods (using derivatizing agents).

1.2.1. Indirect methods

In these methods, the racemates are derivatized using an optically pure derivatizing agent. The resulting diastereomers can then be separated using an achiral stationary phase since they have different physical properties. This method is applied for enantiomers that possess a functional group (e.g. amino, hydroxyl, carboxyl, thiol) that can be easily derivatized. At the same time, the derivatizing agent should possess the following characteristics: 1) be stable, 2) be available in high optical purity, and 3) should not be racemized during the derivatization process. These methods are especially important for trace

analysis of enantiomers in biological samples where sensitive and selective fluorescence labels may be used.⁷ The disadvantages of these methods are the following. First, the procedure lengthens the total analysis time. Second, they cannot be used for compounds without a reactive functional group in the structure. Third, the rates of reactions of the two enantiomers with the chiral molecule may be different.⁸ This results in different proportions of the enantiomers compared to the starting enantiomer composition. Finally, indirect methods are not useful for preparative separations, as the label must be removed to recover the enantiomers.

1.2.2. Direct methods

Direct separation of racemates is usually achieved by the use of chiral mobile phase additives together with an achiral stationary phase or chiral stationary phases in conjunction with an achiral mobile phase. The principle behind both methods is the formation of non-covalent diastereomeric complexes with varying free energy of formation. The magnitudes of these free energies depend on the differences in the interactions between the enantiomers and chiral selector. These interactions may include van der Waals forces, dipole-dipole interactions, hydrogen bonds, ion-dipole interactions, and ionic interactions.

1.2.2.1. Chiral mobile phase additives

Many chiral compounds can be separated on conventional LC columns by adding suitable chiral additives into the mobile phase. Formation of

diastereomeric complexes with chiral mobile phase additives involves three approaches. First, ion pairing agents (e.g. quinine) may be used. They are commonly applied for charged molecules based on the formation of a diastereomeric ion pair between a charged analyte and a counterion of opposite charge.⁹ To promote ion-pair formation, less polar organic solvents such as methylene chloride are commonly used. Second, ligand exchange complexing agents (e.g. L-proline-Cu (II) complex) may be used. They are based on the formation of diastereomeric complexes between transition metal ions and chiral complexing agent with the racemate.¹⁰ Finally, inclusion complexes (e.g. β-cyclodextrin)^{11,12} are commonly used with aqueous mobile phases. The advantages of these additive-based methods include the possibility of using achiral columns with higher loading capacity and using one or more additives to modify solute character. On the other hand, the disadvantage is that the additive should be removed after separation and is used only once.

1.2.2.2. Chiral stationary phases

Direct methods based on chiral stationary phases are preferred over chiral mobile phase additives since they are suitable to resolution of racemates on both small and large scales. The major disadvantage of this method is the difficulty in selecting the best stationary phase and the dependence of the elution order on the stationary phase and/or mobile phase composition. Three modes of separations are commonly employed. These are normal-phase, reversed-phase, and polar-organic modes. In the normal-phase mode, polar stationary phases

and relatively non polar mobile phases (e.g. hexane with alcohols) are used. In the reversed-phase mode, non polar stationary phases and polar mobile phases (e.g. water with methanol or acetonitrile) are used. In the polar-organic mode, moderately polar stationary phases and relatively polar mobile phases (e.g. acetonitrile, alcohols) are used.

During the last twenty five years, several new and improved chiral stationary phases have been developed and made commercially available. The next sections describe these phases.

1.3 TYPES OF CHIRAL STATIONARY PHASES

Chiral stationary phases (CSPs) can be classified into the following main groups: donor-acceptor, protein, inclusion, and polysaccharide.

1.3.1. Donor-acceptor CSPs

Donor-acceptor type CSPs contain a small chiral selector covalently bonded to silica gel. Generally, the chiral selector contains a π -electron donor, a π -electron acceptor, or both a π -donor and a π -acceptor. The most widely known and commercially successful phases are those prepared by Pirkle et al. ^{13,14} For instance, (R)-N-(3,5-dinitrobenzoyl) phenylglycine is considered one of the most popular π -acceptor Pirkle phases. According to Pirkle, chiral recognition in these phases involves π - π interactions, dipole-dipole interactions, and hydrogen bonding. Separation on these phases is mainly explained by the three-point interaction model. ¹⁵ In this model, enantiomers will have three possible

interaction points with the CSP, where at least one of these interactions is stereochemically dependent. One enantiomer will then interact more strongly than the other and, thus, will be retained longer.

1.3.2. Protein-type CSPs

Proteins are naturally occurring, optically active polymers made up of amino acids connected through amide bonds. All proteins are complex in structure because of the different intramolecular hydrogen bonding, disulfide bridges, and other types of bonding. 16 These bonds are responsible for the twisted three-dimensional forms or grooves present in the protein molecule that make it enantioselective in nature. Protein stationary phases are covalently bonded to a silica gel surface and used for liquid chromatography in the reversed-phase mode. Separations on protein stationary phases depend on polar interactions such as dipole-dipole, hydrogen bonding, and ion-ion forces. Several types of proteins have been used as chiral stationary phases including human α_1 -glycoprotein (AGP), 17 human serum albumin (HSA), 18 and ovomucoid. 19 However, they have numerous drawbacks such as low sample capacity, aqueous mobile phase requirements (the proteins denature in organic solvents), and limited durability (limited range of temperature and pH). Hence. their application is limited to analytical purposes.

1.3.3. Inclusion-type CSPs

Cyclodextrins (CDs) are macrocyclic molecules containing six or more D-glucose units connected through α -1,4-glycosidic linkages. They are obtained by the action of cyclodextrin transglycosylase enzyme on starch. The most commonly investigated CDs are α -CD, β -CD, and γ -CD, corresponding to 6, 7, and 8 glucose units, respectively. Cyclodextrin forms a truncated conical cavity, the diameter of which depends on the number of glucopyranose units. Figure 1.1 shows the structure of β -CD.

The CD molecule has secondary 2- and 3-hydroxyl groups at one edge of the cavity and primary 6-hydroxyl groups at the opposite edge. This means that the interior of the cavity itself is relatively hydrophobic and permits inclusion of hydrophobic portions of solute molecules. Depending on the size of the CD cavity relative to the size of the enantiomers, different types of chiral compounds can be resolved.²⁰

Cyclodextrins have been extensively studied by Armstrong et al. $^{21-23}$ as both mobile phase additives and as stationary phases bonded to silica. The mechanism of chiral separation on β -CD in the reversed-phase mode is considered to be the formation of an inclusion complex with the chiral compound. 22 Both native and derivatized CDs are widely used chiral selectors for enantiomer separations in gas chromatography (GC) and LC. The derivatives are formed by bonding various groups onto the surface hydroxyls of the

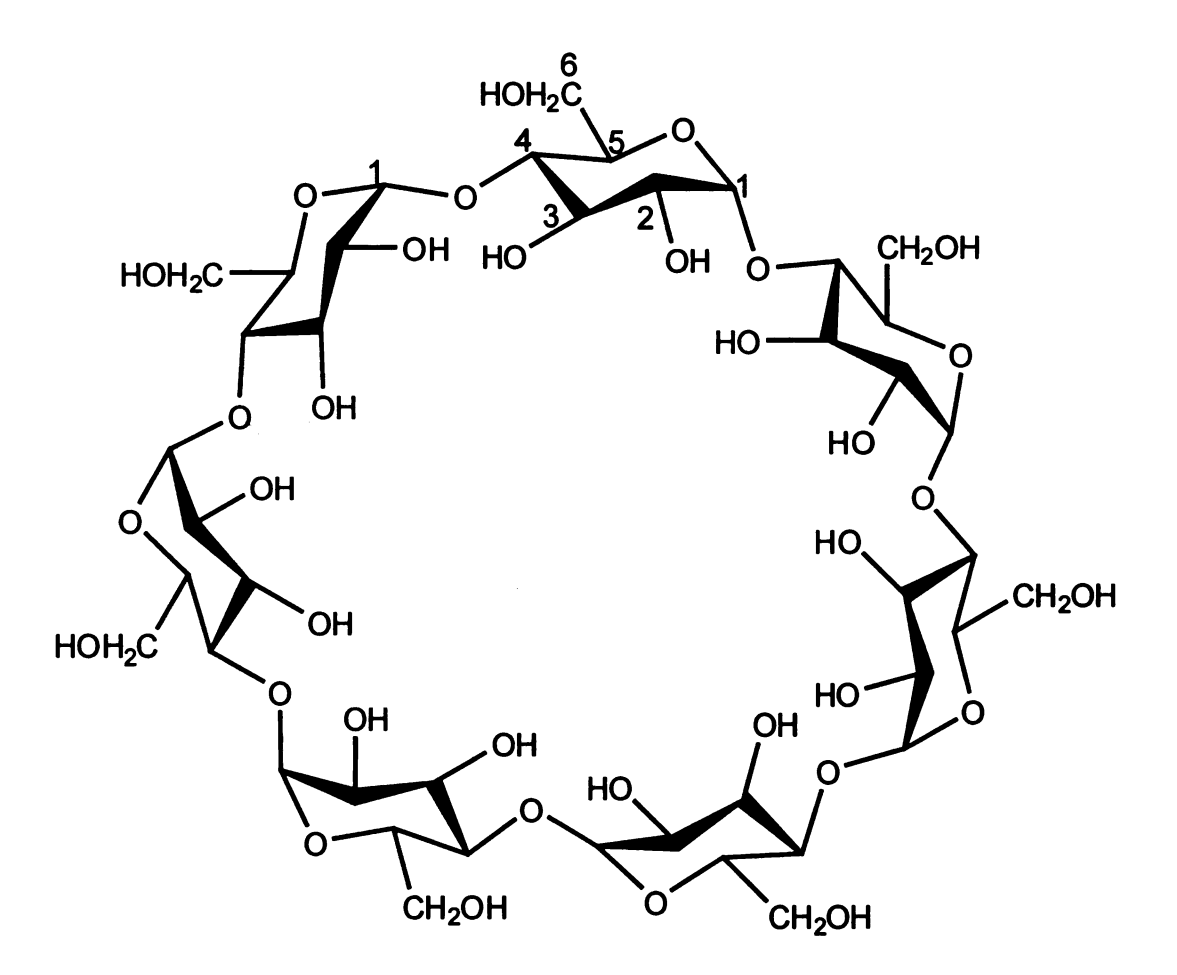


Figure 1.1. Structure of β -cyclodextrin.

cyclodextrin cavity. These include permethylated- β -CD²⁴ for GC, hydroxypropyl β -CD, and tris-3,5-dimethylphenyl carbamate β -CD²⁵ for LC. Section 2.1 gives further information on derivatized β -CDs.

1.3.4. Polysaccharide-type CSPs

Polysaccharides such as amylose and cellulose are optically active biopolymers that can resolve enantiomers. Amylose is a polymer of D-glucose units that are connected by α -1,4-glycosidic bonds and has a helical structure in its native form. In contrast, cellulose is a polymer based on β -1,4-glycosidic bonds and possesses a linear structure. The native forms have low enantioselectivities and poor mechanical properties, unlike the derivatized polysaccharide stationary phases. As a result, the native forms are not practically useful CSPs in LC. 26

Hesse and Hagel²⁷ reported microcrystalline cellulose triacetate (CTA-I) as the first practical CSP derived from polysaccharides in 1973. CTA-I coated on silica gel has higher chiral recognition abilities and mechanical strength compared to the uncoated microcrystalline form.²⁸ In the mid 1980s, four kinds of polysaccharide CSPs were commercially available from Daicel Chemical Industries. These are the tribenzoate,^{28,29} tris-phenyl carbamate,³⁰ and tris-(3,5-dimethylphenyl carbamate)³¹ derivatives of cellulose and the tris-(3,5-dimethylphenyl carbamate) derivative of amylose.³² Today, about 90 % of chiral compounds can be successfully separated with these polysaccharide-based

(a)

Figure 1.2. Structures of tris-(3,5-dimethylphenyl carbamate) a) amylose, b) cellulose.

phases alone.³³ By far, the tris-(3,5-dimethylphenyl carbamates) of cellulose and amylose (Figure 1.2) are generally regarded as the most powerful and popular CSPs for LC.⁴ Interestingly, the chiral selectivities of these two selectors are usually complimentary in nature. Other polysaccharide-based carbamate selectors that show chiral recognition include benzyl carbamates, cycloalkyl carbamates, and benzoyl carbamates of cellulose and amylose.⁴

Finally, polysaccharide chiral packing materials have been traditionally prepared by coating them on silica gel.^{28,31} However, many common organic eluents such as acetone, tetrahydrofuran, ethyl acetate, chloroform, dichloromethane, and toluene, can swell or dissolve these selectors. To improve the solvent compatibility of these phases, different immobilization methods were established over the years.³⁴⁻³⁷ Okamoto et al.³⁸ were the first to chemically bond cellulose derivatives on 3-aminopropyl-functionalized silica gel using a diisocyanate cross linker. Currently, amylose and cellulose derivatives that are chemically bonded to silica gel are commercially available.

1.4. THERMODYNAMIC AND KINETIC THEORIES

1.4.1.Thermodynamics

Liquid chromatographic processes are well described by equilibrium thermodynamics. As a result, separation parameters can be correlated to the energetics of solution-phase interactions.³⁹ During separation, each solute zone proceeds through the column at a rate controlled by competing interactions of the solute with the stationary phase and the mobile phase. This process results in

an increase in the solute retention time (t_r) relative to the movement of a nonretained species (t_0) and is often described with the solute retention factor (k),

$$k = \frac{t_r - t_0}{t_0} \tag{1}$$

The retention factor is the weighted time-average of all possible interactions in the heterogeneous stationary phase environment. It can be related to the changes in molar Gibbs free energy (Δ G) by the following equation

$$\Delta G = -RT \ln K = -RT \ln \frac{k}{\beta}$$
 (2)

where K is the equilibrium constant, R is the universal gas constant, T is the absolute temperature, and β is the volume ratio of the stationary to mobile phase. The molar Gibbs free energy is also a function of the changes in molar enthalpy (Δ H) and molar entropy (Δ S)

$$\Delta G = \Delta H - T \Delta S \tag{3}$$

When Eq. 3 is substituted into Eq. 2,

$$\ln k = \frac{-\Delta H}{RT} + \frac{\Delta S}{R} + \ln \beta \tag{4}$$

The change in molar enthalpy can be determined from the linear slope of a graph of ln k versus 1/T at constant pressure, assuming that the changes in molar enthalpy and entropy are temperature independent. The change in molar entropy is contained in the intercept, but cannot be reliably calculated since the phase ratio (β) is a function of both temperature and pressure. A negative change in the molar enthalpy indicates that the transition from the mobile to stationary phase is an energetically favorable process.

From the definition of molar enthalpy,

$$\Delta H = \Delta E + P \Delta V \tag{5}$$

When Eq. 5 is substituted into Eq. 4, the retention factor can be related to the pressure (P), the change in molar internal energy (ΔE), and the change in molar volume (ΔV)

$$lnk = \frac{-\Delta E + T\Delta S - P\Delta V}{RT} + ln\beta$$
 (6)

The change in molar volume can be calculated from the linear slope of a graph of ln k versus P at constant temperature, assuming that the changes in molar volume, internal energy, and entropy are pressure independent. A negative change in molar volume indicates that the solute occupies less space in the stationary phase than in the mobile phase.

The thermodynamic contributions to enantioselectivity are determined from the selectivity factor (α). This parameter represents the difference in the free energy of interactions of the two enantiomers with the chiral stationary phase and is calculated by

$$\alpha = \frac{k_2}{k_1} \tag{7}$$

where k_2 and k_1 refer to the retention factor of the more retained and less retained enantiomers, respectively. When Eq. 4 is substituted into Eq. 7,

$$\ln \alpha = \frac{-\Delta \Delta H}{RT} + \frac{\Delta \Delta S}{R} \tag{8}$$

where $\Delta\Delta H$ and $\Delta\Delta S$ represent the difference between the changes in molar enthalpy and molar entropy, respectively, for the two enantiomers. They are

determined from the slope and intercept, respectively, of a graph of $\ln \alpha$ versus 1/T. In chiral separations, only stereoselective interaction with the chiral selector leads to a difference in retention. Hence, $\Delta\Delta H$ and $\Delta\Delta S$ represent the difference in chiral contributions from molar enthalpy and entropy, respectively. When Eq. 6 is substituted into Eq. 7,

$$\ln \alpha = \frac{-\Delta \Delta E + T \Delta \Delta S - P \Delta \Delta V}{RT}$$
(9)

where $\Delta\Delta V$ and $\Delta\Delta E$ represent the difference between the changes in molar volume and molar internal energy, respectively, for the two enantiomers. These parameters may be determined from the slope and intercept, respectively, of a graph of ln α versus P.

1.4.1.1. Enthalpy-entropy compensation (EEC)

Analysis of physicochemical processes, such as chromatographic retention, can be performed by investigating the enthalpy-entropy compensation behavior. The experimental observation of a linear relationship between ΔH and ΔS for a series of related processes is known as enthalpy-entropy compensation. Mathematically, it can be expressed as

$$\Delta H = T_c \Delta S + \Delta G_{T_c}$$
 (10)

where T_C is the compensation temperature and ΔG_{Tc} is the change in Gibbs free energy at the compensation temperature.⁴⁰ The compensation temperature represents the temperature at which ΔH and ΔS are completely compensated, i.e., the temperature at which there is no enantioselectivity (ΔG =0). For statistical

reasons, it is unfortunately true that a linear correlation could be expected between ΔH and ΔS when both are determined from the van't Hoff equation, even when there is no real compensation effect. Krug et al. 40,41 have shown that linear plots of enthalpy-entropy data may be due to propagation of measurement errors rather than a real EEC. When there is a linear plot between ΔH and ΔS , without real EEC, the slope of the plot is equal to the harmonic mean of the experimental temperatures (T_{hm}), while the correlation coefficient is close to unity. Krug⁴² proposed two conditions for a compensation that results from physicochemical effects. First, plots of ΔG (or ln k) vs. 1/T must intersect at a single temperature for all compounds. Second, plots of ΔG_{hm} (or ln k_{hm}) vs. ΔH must provide a linear plot. These linear plots are usually indicative of compensation resulting from similar solute-stationary phase interactions. When Eq. 10 is rearranged to solve for ΔS and is substituted into Eq. 3,

$$\Delta G = \Delta H \left[1 - \frac{T}{T_C} \right] + \frac{T \Delta G_{T_C}}{T_C}$$
 (11)

Upon substituting Eq. 11 into Eq. 2,

$$\ln k = \frac{-\Delta H}{R} \left[\frac{1}{T_{hm}} - \frac{1}{T_C} \right] - \frac{\Delta G_{T_C}}{RT_C} + \ln \beta$$
 (12)

where T_{hm} is the harmonic mean temperature (<1/T>-1). Eq. 12 shows that if compensation occurs, a plot of ln k versus - ΔH will be linear, and the slope of the line contains information to determine the compensation temperature. If the compensation temperature is sufficiently higher than the ambient temperature, the separation is usually considered as enthalpy dominated.⁴⁴ In contrast, if the

compensation temperature is lower than the ambient temperature, the separation is entropy dominated.⁴⁴ At values close to the compensation temperature, enantioseparations cannot be obtained.

Two processes with similar compensation temperatures are considered to proceed via the same mechanism.¹⁴ However, this idea was challenged by Ranatunga et al.¹⁵ According to the authors, the only conclusion that can be made is that the enthalpy and entropy contributions to the total free energy is the same in the two processes. The authors argue that in systems with similar compensation temperatures, the processes occurring may or may not be the same, since the fraction of enthalpy and entropy in the overall free energy for two different processes may be identical. However, if the compensation temperatures are different, then the mechanisms of the two processes must be different. Thus, enthalpy-entropy compensation studies may provide important information about retention mechanisms under different chromatographic conditions.

1.4.2. Kinetics

The rate at which solute molecules undergo transfer between the mobile and stationary phases can be described by kinetic parameters such as rate constants and activation energies. Generally, the kinetic rate constants are the energy-weighted average of the different initial and final states and the different paths taken by the solute to transfer between them. They can be related to the thermodynamic retention factor by the following expression

$$k = \frac{k_{sm}}{k_{ms}} \tag{13}$$

where k_{sm} and k_{ms} are the rate constants for the solute transfer from mobile to stationary phase and from stationary to mobile phase, respectively. The determination of the individual rate constants is shown in chapters 3 and 4. When the solute transfers between the mobile and stationary phases, it passes through a short-lived, high-energy transition state (‡) that uniquely characterizes the path-dependent aspects of the retention mechanism. The kinetic rate constants can be related to the activation energy by means of the Arrhenius equation

$$lnk_{sm} = lnA_{\ddagger m} - \frac{\Delta E_{\ddagger m}}{RT}$$
 (14)

$$lnk_{ms} = lnA_{\ddagger s} - \frac{\Delta E_{\ddagger s}}{RT}$$
 (15)

where $A_{\pm m}$ and $A_{\pm s}$ are the pre-exponential factors and $\Delta E_{\pm m}$ and $\Delta E_{\pm s}$ are the activation energies arising from the mobile phase to transition state and stationary phase to transition state, respectively. The activation energy for the sorption process can be determined by plotting ln k_{sm} versus 1/T, if $\Delta E_{\pm m}$ is temperature independent. Likewise, the activation energy for the desorption process can be determined by plotting ln k_{ms} versus 1/T, if $\Delta E_{\pm s}$ is temperature independent. When one of these transitions is slow with respect to the mobile phase velocity, it will be manifested chromatographically in the asymmetrical

broadening of a solute zone.³⁹ These thermodynamic and kinetic parameters are used to characterize different achiral or chiral stationary phases.

1.5. PREVIOUS THERMODYNAMIC AND KINETIC STUDIES

There have been some thermodynamic and kinetic studies on inclusion phases (β -cyclodextrin) and polysaccharide phases (derivatized cellulose and amylose). These studies involve investigation of the effect of different chromatographic conditions, mobile phase, temperature, and pressure, on their retention mechanisms.

1.5.1. Inclusion phases

One of the earliest temperature studies in chiral separations on β -CD stationary phases was performed by Feitsma et al.⁴⁵ The authors varied temperature from 25 to 57 °C to separate aromatic carboxylic acids. Although the selectivity of the separation decreases with an increase in temperature, the resolution increases. The authors attributed this observation to reduced tailing of the peaks at higher temperature.

The effect of temperature on the separation of two chiral pharmaceuticals, oxazepam and prominal, was investigated by Cabrera and Lubda⁴⁶ using immobilized β -CD in the reversed-phase mode. For both solutes, linear van't Hoff plots were observed in the range of 5 to 40 °C. Moreover, a decrease in temperature caused an increase in their retention. However, the effect of temperature on the enantioselectivity was quite unusual. For oxazepam, the

enantioselectivity improved with decreasing temperature, whereas for prominal it improved with increasing temperature. As a result, the separation of oxazepam was found to be enthalpy controlled ($\Delta\Delta H = -1.39 \text{ kJ/mol}$, $\Delta\Delta S = 0.23 \text{ kJ/mol}$), while that of prominal was entropy controlled ($\Delta\Delta H = 1.56 \text{ kJ/mol}$), $\Delta\Delta S = 1.75 \text{ kJ/mol}$).

Morin et al.47 also investigated the effect of temperature and pH for six imidazole derivatives using a β-CD bonded chiral stationary phase. The van't Hoff plots, determined for the temperature range of 20 to 55 °C, were linear at pH 7.0 and 7.5. However, these plots were curved (non-linear) with minima between 35 and 40 °C at pH 6.5, 8.0, and 8.5. The observed van't Hoff plots were different with mobile phase pH values, suggesting a change in the retention mechanism with pH. Enthalpy-entropy compensation studies (ln k vs. -ΔH) at pH 7.0 and 7.5 showed that the retention mechanism was not dependent on the structures of the imidazole derivatives. To further investigate the effect of temperature on the stationary phase, differential scanning calorimetry and thermogravimetric analysis were used at pH values of 6.5, 7.0, 7.5, and 8.0. The results indicate that the stationary phase showed an exothermic peak at around 43 °C at pH 6.5, 8.0, and 8.5. This change was attributed to a phase transition between the ordered (relaxed) and disordered (distorted) state of the cyclodextrin cavity.

Li and McGuffin⁴⁸ investigated the thermodynamics and kinetics of the separation of coumarin-based anticoagulants on native β-cyclodextrin stationary phase using polar-organic eluents. For all the coumarins, an increase in

temperature decreased the thermodynamic retention factor and chiral selectivity, and the van't Hoff plots were linear. The changes in molar enthalpy and entropy were obtained from the slopes and intercepts of these plots. Estimated values of $\Delta\Delta H$ ranged from -0.50 to -1.55 kJ/mol, while those of $T\Delta\Delta S$ ranged from -0.15 to -0.94 kJ/mol. The enthalpy-entropy compensation plot (ln k vs. - ΔH), showed that the coumarins have different retention mechanisms. The estimated values for the compensation temperature (T_C) were above room temperature, suggesting that the separation is enthalpy dominated. Pressure had a negligible effect on the enantioselectivity of these solutes. The inclusion in the chiral cavity was negligible, as the change in the molar volume of the solutes was positive. This observation suggested that, unlike the reversed-phase mode, inclusion was not the dominant retention mechanism in the polar-organic mode. The kinetics rate constants for mass transfer in this phase increased with an increase in temperature.

The effect of pressure on retention, selectivity, and plate height for hexobarbital, warfarin, and other pharmaceuticals on β -CD bonded phase was studied by Ringo and Evans. The pressure dependence of the retention factor showed a clear trend between reversed-phase and polar-organic separation modes. In the reversed-phase mode, the retention factor showed an increase or no change with a concomitant change in molar volume that was negative or negligible. In contrast, a decrease in retention factor with a concomitant change in molar volume that was positive or negligible was observed in the polar-organic mode. The change in molar volume ranged from -12 to 17 cm³/mol. The

pressure dependence of chiral selectivity was determined by the enantiomeric differences in the partial molar volume of the complexes formed upon retention. Unlike retention factor and selectivity, differences in the binding kinetics primarily govern the pressure dependence on plate height. For both reversed-phase and polar-organic separation modes, pressure-induced changes resulted in an increase in the plate height of up to 240%.

The role of pressure in separation of positional isomers of nitrophenol on β -CD bonded phase, where inclusion complexation is the dominant mechanism, was investigated by Ringo and Evans.⁵⁰ The change in the retention factor of these positional isomers ranged from -2.1 % to -35 % for pressure changes of 40 to 340 bar. The magnitude of solute retention was found to be a function of solvent strength of the mobile phase.

Finally, Ringo and Evans⁵¹ studied the effect of pressure on the change in partial molar volume of warfarin enantiomers separated with β -CD. Both enantiomers of warfarin showed modest changes in molar volume upon complexation (17 and 16 cm³/mol), resulting in a small variation in the differential change in molar volume (1.0 cm³/mol). The difference in their molar volume was mainly attributed to their solvated complexes and may contribute to chiral recognition of the enantiomers.

1.5.2. Polysaccharide phases

The role of temperature in chiral separations on derivatized cellulose was reported by Smith et al.⁵² Cellulose derivatized with tris-(3,5-dimethylphenyl

carbamate) was used to separate two analogues of Cromakalim, a potassium channel activator, in the temperature range of 0 to 42 °C. Two of the compounds, which differed only by substitution of a benzoyl group by an npentanovi group, showed guite different dependence on temperature. The npentancyl enantiomers showed increasing resolution with a decrease in temperature, while the benzovl enantiomers showed the opposite. The differential changes in molar enthalpy ($\Delta\Delta H$) and entropy ($\Delta\Delta S$) were determined from the van't Hoff plots. The calculated $\Delta\Delta H$ values were 1.93 and -4.27 kJ/mole, whereas the $T\Delta\Delta S$ values were 3.07 and -4.05 kJ/mole for the benzovl and *n*-pentanoyl enantiomers, respectively. The compensation temperatures varied greatly, and the magnitudes were -86 and 41 °C, respectively. As a result, the separation of benzoyl enantiomers was entropy dominated, whereas that of *n*-pentancyl enantiomers was enthalpy-dominated. The authors concluded that the enantioselectivity of chiral compounds that involve more π - π interactions were favored by an increase in temperature whereas enantioseparations that were more dependent upon hydrogen bonding interactions were favored by a decrease in temperature.

The temperature dependence of the separation of Rolipram enantiomers (an anti-inflamatory drug) on a tris-(3,5-dimethylphenyl carbamate) cellulose stationary phase (Chiralcel-OD) was investigated by Kusters and Spondlin.⁵³ For these studies, methanol, 2-propanol, and 4-methyl-2-pentanol were used as modifiers in *n*-hexane mobile phase for temperatures ranging from 10 to 60 °C. At 10 and 20 °C, no separation was observed. In contrast, adequate separation

was observed at 60 °C, suggesting that the separation is entropy dominated. The estimated values of $\Delta\Delta H$ and $T\Delta\Delta S$ in 4 % 2-propanol/*n*-hexane mobile phase were 1.62 kJ/mol and 1.78 kJ/mol, respectively. The authors concluded that chiral resolution is due to additional weak π - π interaction or weak hydrogen bonding.

The effect of temperature on the separation of α -aminobenzyl substituted 1- and 2-naphthol analogs on a tris-(3,5-dimethylphenyl carbamate) cellulose stationary phase was reported by Sztojkov-Ivanov et al. 54 The authors observed linear van't Hoff plots in the temperature range of 5 to 35 °C for all the analogs of naphthol. From the slopes of the van't Hoff plots, the - $\Delta\Delta$ H values for the binding of 2-naphthol analogs ranged from 9.4 to 13.4 kJ/mol, while that for the 1-naphthol analogs ranged from 1.5 to 7.6 kJ/mol. This indicates that a change in the position of α -aminobenzyl substitution from position 1 to position 2 caused 60-80 % reduction in the binding energy. Although more favorable enthalpic contributions were observed for the 2-naphthol analogs, they also had larger unfavorable entropic contributions compared to the 1-naphthol analogs. For both analogs, the values for $\Delta\Delta$ H and $\Delta\Delta$ S were negative, indicating that the separation was enthalpy dominated.

O'Brien et al.⁵⁵ elucidated the types of interactions occurring between a diol intermediate for a leukotriene D_4 antagonist and a tris-(4-methylbenzoate) cellulose stationary phase. The observed van't Hoff plots were non-linear over the temperature range of 5 to 50 °C for both retention and selectivity, with a transition occurring between 18 and 20 °C. The van't Hoff plot for α had two

linear regions ($R^2 > 0.99$): region I occurred at temperatures between 18 and 50 °C, and region II occurred below 18 °C. The calculated values of $\Delta\Delta H$ and $\Delta\Delta S$ were negative in region I (high temperature) indicating an enthalpy-controlled separation, whereas those in region II (low temperature) were positive, indicating an entropy-controlled separation. The authors attributed this unsual temperature dependence to a conformational change in the stationary phase, that was further confirmed by infrared spectroscopy and differential scanning calorimetry. A trend was also observed between the thermodynamic parameters and the concentration of the alcohol modifiers used in the normal-phase mode. For both temperature regions, an increase in the concentration of 2-propanol caused an increase in both the $\Delta\Delta H$ and $\Delta\Delta S$ values. The changes in the two quantities canceled each other, resulting in only small changes in the molar free energy $(\Delta\Delta G)$ and, hence, the selectivity. The authors speculated that the loss of interaction of the more retained R-enantiomer relative to the S-enantiomer with increasing 2-propanol concentration was balanced by a relative increase in the space available for the R-enantiomer when it entered the stationary phase. This behavior was attributed to swelling of the cellulose phase (more positive $\Delta\Delta S$). Conformational changes of the cellulose phase were also accompanied by differences in solute sorption/desorption rates as measured by their plate height. For the R-enantiomer, the reduced plate height was large for temperatures up to 10 °C, but sharply decreased at about 15 °C, followed by a gradual decrease with further increase in temperature. For the S-enantiomer, the reduced plate height decreased gradually over the entire temperature range of 5 to 50 °C. This observation was explained by an inclusion-type interaction of the R-enantiomer in the chiral cavity of the stationary phase. At low temperature, the mass transfer of the R-enantiomer was slow due to inclusion in the chiral cavities. At this temperature, the cellulose chains were rigid and the reduced plate height remained relatively high. At higher temperature, the stationary phase was relaxed, the mass transfer was faster, and the reduced plate height was reduced.

Unsual temperature effects were also reported by Wang et al.⁵⁶ The separation of dihydropyrimidinone (DHP) acid and its methyl ester were investigated using tris-(3,5-dimethylphenyl carbamate) amylose (Chiralpak-AD) and cellulose (Chiralcel-OD) with an ethanol/n-hexane mobile phase. Non-linear van't Hoff plots of the retention factor and selectivity were obtained for the DHP acid on the amylose stationary phase, while linear plots were observed on the cellulose phase. Furthermore, the van't Hoff plot obtained when heating the amylose column from 5 to 50 °C was not superimposable on that obtained upon cooling from 50 to 5 °C. This observation indicated that the amylose phase had undergone a thermally induced, irreversible conformational change between the heating and cooling cycles. The conformational change was also found to depend on the polar component of the mobile phase. The van't Hoff plot of the DHP acid was linear and thermally reversible when 2-propanol was used instead of ethanol as a modifier. Solid state NMR was identified for structural changes in the amylose phase as a function of mobile phase composition.⁵⁷ The 2-Propanol modifier displayed more efficient displacement of incorporated n-hexane and formed relatively more ordered solvent complexes compared to ethanol.

In a related study, Wang et al.⁵⁸ extended their investigations to other polysaccharide phases. These include immobilized tris-(3,5-dimethylphenyl carbamate) of amylose and cellulose (Chiralpak IA and IB, respectively), and coated tris-(S-α-methylbenzyl carbamate) of amylose (Chiralpak AS-H) columns solvated with ethanol and 2-propanol in *n*-hexane mobile phases. For these studies, four different commercially available DHP compounds were used. The van't Hoff plots were non-superimposable on Chiralpak IA and Chiralpak AS-H columns solvated with 2-propanol and on Chiralpak IB and Chiralpak AS-H columns solvated with 2-propanol in *n*-hexane mobile phases. The authors concluded that this thermally induced path-dependent behavior resulted from slow equilibration of the stationary phase. These conclusions were supported by the observation of superimposable heating and cooling curves during the second cycle of heating and cooling steps.

Finally, Wang et al.⁵⁹ compared the effect of heating and cooling cycles on the apparent retention factors and selectivities of the above compounds. For this study, the mobile phases were 1-propanol, 1-butanol, 2-butanol, *i*-butanol and *t*-butanol in *n*-hexane, and the stationary phase was tris-(S-α-methylbenzyl carbamate) amylose coated on 5 and 10 μm silica gel (Chiralpak AS-H and AS, respectively). The authors reported that the apparent change in the retention factor of these compounds varied with the particle size of the stationary phase and alcohol modifiers used. The highest reduction in the apparent retention factor was observed in *t*-butanol/*n*-hexane mobile phase on the Chiralpak AS phase (> 27 %) as compared to Chiralpak AS-H phase (< 4 %). The other

alcohol modifiers did not show any clear trend in changing the apparent retention factors in both phases. Step temperature studies indicated that slow thermal equilibration behavior (change in apparent retention factor with time) was observed with mobile phases of 1-butanol, 2-butanol, *i*-propanol, and *t*-butanol in *n*-hexane for the Chiralpak AS phase at 50 °C. In contrast, this behavior was observed for only *t*-butanol in *n*-hexane for the Chiralpak AS-H phase. These observation indicated that the solvation of the CSPs and/or the probe compounds governed the thermodynamic and kinetics of the chromatographic behavior.

Kazusaki and Ohgami⁶⁰ showed enthalpy-entropy compensation for enantioseparation of N-carbobenzyloxy-D,L-leucine on tris-(3,5dimethylbenzoate) amylose stationary phase in reversed-phase chromatography. The van't Hoff plots of retention factor and selectivity were linear over the temperature range of 25 to 45 °C. Estimated values of $\Delta\Delta H$, $\Delta\Delta S$, and $\Delta\Delta G$ were negative, indicating that the separation was enthalpy dominated. Using the methods proposed by Krug et al., 40-42 the authors were able to demonstrate enthalpy-entropy compensation, where plots of $\Delta\Delta H$ vs. $\Delta\Delta G$ were linear and the compensation temperature (69.4 °C) was statistically different from the harmonic mean of the experimental temperatures (43.8 °C). These observations indicated that the mechanism of separation of the two enantiomers was basically similar under the experimental conditions.

Recently, Yao et al.⁴⁴ have reported the temperature-induced inversion of elution order for 1,1'-bi-2-naphthol, when 2-propanol/n-hexane (8/92, % v/v) was used as mobile phase. The estimated compensation temperature (T_C) was 31.4

 $^{\circ}$ C and the corresponding selectivity was marginal, as T_C was around room temperature. Interestingly, when 2-propanol/tetrahydrofuran/n-hexane (2/5/93, % v/v) was used as the mobile phase, the T_C value decreased to -8.2 $^{\circ}$ C. Consequently, the selectivity was 1.189 and 1.332 at 25 and 50 $^{\circ}$ C, respectively, indicating an entropically-driven enantioseparation. The authors demonstrated the existence of compensation temperature and how the mobile phase composition could be used to improve the enantioseparation by shifting T_C sufficiently away from room temperature, but did not explain why T_C shifts. Although many studies are reported in the literature, there is no comprehensive view about the different chiral stationary phases. Most of these studies are conducted using different solute probes and mobile phases. Hence, it is difficult to find general trends from these reports.

1.6. CONCLUSIONS

The separation of enantiomers has continued to be the most challenging problem in the use and development of pharmaceutical drugs and agrochemicals. A large number of chiral selectors have been developed for the analysis of these compounds. Among these, natural oligosaccharides including cyclodextrin and polysaccharides such as amylose and cellulose have been used as important enantioselective adsorbents for many enantiomers. Still, none of these phases are universal in their application. The major problem with these phases is their structural complexity and an incomplete understanding of their separation mechanism.

The goal of this research is to explore the detailed thermodynamics and kinetics of chiral separations on derivatized β -cyclodextrin, amylose and cellulose phases. These chiral selectors have the same primary structure (D-glucose units) but different secondary structures. By using the same chiral probes (warfarin and related coumarin anticoagulants), and mobile phase composition, systematic comparison of the retention mechanism of these stationary phases is performed. First, mobile phase studies on derivatized β -CD stationary phases will be compared (Chapter 2). Second, mobile phase studies on derivatized amylose and cellulose phases will be compared (Chapter 3). Third, detailed thermodynamic studies (changes in enthalpy, entropy, and free energy of association as well as enthalpy-entropy compensation analysis) and kinetic studies (rate constants and activation energies) will be discussed (Chapter 4).

Computational studies such as molecular dynamics can provide thermodynamic and kinetic information that are not easily observed from experiment. In this regard, the conformational sampling of warfarin conformers in polar solvents will be investigated. This study will show how each conformer (R-and S-warfarin structures) is favored over the other in each solvent environment and ultimately affect chiral recognition. In addition, docking of these conformers with β -cyclodextrin will be shown. These docking studies will provide information on how each warfarin conformer might bind differently in the β -cyclodextrin cavity. Such studies are believed to give some insight into understanding enantioselective interactions and will be shown in Chapter 5. Finally, conclusions and future directions will be discussed in Chapter 6.

1.7. REFERENCES

- (1) Silber, B.; Holford, N. H. G.; Riegelman, S. *J. Pharm. Sci.* **1982**, *71*, 699-704.
- (2) Rentsch, K. M. J. Biochem. Biophys. Meth. 2002, 54, 1-9.
- (3) U.S. Food and Drug Administration *Chirality* **1992**, *4*, 338-340.
- (4) Ikai, T.; Okamoto, Y. Chem. Rev. 2009, 109, 6077-6101.
- (5) Tian, Q.; Lv, C. G.; Wang, P.; Ren, L. P.; Qiu, J.; Li, L.; Zhou, Z. Q. *J. Sep. Sci.* **2007**, *30*, 310-321.
- (6) Williams, A. Pestic. Sci. 1996, 46, 3-9.
- (7) Toyooka, T. *Biomed. Chromatogr.* **1996**, *10*, 265-277.
- (8) Krull, I. S.; Giddings, J. C.; Grushka, E.; Cazes, J.; Brown, P. R.; (Eds.) *Advances in chromatography, Lippincott, Philadelphia* **1977**, *16*, 146.
- (9) Pettersson, C.; Schill, G. J. Liq. Chromatogr. 1986, 9, 269-290.
- (10) Davankov, V. A.; Kurganov, A. A. Chromatographia 1983, 17, 686-690.
- (11) Debowski, J.; Sybilska, D.; Jurczak, J. *J. Chromatogr.* **1982**, *237*, 303-306.
- (12) Sybilska, D.; Zukowski, J.; Bojarski, J. *J. Liq. Chromatogr.* **1986**, *9*, 591-606.
- (13) Pirkle, W. H.; Finn, J. M.; Schreiner, J. L.; Hamper, B. C. *J. Am. Chem. Soc.* **1981**, *103*, 3964-3966.
- (14) Pirkle, W. H.; House, D. W.; Finn, J. M. J. Chromatogr. 1980, 192, 143-158.
- (15) Dalgliesh, C. J. J. Chem. Soc. 1952, 137, 3940.
- (16) Aboul-Enein, H. Y.; Ali, I. Chiral Separations by Liquid Chromatography and Related Technologies, Marcel Dekker, Inc. 2003, 90, 210.
- (17) Hermansson, J. J. Chromatogr. 1983, 269, 71-80.
- (18) Allenmark, S.; Bomgren, B.; Boren, H. *J. Chromatogr.* **1983**, *264*, 63-68.

- (19) Miwa, T.; Ichikawa, M.; Tsuno, M.; Hattori, T.; Miyakawa, T.; Kayano, M.; Miyake, Y. Chem. Pharm. Bull. 1987, 35, 682-686.
- (20) Armstrong, D. W.; Ward, T. J.; Armstrong, R. D.; Beesley, T. E. *Science* **1986**, *232*, 1132-1135.
- (21) Armstrong, D. W.; Demond, W. Journal of Chromatographic Science 1984, 22, 411-415.
- (22) Armstrong, D. W.; Han, Y. I.; Han, S. M. *Anal. Chim. Acta* **1988**, *208*, 275-281.
- (23) Armstrong, D. W.; Ward, T. J.; Armstrong, R. D.; Beesley, T. E. Science 1986, 232, 1132-1135.
- (24) Schurig, V.; Schmaizing, D.; Miihleck, U.; Jung, M.; Schleimer, M.; Mussche, P.; Duvekot, C.; Buyten, J. C. *J. High Resolut. Chromatogr.* **1990**, *13*, 713-717.
- (25) Han, X.; Zhong, Q.; Yue, D.; Della Ca, N.; Larock, R. C.; Armstrong, D. W. *Chromatographia* **2005**, *61*, 205-211.
- (26) Okamoto, Y.; Yashima, E. Angew. Chem. Int. Ed. 1998, 37, 1020-1043.
- (27) Hesse, G.; Hagel, R. Chromatographia 1973, 6, 277-280.
- (28) Okamoto, Y.; Kawashima, M.; Yamamoto, K.; Hatada, K. *Chem. Lett.* **1984**, 739-742.
- (29) Ichida, A.; Shibata, T.; Okamoto, I.; Yuki, Y.; Namikoshi, H.; Toga, Y. *Chromatographia* **1984**, *19*, 280-284.
- (30) Okamoto, Y.; Kawashima, M.; Hatada, K. *J. Am. Chem. Soc.* **1984**, *106*, 5357-5359.
- (31) Okamoto, Y.; Kawashima, M.; Hatada, K. *J. Chromatogr.* **1986**, *363*, 173-186.
- (32) Okamoto, Y.; Aburatani, R.; Fukumoto, T.; Hatada, K. *Chem. Lett.* **1987**, 1857-1860.
- (33) Zhang, T.; Kientzy, C.; Franco, P.; Ohnishi, A.; Kagamihara, Y.; Kurosawa, H. J. Chromatogr. A 2005, 1075, 65-75.
- (34) Ali, I.; Aboul-Enein, H. Y. J. Sep. Sci. 2006, 29, 762-769.

- (35) Chenl, X. M.; Yamamoto, C.; Okamoto, Y. *Pure Appl. Chem.* **2007**, 79, 1561-1573.
- (36) Ikai, T.; Yamamoto, C.; Kamigaito, M.; Okamoto, Y. *Polym. J. (Tokyo, Jpn.)* **2006**, *38*, 91-108.
- (37) Ikai, T.; Yamamoto, C.; Kamigaito, M.; Okamoto, Y. *J. Chromatogr. B* **2008**, *875*, 2-11.
- (38) Okamoto, Y.; Aburatani, R.; Miura, S.; Hatada, K. *J. Liq. Chromatogr.* **1987**, *10*, 1613-1628.
- (39) Giddings, J. C. Dynamics of Chromatography, Part I: Principles and Theory, Dekker, Inc., NY 1965.
- (40) Krug, R. R.; Hunter, W. G.; Grieger, R. A. *J. Phys. Chem.* **1976**, *80*, 2341-2351.
- (41) Krug, R. R.; Hunter, W. G.; Grieger, R. A. *J. Phys. Chem.* **1976**, *80*, 2335-2341.
- (42) Krug, R. R. Ind. Eng. Chem. Fundam. 1980, 19, 50-59.
- (43) Li, J. J.; Carr, P. W. J. Chromatogr. A 1994, 670, 105-116.
- (44) Yao, B. X.; Zhan, F. P.; Yu, G. Y.; Chen, Z. F.; Fan, W. J.; Zeng, X. P.; Zeng, Q. L.; Weng, W. J. Chromatogr. A 2009, 1216, 5429-5435.
- (45) Feitsma, K. G.; Bosman, J.; Drenth, B. F. H.; Dezeeuw, R. A. *J. Chromatogr.* **1985**, 333, 59-68.
- (46) Cabrera, K.; Lubda, D. *J. Chromatogr. A* **1994**, *666*, 433-438.
- (47) Morin, N.; Guillaume, Y. C.; Peyrin, E.; Rouland, J. C. *Anal. Chem.* **1998**, 70, 2819-2826.
- (48) Li, X. P.; McGuffin, V. L. *J. Liq. Chromatogr. Relat. Technol.* **2007**, *30*, 965-985.
- (49) Ringo, M. C.; Evans, C. E. Anal. Chem. 1997, 69, 4964-4971.
- (50) Ringo, M. C.; Evans, C. E. Anal. Chem. 1997, 69, 643-649.
- (51) Ringo, M. C.; Evans, C. E. J. Phys. Chem. B 1997, 101, 5525-5530.

- (52) Smith, R. J.; Taylor, D. R.; Wilkins, S. M. *J. Chromatogr. A* **1995**, 697, 591-596.
- (53) Kusters, E.; Spondlin, C. J. Chromatogr. A 1996, 737, 333-337.
- (54) Sztojkov-Ivanov, A.; Szatmari, I.; Peter, A.; Fulop, F. *J. Sep. Sci.* **2005**, *28*, 2505-2510.
- (55) O'Brien, T.; Crocker, L.; Thompson, R.; Thompson, K.; Toma, P. H.; Conlon, D. A.; Feibush, B.; Moeder, C.; Bicker, G.; Grinberg, N. *Anal. Chem.* **1997**, *69*, 1999-2007.
- (56) Wang, F.; O'Brien, T.; Dowling, T.; Bicker, G.; Wyvratt, J. *J. Chromatogr. A* **2002**, *958*, 69-77.
- (57) Wang, F.; Wenslow, R. M.; Dowling, T. M.; Mueller, K. T.; Santos, I.; Wyvratt, J. M. *Anal. Chem.* **2003**, *75*, 5877-5885.
- (58) Wang, F.; Yeung, D.; Han, J.; Semin, D.; McElvain, J. S.; Cheetham, J. J. Sep. Sci. **2008**, *31*, 604-614.
- (59) Wang, F.; Han, J.; Yeung, D.; Semin, D.; Cheetham, J. J. Sep. Sci. 2008, 31, 1027-1033.
- (60) Kazusaki, M., Ohgami, Y. Chromatography 2007, 28, 125-130.

CHAPTER 2

COMPARISON OF DERIVATIZED β -CYCLODEXTRIN STATIONARY PHASES 2.1 INTRODUCTION

Numerous articles have been published on the use of cyclodextrins (CDs) in chiral separations¹⁻³ and pharmaceutical applications.⁴ In chiral separations, cyclodextrins represent the most common and successful class of chiral selectors for separation of racemates by gas chromatography (GC), liquid chromatography (LC), and supercritical fluid chromatography (SFC). In pharmaceutical applications, cyclodextrins can enhance the solubility, stability, and bioavailability of drug molecules. Their potential as drug carriers stems from their well-defined structure, size of their cavities, ease of chemical modification, low toxicity, pharmacological activity, and protection of guest molecules from biodegradation.⁵

β-Cyclodextrin, the most common cyclodextrin, has been widely used as a chiral selector for separating several classes of racemic drugs in pharmaceutical research and development. It is inherently chiral, with each glucose unit containing five chiral centers. It has a truncated conical cavity with 14 secondary 2- and 3-OH groups at the wider end of the cavity and 7 primary 6-OH groups at the narrow end (Figure 1.1). The secondary hydroxyl groups are held relatively rigid, while the primary hydroxyl groups can rotate freely and may partially block the narrow end of the cavity.⁶

The chiral recognition mechanism of cyclodextrins in the reversed-phase mode is considered to be the formation of an inclusion complex. 1,2,7,8 However,

in the normal-phase and polar-organic modes, the mechanism is due mainly to interaction with the hydroxyl groups that line the exterior surface of the CD cavity. 9,10

One of the most important developments in β-cyclodextrin stationary phases is their derivatization, which expanded the scope of their application as The OH functional groups can be derivatized by different chiral selectors. reagents and many such phases have been reported in the literature. These β-CD.¹¹ hydroxyalkylated include methylated (hydroxyethylated and hydroxypropylated) β-CD.¹² acetylated β-CD.¹³ and sulphated β-CD.^{14,15} Unlike the native β-CDs, the modes of interaction in derivatized cyclodextrins may not require the formation of an inclusion complex.^{9,16} Armstrong et al.⁹ have synthesized β-CDs based on naphthylethyl carbamates, 2,6-dimethylphenyl carbamates, and acetyl esters. The average degree of substitution with these derivatives is found to be 6, 10, and 19, respectively, of the 21 available OH groups. This suggests that the size of the derivatizing agent affects the degree of substitution. Higher degree of substitution is usually found to correlate with decreased enantioselectivity. 17,18

β-Cyclodextrin phases with π -electron donating (π -basic) and π -electron deficient (π -acidic) derivatizing agents have gained greater interest in chiral separation. These include π -basic groups such as naphthylethyl and tris-3,5-dimethylphenyl carbamates (DMPC), and π -acidic groups such as 2,6-dinitro-4-trifluoromethyl phenyl ether (DNP). As opposed to the native β -CD, these π -basic and π -acidic groups introduce new sites for π - π and dipole-dipole

interactions. Chiral solutes with π -basic functional groups are likely to be separated by β -CDs derivatized with π -acidic groups, and vice versa.²⁰

In this chapter, the separation of coumarin-based anticoagulants on β -CD derivatized with DMPC and DNP will be compared with native β -CD. This comparison will help to investigate the thermodynamics (retention and selectivity) of the two stationary phases and understand their mechanistic differences using the probe compounds.

2.2. EXPERIMENTAL METHODS

2.2.1. Chemicals

Coumarin-based anticoagulants, consisting of warfarin, coumachlor, coumafuryl, coumatetralyl, and 4-hydroxycoumarin, are used as solutes in this study. With the exception of 4-hydroxycoumarin, all model solutes are chiral. The structures are shown in Figure 2.1. The solutes are obtained from Sigma-Aldrich as solids and are dissolved in high-purity acetonitrile (Burdick and Jackson, Honeywell) to yield standard solutions at 10⁻³ M concentration. For mobile phase preparation, deionized water, methanol (Burdick & Jackson, Honeywell), iso-propanol (HPLC grade, Sigma-Aldrich), and hexane (Burdick & Jackson, Honeywell) are used as modifiers, while acetic acid (Sigma-Aldrich) and triethylamine (Sigma-Aldrich) are used as additives.

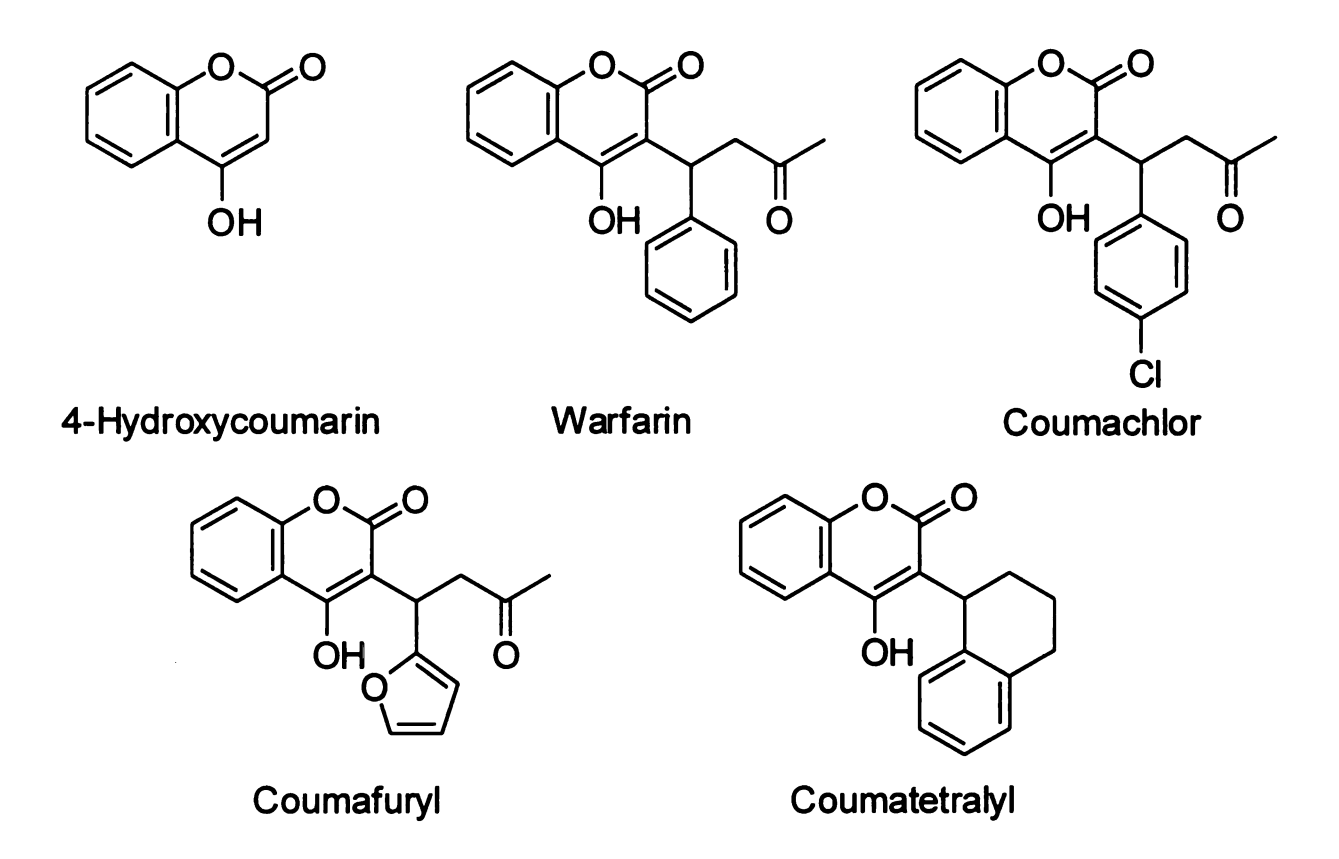


Figure 2.1. The structures of coumarin anticoagulants.

2.2.2. Column preparation and packing

For this study, liquid chromatography is employed with an optically transparent fused-silica capillary column (200- μ m i.d., 100 cm length, Polymicro Technologies). The silica packing is characterized by a 5- μ m particle size that is immobilized with native β -CD (Cyclobond I 2000, Astec), tris-(3,5-dimethylphenyl carbamate) β -CD (Cyclobond I 2000 DMP, Astec), and 2,6-dinitro-4-trifluoromethylphenyl ether β -CD (Cyclobond I 2000 DNP, Astec). Before the column is packed, the polyimide coating is removed to create a detection window (at 90, 90, and 74 cm, respectively) and the outlet is terminated with a quartz wool frit. The slurry method is used to pack each of the stationary phases. This method involves selection of a solvent that will result in slow settling and minimal aggregation of the stationary phase particles. Methanol, acetonitrile, acetone, ethyl acetate, tetrahydrofuran, and hexane are tested for this purpose. Among these solvents, methanol is found to be the most appropriate.

2.2.3. Chromatographic system

For this study, capillary liquid chromatography is used. The mobile phase is delivered by a single-piston reciprocating pump (Model 114M, Beckman Instruments), operated in the constant-pressure mode at 1100 psi. After injection (Model EC14W1, Valco Instruments), the samples are split between the column and a fused-silica capillary (50-μm i.d., Polymicro Technologies) to prevent excessive broadening and overload of the stationary phase. The injection volume is about 16 nL (split ratio 1:60).

Laser-induced fluorescence is used for on-column detection. A helium-cadmium laser (Model 3074-20M, Melles Griot) provides excitation at 325 nm. The fluorescence emission is isolated by a liquid filter (1% aqueous NaNO₃) and two interference filters (420 nm, S10-410-F, Corion), and is detected by a photomultiplier tube (Centronic Model Q4249BA, Bailey Instruments). The resulting photocurrent is amplified, converted to the digital domain (Model PCIMIO-16XE-50, National Instruments), and stored by a user-defined program (Labview v5.1, National Instruments). The instrumental system is shown in Figure 2.2. A conventional fluorescence spectrometer (Model F-4500, Hitachi) is used to record the fluorescence of warfarin in hexane that contains *i*-propanol modifier.

2.2.4. Data analysis

For each solute zone, the retention time of the solutes is taken from the center of the chromatographic peak. The retention factor (k) is then calculated as

$$k = \frac{t_r - t_0}{t_0} \tag{3}$$

where t_r and t_0 are the mean elution times of a retained and non-retained solute, respectively. The chiral selectivity (α) is calculated as

$$\alpha = \frac{k_2}{k_1} \tag{4}$$

where k_1 and k_2 are the retention factors for the first- and second-eluted enantiomers, respectively.

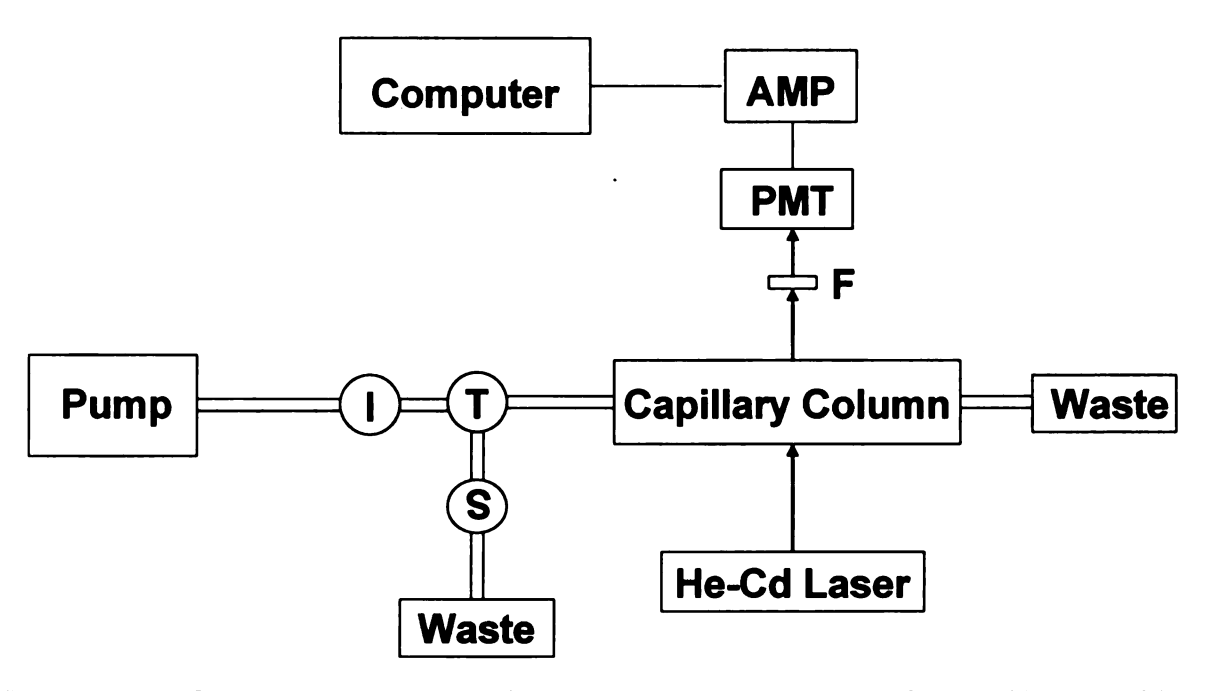


Figure 2.2. Schematic diagram of the experimental system for capillary liquid chromatography with on-column laser-induced fluorescence detection. I: injection valve, T: splitting tee, S: splitting capillary, F: filter, PMT: photomultiplier tube, AMP: current to voltage amplifier.

2.3. RESULTS AND DISCUSSIONS

2.3.1. Effect of mobile phase composition

The effect of mobile phase composition on the separation of coumarins using derivatized β -cyclodextrin stationary phases is investigated in the polar-organic, reversed-phase, and normal-phase modes. In the polar-organic and reversed-phase modes, acetic acid and triethylamine are also used as mobile phase additives.

2.3.1.1. DMPC-CD stationary phase

The separation of coumarins in DMPC-CD is investigated using the polar-organic mode and is shown in Figure 2.3. In the polar-organic mode, warfarin, coumafuryl, coumachlor, and coumatetralyl are found to have no chiral recognition. However, literature reports indicate that these solutes are resolved in the native β -CD stationary phase in the polar-organic mode. The fact that there is no chiral selectivity in this phase suggests that the chiral recognition mechanism in the derivatized β -CD phase is different from that in the native cyclodextrin. The tris-(3,5-dimethylphenyl carbamate) functional group of the chiral selector is a π -electron donor (π -basic) in its properties. The coumarin solutes may also be regarded as π -basic in their properties. Hence, weak π - π interactions between the solute and selector are expected. In the derivatized stationary phase, some of the OH selective sites are blocked and the solutes may have limited access to the cavity.

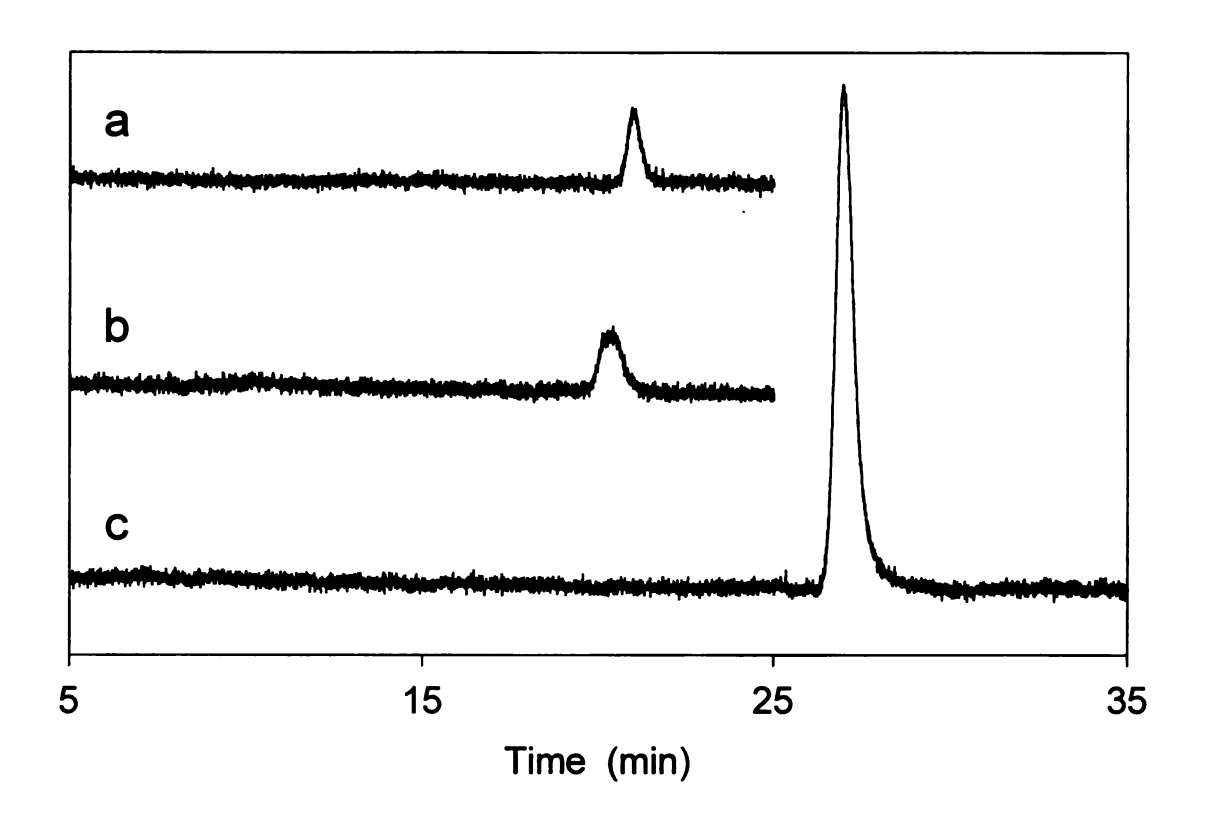


Figure 2.3. Separation of a) warfarin, b) coumachlor, and c) coumatetralyl enantiomers in DMPC-CD stationary phase. Mobile phase contains acetonitrile with 1 % methanol, 0.1 % acetic acid, and 0.4 % triethylamine.

The separation of coumarins is also investigated in the reversed-phase and normal-phase modes. In the reversed phase, 5 – 60 % water is used in acetonitrile mobile phase and has a detrimental effect on the resolution of these solutes. In the normal phase, hexane serves as the bulk component with *i*-propanol as a modifier. However, no elution peaks are observed for any solute. To investigate whether the lack of response is due to a detection problem, the fluorescence of warfarin in hexane with *i*-propanol modifier is recorded. The resulting emission spectrum is found to have a maximum at 360 nm as compared to the peak maximum at 405 nm in acetonitrile. To address this problem, a low-pass optical filter with wavelength of 380 nm is substituted in the laser-induced fluorescence detector. However, peaks are still not observed. When an open column is used with a UV-detector, warfarin peak is observed at wavelengths ranging from 210 to 225 nm. This suggests that a lower excitation wavelength should be used instead of the 325 nm of the helium-cadmium laser.

2.3.1.2. DNP-CD stationary phase

The separation of coumarins in DNP-CD using the polar-organic mode is shown in Figure 2.4. For warfarin and coumafuryl, relatively modest chiral resolution is observed, but for coumachlor, the chiral resolution is quite low. However, none of the solutes show baseline separation in this stationary and mobile phase. The dinitro and trifluoromethyl functional groups in the DNP derivatizing agent can withdraw electron density from the phenyl ring through

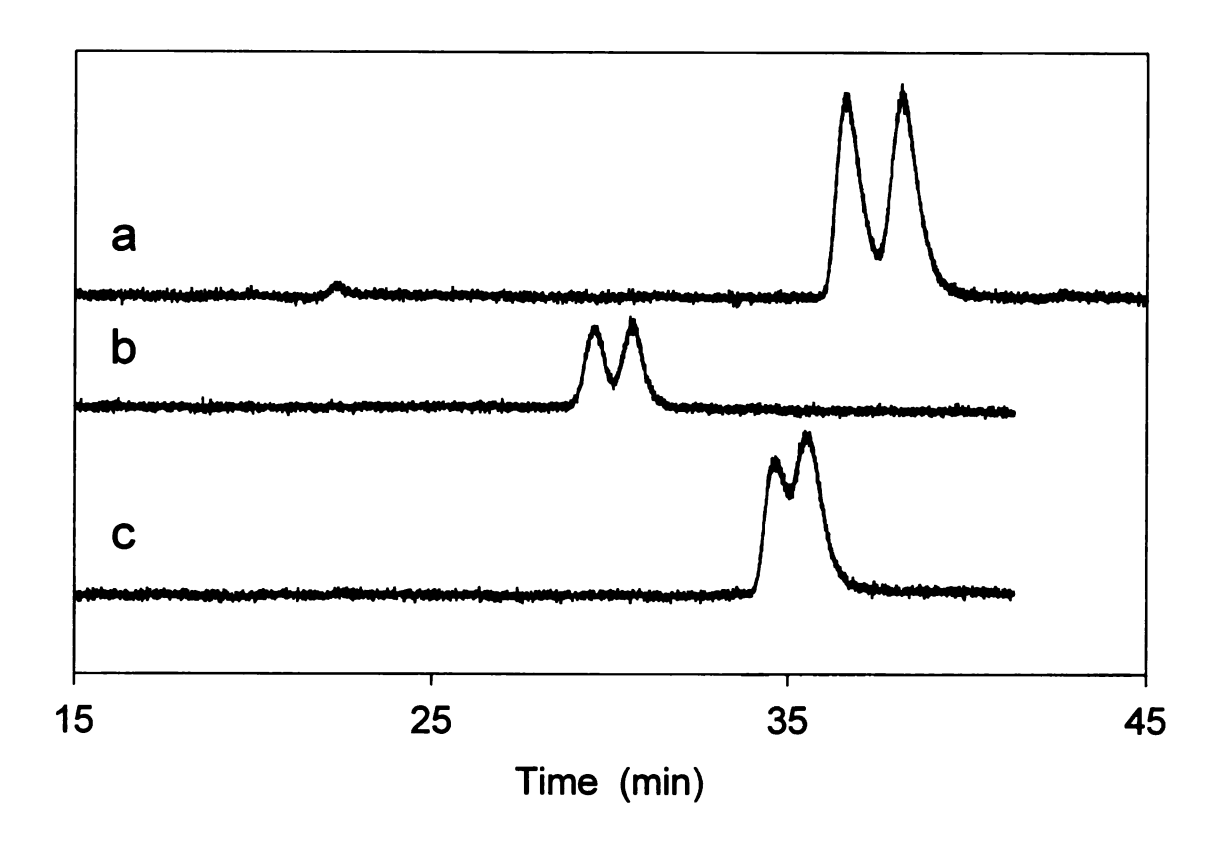


Figure 2.4. The separation of a) warfarin, b) coumafuryl, and c) coumachlor in DNP-CD using acetonitrile mobile phase. Mobile phase also contains 0.1 % acetic acid and 0.2 % triethylamine.

electron resonance as well as inductive effects. As a result, they are π -acidic in their properties. These π -acidic groups of the chiral selector may have stronger π - π interactions with the π -basic coumarins than the π -basic DMPC groups. Despite these additional interactions, together with the possible hydrogen bonding, dipole-dipole, and van der Waals forces, baseline chiral separation of these solutes is not achieved.

The effect of acetic acid and triethylamine additives is investigated by systematically varying their concentration using acetonitrile as the bulk mobile phase and warfarin as a probe (Table 2.1). In general, as the concentration of acetic acid increases, the retention factor of the warfarin enantiomers decreases. Doubling the acetic acid concentration causes a decrease in the retention factor of warfarin enantiomers by about 13 % and 14 % for the first- and second-eluted enantiomers, respectively. However, an increase in acetic acid concentration does not change the chiral selectivity of the separation, suggesting that the acid has no effect on the chiral selective sites. Similarly, an increase in triethylamine concentration causes a decrease in the retention factor of the solutes without causing substantial changes in the selectivity. Doubling the concentration of triethylamine causes a decrease in the retention factor of warfarin by about 27 % for both enantiomers. These results suggest that both the acid and amine are acting as displacing agents. The effect of acetic acid and triethylamine on chiral separation of warfarin are discussed in detail in Section 3.3.1.

Table 2.1. Effect of acetic acid and triethylamine additives on the retention (k) and chiral selectivity (α) of warfarin using DNP-CD.

Parameter	Acetic acid (%) ^b			Triethylamine (%) ^c		
	0.15	0.2	0.3	0.2	0.3	0.4
k ₁ ^a	2.34	2.26	2.04	1.78	1.51	1.29
k ₂ ^a	2.48	2.38	2.13	1.90	1.60	1.39
α	1.06	1.05	1.05	1.06	1.06	1.08

^aRetention factor for the first (1) and the second (2) eluted enantiomers.

^bTriethylmine concentration at 0.1 %.

^cAcetic acid concentration at 0.1 %.

The effect of modifiers on the separation of coumarins in the DNP-CD stationary phase is investigated using methanol and water. The separation of warfarin in the presence of different concentrations of methanol is shown in Figure 2.5. An increase in the concentration of methanol has a detrimental effect on the chiral selectivity of warfarin enantiomers. This suggests that hydrogen bonding is important in the chiral recognition process. The retention time of warfarin also decreases with an increase in methanol concentration, suggesting that it competes for hydrogen bonding sites in the stationary phase and thereby acts as a displacing agent. The use of water as a mobile phase modifier also has a detrimental effect on the separation probably due to strong hydrogen bonding with the residual hydroxyl groups. Water also shows a memory effect i.e., solutes are less retained after the column is exposed to water due to strong hydrogen bonding interactions with the hydroxyl groups of the stationary phase.

2.2.1.3. COMPARISON OF NATIVE, DMPC- AND DNP-CD PHASES

To compare the chiral discriminating abilities of the native and derivatized β -CD stationary phases in the polar-organic mode, warfarin is used as a probe solute (Figure 2.6). As can be seen from the chromatogram, excellent chiral resolution of warfarin is obtained in the native cyclodextrin, while modest resolution is obtained in the DNP-cylodextrin. In contrast, no chiral resolution is observed in the DMPC-CD stationary phase.

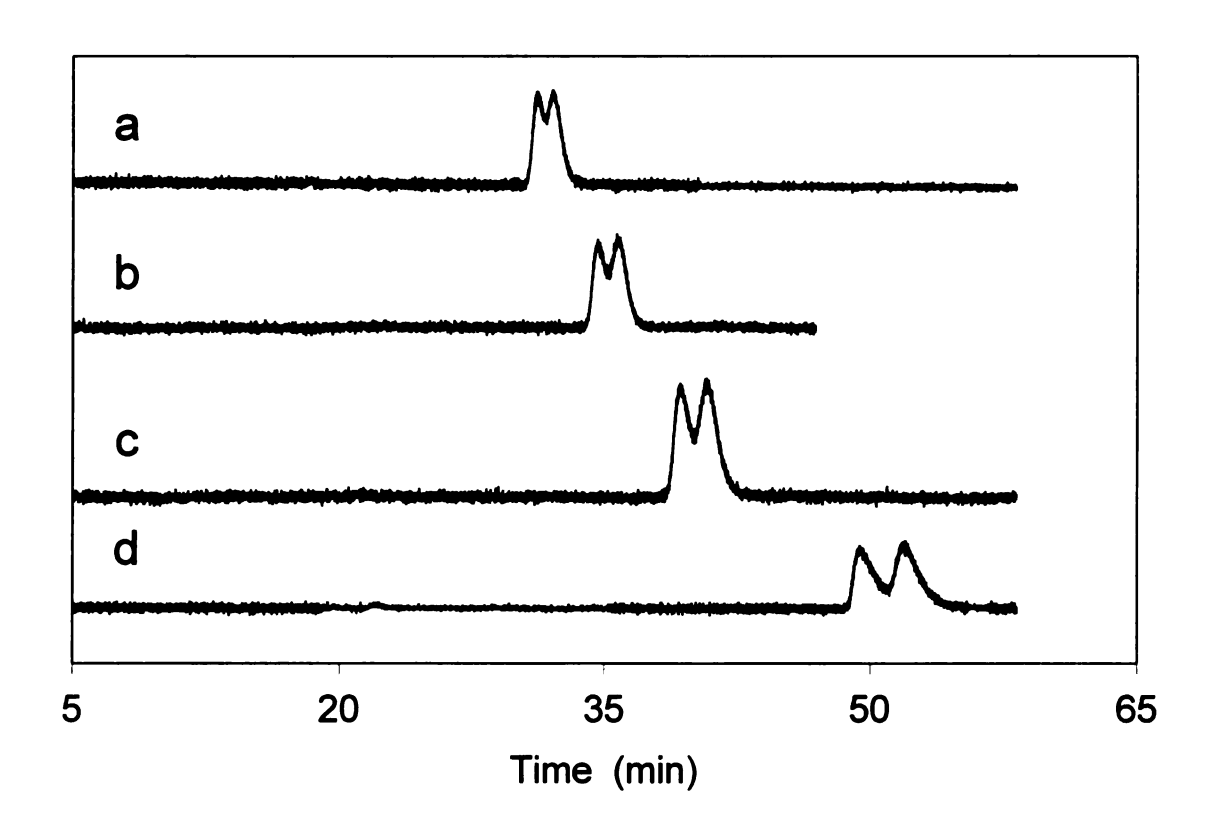


Figure 2.5. Effect of methanol concentration a) 5 %, b) 3 %, c) 1 %, and d) 0 % on the separation of warfarin enantiomers in DNP-CD. Mobile phase also contains acetonitrile with 0.1 % acetic acid and triethylamine.

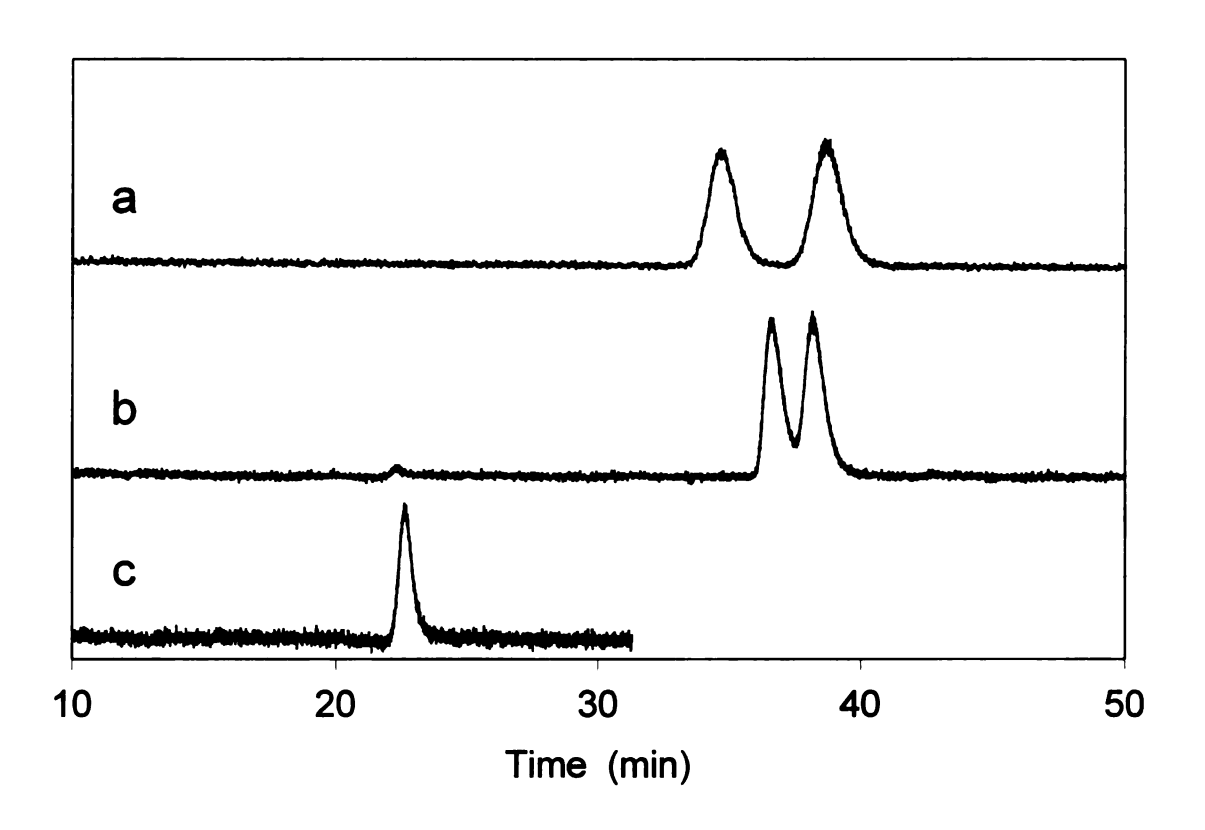


Figure 2.6. Separation of warfarin enantiomers in a) native β -CD, b) DNP-CD, and c) DMPC-CD. Mobile phase contains acetonitrile with 0.1 % acetic acid and 0.2 % triethylamine

Table 2.2 summarizes the retention and selectivity of the three stationary phases. The retention factor for the first-eluted enantiomer of warfarin is 37 % higher in the DNP-CD than that for the native β -CD stationary phase, but virtually non-retained in the DMPC-CD. This suggests that the achiral interactions are stronger for DNP-CD than for native and DMPC-CD. The chiral selectivity of warfarin is excellent in the native β -CD (α = 1.20) and modest in DNP-CD (α = 1.07), but non-existent in DMPC-CD (α = 1.00). This indicates that the chiral selective interactions are stronger for the native β -CD than that for DMPC- and DNP-CD stationary phases. These observations suggest that the resolution of coumarins on these stationary phases requires strong hydrogen bonding and inclusion interactions.

2.4. CONCLUSIONS

The DMPC-CD stationary phase, which is π -basic in its properties, has little retention and no chiral recognition for all coumarins using the polar-organic and reversed-phase modes. In contrast, the DNP-CD stationary phase, which is π -acidic in its properties, has modest chiral recognition for warfarin and coumafuryl in the polar-organic mode. These results suggest that the chiral discrimination mechanism in the derivatized β -CD phases is different from that for the native β -CD phase. It seems that derivatization has a negative effect on the chiral recognition of these solutes. The derivatizing groups can potentially block the chiral selective sites and/or the cavity of the CD from having inclusion

Table 2.2. Comparison of retention factor (k) and selectivity (α) of warfarin in native and derivatized cyclodextrins.

Parameter	Native CD	DNP-CD	DMPC-CD
k ₁ ^a	1.30	1.78	0.58
k ₂ ^a	1.57	1.90	0.58
α	1.20	1.07	1.00

^aRetention factor for the first (1) and the second (2) enantiomers.

interactions. Consequently, the native CD is more useful than the derivitized ones and no detailed thermodynamic and kinetic study is required.

interactions. Consequently, the native CD is more useful than the derivitized ones and no detailed thermodynamic and kinetic study is required.

2.5. REFERENCES

- (1) Armstrong, D. W.; Ward, T. J.; Armstrong, R. D.; Beesley, T. E. *Science* **1986**, 232, 1132-1135.
- (2) Armstrong, D. W.; Demond, W. J. Chromatogr. Sci. 1984, 22, 411-415.
- (3) Chang, S. C.; Reid, I. G.; Chen, S.; Chang, C. D.; Armstrong, D. W. *Trends Anal. Chem.* **1993**, *12*, 144-153.
- (4) Szejtli, J. Chem. Rev. 1998, 98, 1743-1753.
- (5) Uekama, K.; Hirayama, F.; Irie, T. Chem. Rev. 1998, 98, 2045-2076.
- (6) Crini, G.; Morcellet, M. J. Sep. Sci. 2002, 25, 789-813.
- (7) Armstrong, D. W.; Ward, T. J.; Czech, A.; Czech, B. P.; Bartsch, R. A. *J. Org. Chem.* **1985**, *50*, 5556-5559.
- (8) Armstrong, D. W.; Demond, W.; Czech, B. P. *Anal. Chem.* **1985**, *57*, 481-484.
- (9) Armstrong, D. W.; Stalcup, A. M.; Hilton, M. L.; Duncan, J. D.; Faulkner, J. R.; Chang, S. C. *Anal. Chem.* **1990**, *62*, 1610-1615.
- (10) Stalcup, A. M.; Chang, S. C.; Armstrong, D. W. *J. Chromatogr.* **1991**, *540*, 113-128.
- (11) Casu, B.; Reggiani, M.; Sanderson, G. R. *Carbohydr. Res.* **1979**, *76*, 59-66.
- (12) Szente, L.; Szejtli, J. Adv. Drug Delivery Rev. 1999, 36, 17-28.
- (13) Casu, B.; Reggiani, M.; Gallo, G. G.; Vigevani, A. *Carbohydr. Res.* **1970**, *12*, 157-170.
- (14) Wu, W. H.; Stalcup, A. M. J. Liq. Chromatogr. 1995, 18, 1289-1315.
- (15) Stalcup, A. M.; Gahm, K. H. Anal. Chem. 1996, 68, 1369-1374.
- (16) Zhong, Q. Q.; He, L. F.; Beesley, T. E.; Trahanovsky, W. S.; Sun, P.; Wang, C. L.; Armstrong, D. W. *J. Chromatogr. A* **2006**, *1115*, 19-45.
- (17) Hargitai, T.; Kaida, Y.; Okamoto, Y. *J. Chromatogr.* **1993**, *628*, 11-22.

- (18) Zhong, Q. Q.; He, L. F.; Beesley, T. E.; Trahanovsky, W. S.; Sun, P.; Wang, C. L.; Armstrong, D. W. *J. Chromatogr. A* **2006**, *1115*, 19-45.
- (19) Zhong, Q.; He, L.; Beesley, T. E.; Trahanovsky, W. S.; Sun, P.; Wang, C.; Armstrong, D. W. *Chromatographia* **2006**, *64*, 147-155.
- (20) Ilisz, I.; Berkecz, R.; Forro, E.; Fulop, F.; Armstrong, D. W.; Peter, A. *Chirality* **2009**, *21*, 339-348.
- (21) Gluckman, J. C.; Hirose, A.; McGuffin, V. L.; Novotny, M. *Chromatographia* **1983**, *17*, 303-309.
- (22) Li, X. P.; McGuffin, V. L. *J. Liq. Chromatogr. & Relat. Technol.* **2007**, *30*, 937-964.

CHAPTER 3

COMPARISON OF DERIVATIZED POLYSACCHARIDE PHASES FOR SEPARATION OF WARFARIN AND RELATED DRUGS

3.1. INTRODUCTION

Successful resolution of racemates depends on the proper selection of chiral stationary phases and mobile phases. Polysaccharide-based stationary phases, such as derivatized amylose and cellulose, are particularly versatile and durable chiral stationary phases. 1-8 Okamoto et al. 4,6,9 developed several phenylcarbamate derivatives of amylose and cellulose, physically coated on a silica gel matrix. Among these phases, the 3,5-dimethylphenylcarbamate (DMPC) derivatives of amylose and cellulose, commercially available as Chiralpak AD and Chiralcel OD, respectively, are the most successful for separating a wide variety of racemic compounds. 4,9,10 However, these coated forms can only be used with mobile phases such as acetonitrile, alcohols, and their mixtures in alkanes. More recently, immobilized forms of these stationary phases, known as Chiralpak IA and Chiralpak IB respectively, became commercially available. The immobilized phases are compatible with a wide range of solvents, including chlorinated hydrocarbons, acetone, tetrahydrofuran, and ethyl acetate. 11-13

Mobile phase composition likely governs solute retention and selectivity by modifying the shape, crystallinity, and size of the chiral cavities of the stationary phases. Wenslow and Wang 14,15 used 1H/13C cross polarization and magic angle spinning (CPMAS) solid-state NMR to study the structural differences in

Chiralpak AD caused by different alcohol modifiers in hexane-based mobile phases. The authors proposed that the alcohols are incorporated into the chiral stationary phase and form polymer–alcohol complexes that are more ordered than the polymer–hexane complexes. Concomitantly, the steric environment of the chiral cavities is affected due to differences in the degree of twisting of glucose units in the helical structure. Kasat et al. 16 also studied the polymer–solvent interactions in Chiralpak AD with alcohols, acetonitrile, and hexane by using NMR, infrared spectroscopy, and X-ray diffraction. The authors concluded that the change in polymer crystallinity is solvent dependent and is more pronounced in alcohols and less in hexane.

The polysaccharide stationary phases are most commonly used with normal-phase eluents, such as hexane/alcohol mixtures, and reversed-phase eluents, such as water/acetonitrile or water/alcohol. More recently polar-organic eluents, which are mainly used for cyclodextrin stationary phases, have become more widely used. The polar-organic eluents, which Armstrong et al. Introduced, contain pure acetonitrile, methanol, ethanol, propanol, or their mixtures. The high solubility of polar analytes combined with the relative simplicity for solvent removal accounts for the popularity of polar-organic eluents in preparative-scale separations.

The effect of mobile phase modifiers has been studied on both DMPC-amylose and DMPC-cellulose stationary phases. 18,20-24 Most of these studies indicate that these stationary phases are complementary in their properties. Despite the numerous research articles on polysaccharide phases, molecular-

level understanding of their chiral recognition mechanism has not been elucidated. One way of understanding the chiral recognition mechanism in these phases is to investigate the effects of mobile phase modifiers on the retention, selectivity, and kinetics of the separation. The aim of this work is, therefore, to compare DMPC-amylose and DMPC-cellulose in the polar-organic mode in an effort to understand the chiral recognition mechanism in these phases.

3.2. EXPERIMENTAL

3.2.1. Chemicals

Coumarin-based anticoagulants, consisting of warfarin, coumachlor, coumafuryl, coumatetralyl, and 4-hydroxycoumarin, are used as solutes in this study. With the exception of 4-hydroxycoumarin, all model solutes are chiral. The structures are shown in Figure 2.1. The solutes are obtained from Sigma-Aldrich as solids and are dissolved in high-purity acetonitrile (Burdick and Jackson, Honeywell) to yield standard solutions at 10⁻³ M concentration. Mobile phase is prepared using bulk acetonitrile with some modifiers and additives. Methanol, acetone (Burdick and Jackson, Honeywell), and tetrahydrofuran (Jade Scientific) are used as organic modifiers, while acetic acid and triethylamine (Sigma-Aldrich) are used as additives.

3.2.2. Instrumental system

For this study, liquid chromatography is employed with an optically transparent fused-silica capillary column (200-μm i.d., 110 cm length, Polymicro

Technologies). The silica packing is characterized by a 5- μ m particle size that is immobilized with tris-(3,5-dimethylphenyl carbamates) of amylose and cellulose (Chiralpak IA and Chiralpak IB, respectively, Chiral Technologies). Before the column is packed, the polyimide coating is removed to create a detection window (~86 cm from inlet) and the outlet is terminated with a quartz wool frit. The slurry method is used to pack each of the stationary phases. This method involves selection of a solvent that will result in slow settling and minimal aggregation of the stationary phase particles. Methanol, acetonitrile, acetone, ethyl acetate, tetrahydrofuran, and hexane are tested for this purpose. Among these solvents, methanol meets the above criteria most appropriately. The resulting DMPC-amylose and DMPC-cellulose columns have plate heights of 23 μ m and 25 μ m, respectively, determined with a neutral solute (pyrene).

The mobile phase is delivered by a single-piston reciprocating pump (Model 114M, Beckman Instruments), operated in the constant-pressure mode. After injection (Model EC14W1, Valco Instruments), the samples are split between the column and a fused-silica capillary (50-µm i.d., Polymicro Technologies) to prevent excessive broadening and overload of the stationary phase. The injection volume is about 16 nL (split ratio 1: 60).

Laser-induced fluorescence is used for on-column detection. A helium-cadmium laser (Model 3074-20M, Melles Griot) provides excitation at 325 nm. The fluorescence emission is isolated by a liquid filter (1% aqueous NaNO₃) and two interference filters (420 nm, S10-410-F, Corion), and is detected by a photomultiplier tube (Centronic Model Q4249BA, Bailey Instruments). The

resulting photocurrent is amplified, converted to the digital domain (Model PCIMIO-16XE-50, National Instruments), and stored by a user-defined program (Labview v5.1, National Instruments). The instrumental system is shown in Figure 2.2. A conventional fluorescence spectrometer (Model F-4500, Hitachi) is used to record the fluorescence of warfarin in acetonitrile that contains acetic acid and triethylamine additives.

3.2.3. Data analysis

In this study, zone profiles from each solute are analyzed by regression to an exponentially modified Gaussian (EMG) function by using a commercially available program (Peakfit, v4.14, SYSTAT Software). The EMG equation is the convolution of Gaussian and exponential functions, having the following form

$$C(t) = \frac{A}{2\tau} \exp\left(\frac{\sigma^2}{2\tau^2} + \frac{t_g - t}{\tau}\right) \left(1 + \operatorname{erf}\left(\frac{t - t_g}{\sqrt{2}\sigma}\right) - \frac{\sigma}{\sqrt{2}\tau}\right)$$
 (1)

where C(t) is the concentration as a function of time, A is the peak area, t_g is the retention time of the Gaussian component, σ^2 is the variance of the Gaussian component, and τ^2 is the variance of the exponential component. The symmetrical and asymmetrical broadening of the solute zones are represented by σ and τ , respectively. Processes that are fast on the time scale of the separation, such as diffusion and resistance to mass transfer in the mobile and stationary phases, result in symmetrical zone broadening. In contrast, slow kinetics and non-linear isotherms result in asymmetrical broadening. By injecting solutes at low concentrations and in small volumes, non-linear

isotherms can be minimized. Under these conditions, the asymmetrical broadening is dominated by slow kinetics. From the regression parameters of the EMG function, thermodynamic and kinetic quantities can be determined.²⁷ The retention time of the solute is calculated as

$$t_r = t_q + \tau \tag{2}$$

The retention factor (k) is then calculated as

$$k = \frac{t_r - t_0}{t_0} \tag{3}$$

where t_r and t_0 are the elution times of a retained and non-retained solute, respectively. The chiral selectivity (α) is calculated as

$$\alpha = \frac{\mathbf{k_2}}{\mathbf{k_1}} \tag{4}$$

where k_1 and k_2 are the retention factors for the first- and second-eluted enantiomers, respectively. The rate constants for sorption (k_{sm}) and desorption (k_{ms}) of the solute are related to the asymmetric variance by^{26, 28}

$$k_{ms} = \frac{2kt_0}{r^2} \tag{5}$$

$$k_{sm} = kk_{ms} = \frac{2k^2t_0}{\tau^2}$$
 (6)

3.3. RESULTS AND DISCUSSION

The success of chiral chromatographic separations is dependent on the selection of the appropriate stationary phase and mobile phase composition.

This study compares, amylose and cellulose derivatized with 3,5-dimethylphenyl

carbamate (DMPC). The polar-organic mode, which contains acetonitrile as the bulk component, is used as the mobile phase. Modifiers such as methanol (MeOH), acetone, and tetrahydrofuran (THF) and additives such as acetic acid and triethylamine are also used. A series of coumarin-based anticoagulants is chosen as the model solutes (Figure 2.1). These solutes share a common structural backbone, for which 4-hydroxycoumarin will serve as a model to establish achiral contributions. Warfarin is a pharmaceutical drug, while the others are used as pesticides.

3.3.1. Effect of additives

Chiral separation commonly requires the use of mobile phase additives.

Normally, a small amount of achiral acid and/or base is added to the mobile phase to minimize tailing or fronting of chromatographic peaks.^{29,30} These additives can also affect retention and selectivity of many chiral solutes.³¹

The effect of acetic acid and triethylamine on the separation of warfarin on the DMPC-amylose phase is investigated. In the presence of 0.2 % triethylamine, warfarin enantiomers have low retention (Figure 3.1a). In addition, the unresolved peaks show fronting that is characteristic of a non-linear isotherm of BET Type III (adsorbate has greater affinity for itself than for adsorbent).³² In the presence of 0.1 % acetic acid, the peaks have gained some selectivity and better symmetry (Figure 3.1b). The second-eluted enantiomer retains a slightly fronting shape characteristic of the BET Type III isotherm, whereas the

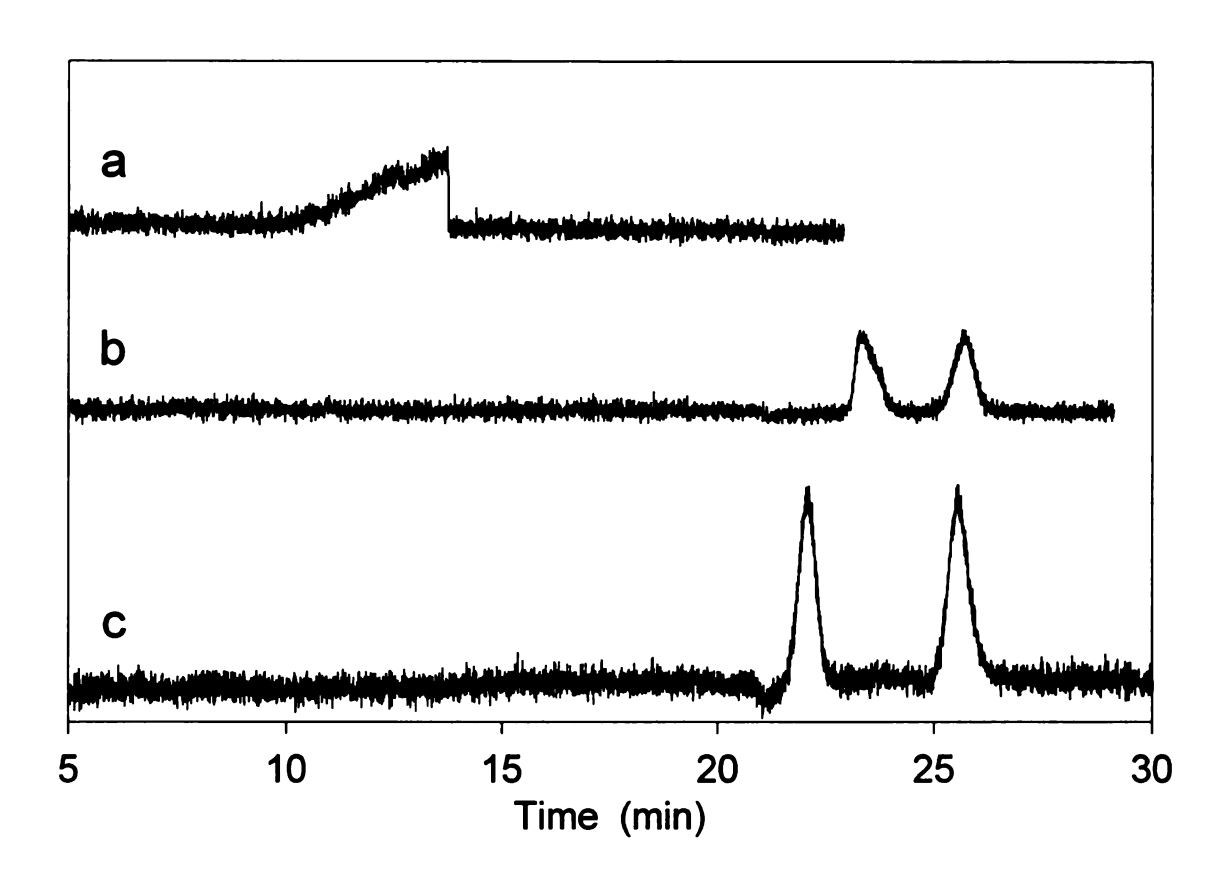


Figure 3.1. Representative chromatograms showing the separation of warfarin enantiomers using DMPC-amylose phase and acetonitrile mobile phase that contains a) 0.2 % triethylamine; b) 0.1 % acetic acid; c) 0.1 % acetic acid and 0.2 % triethylamine.

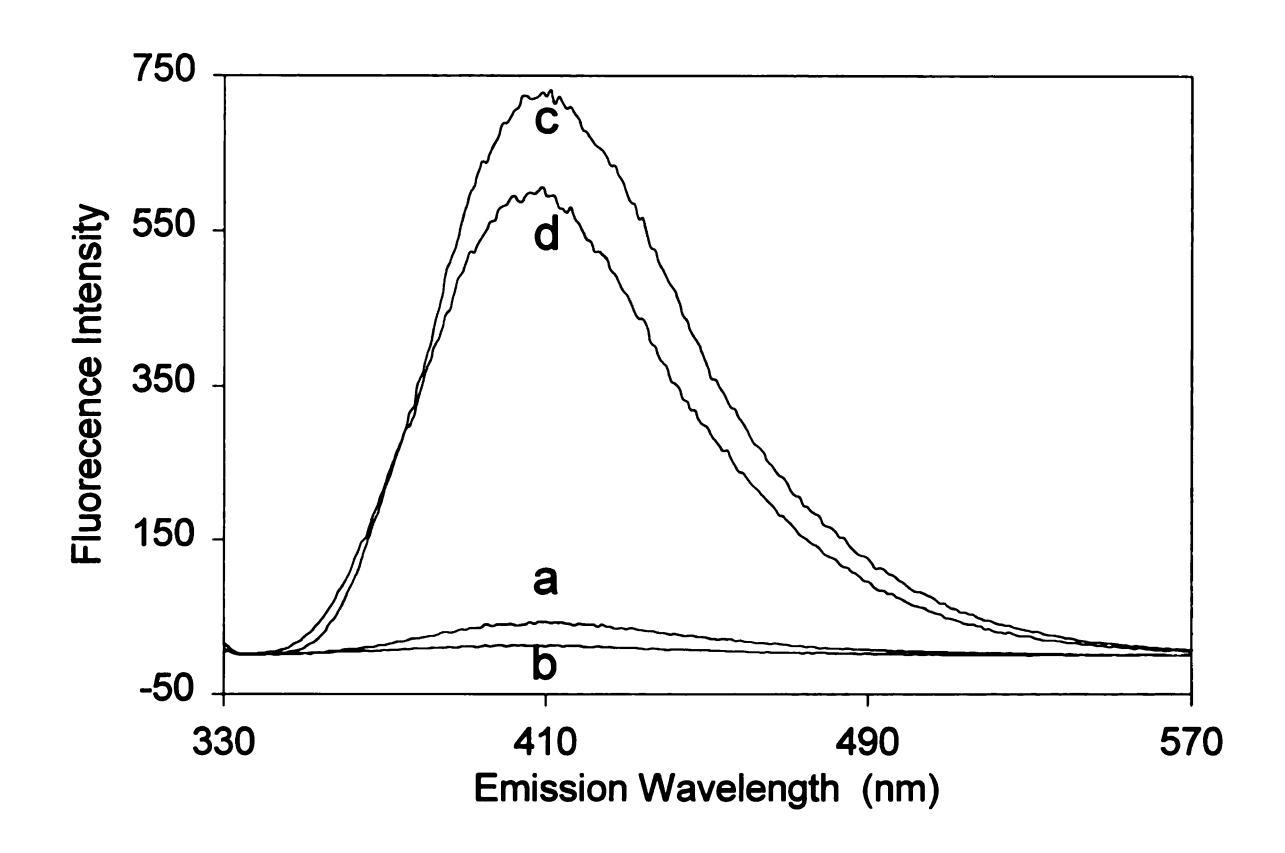


Figure 3.2. Fluorescence spectrum of warfarin (25 μ M) in acetonitrile mobile phase that contains a) no additives; b) 0.1 % acetic acid; c) 0.2 % triethylamine; d) 0.1 % acetic acid and 0.2 % triethylamine.

I isotherm (sites are used up or monolayer adsorption). When both 0.1 % acetic acid and 0.2 % triethylamine are present, the peaks are well resolved and have symmetric shape, as expected for a linear isotherm (Figure 3.1c). This behavior is observed for both the DMPC-amylose and DMPC-cellulose stationary phases.

The effect of acetic acid and triethylamine additives on warfarin is also investigated by using fluorescence spectroscopy. Figure 3.2a shows the fluorescence spectrum of warfarin in bulk acetonitrile (no additives). When 0.1 % acetic acid is added, the fluorescence intensity of warfarin decreases by a factor of 3 (Figure 3.2b). In contrast, the intensity increases by a factor of 17 in the presence of 0.2 % triethylamine (Figure 3.2c). When both 0.1 % acetic acid and 0.2 % triethylamine are present, the fluorescence intensity increases by a factor of 14. These results suggest that acetic acid and triethylamine can interact with warfarin and change its structural form. Warfarin is known to exist in various isomeric forms in solution (Figure 3.3).34-37 Valente et al.33, 34 reported that the isomeric distribution is dependent upon the polarity of the solvent, proton donor/acceptor ability, and pH. In organic solvents, warfarin exists predominantly in two diastereometric cyclic hemiketal structures (cyclic I and II, Figure 3.3). As solvent polarity increases, the tautomeric equilibrium begins to favor the corresponding open-ring forms (open I and II, Figure 3.3). 33-36 In aqueous solutions at physiological pH $(pK_a = 5.1)^{37}$, the dominant structures are the

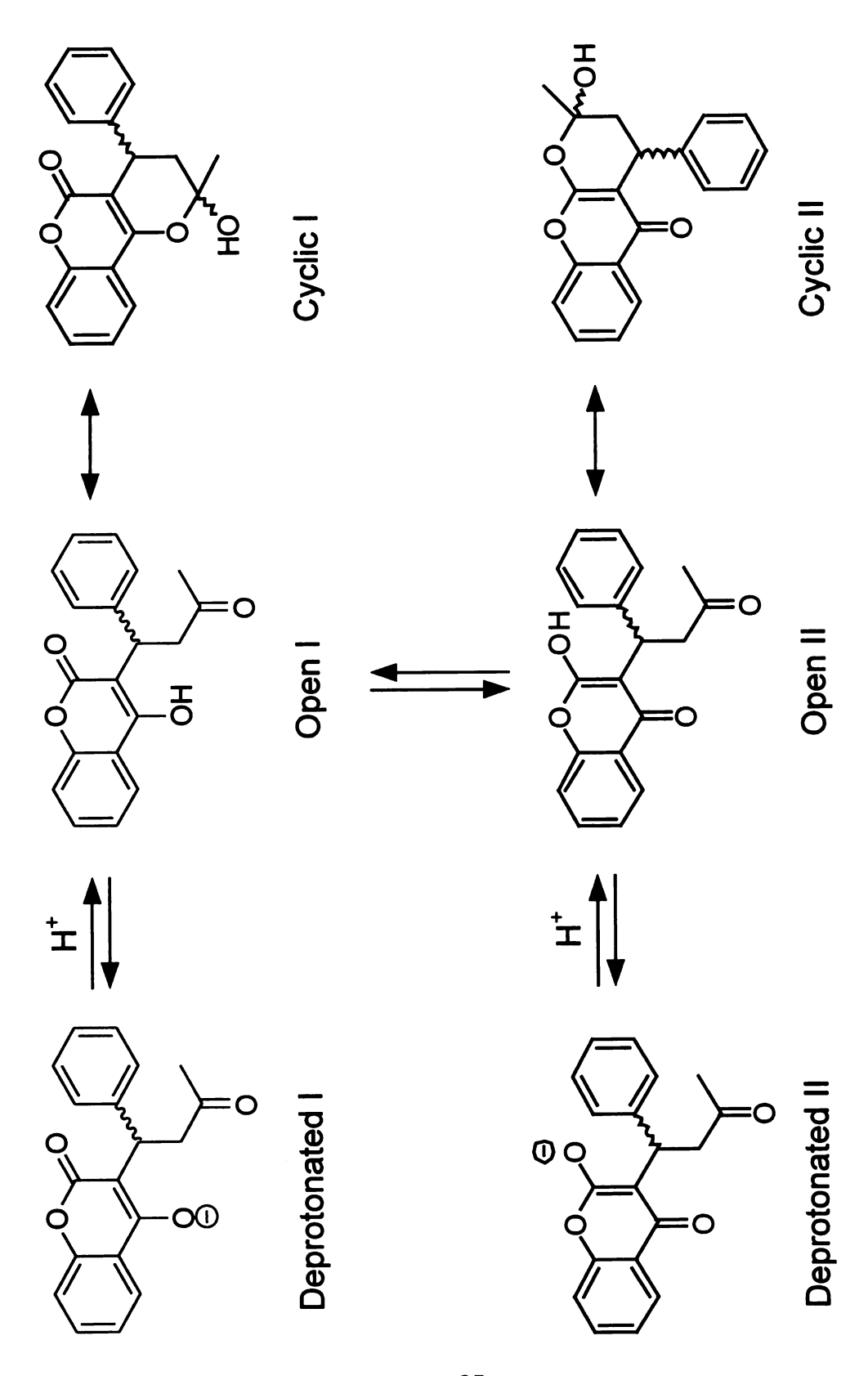


Figure 3.3. Structures of warfarin isomers in cyclic, open, and deprotonated form

resonance stabilized, open-ring anionic forms (deprotonated I and II, Figure 3.3).³⁵ These changes in structure are responsible, in large part, for the observed changes in peak shape and retention with acid/base additives shown in Figure 3.1.

A systematic study is also conducted by using different concentrations (0.1 – 0.5 %) of acetic acid and triethylamine in bulk acetonitrile mobile phase (Table 3.1). This study reveals that an increase in the concentration of acetic acid slightly increases the retention factor of the coumarins. In contrast, an increase in the concentration of triethylamine decreases the retention factor. Triethylamine, a proton acceptor, may compete with warfarin for hydrogen bonding sites on the stationary phase, thereby causing to undergo earlier elution. The chiral selectivity varies only slightly with the concentration of acetic acid and triethylamine, which suggests that these additives affect retention sites that are achiral. Based on the observed trend in selectivity, 0.1 % acetic acid (~0.18 M) and 0.2 % triethylamine (~0.14 M) are chosen for all subsequent studies.

3.3.2. Effect of stationary phase

Amylose is composed of D-glucose units connected with α -1,4 glycosidic bonds, having a helical structure in its native form. In contrast, cellulose is composed of D-glucose units connected with β -1,4 glycosidic bonds, having a more linear structure. Table 3.2 compares the retention factors of the coumarins

Table 3.1. Effect of acetic acid and triethylamine concentration on retention and selectivity of warfarin enantiomers using DMPC-amylose phase. Mobile phase contains acetonitrile. Standard deviations in k and α are \pm 0.01.

Parameter	Percent ratio of acetic acid to triethylamine							
raiametei	0.1 : 0.0	0.1 : 0.2	0.1 : 0.5	0.2 : 0.2	0.4 : 0.2			
k ₁ ^a	1.20	1.08	1.01	1.31	1.44			
k ₂ ^a	1.42	1.40	1.32	1.63	1.74			
α	1.18	1.30	1.31	1.25	1.21			

^aSubscripts denote the first (1) and second (2) eluted enantiomers.

Table 3.2. Comparison of retention and selectivity of coumarins using DMPC-amylose and DMPC-cellulose phases. Mobile phase contains acetonitrile with 0.1 % acetic acid and 0.2 % triethylamine. Standard deviations in k and α are \pm 0.01.

Solute	DM	IPC-Amylo	ose	DMPC-Cellulose			
Solute	k ₁ ^a	k ₂ ^a	α	k ₁	k ₂	α	
Warfarin	1.08	1.40	1.30	0.98	0.98	1.00	
Coumachlor	1.10	1.50	1.36	0.93	1.02	1.09	
Coumafuryl	1.21	1.29	1.07	0.93	0.93	1.00	
Coumatetralyl	3.32	4.82	1.45	1.53	1.82	1.18	
4-Hydroxycoumarin	3.90	N/A ^b	N/A	4.55	N/A	N/A	

^aSubscripts denote the first (1) and second (2) eluted enantiomers.

^bNot applicable (N/A).

on the DMPC-amylose and DMPC-cellulose stationary phases. As can be seen, the coumarins are more retained on DMPC-amylose than on DMPC-cellulose, except for the achiral solute 4-hydroxycoumarin. Okamoto et al. $^{2.5}$ proposed that the chiral recognition mechanism in polysaccharides derivatized with phenylcarbamates involves inclusion (in the helical grooves) together with a combination of weak attractive forces. These forces include hydrogen bonding, dipole-dipole interactions, and π - π interactions. The structures of warfarin, coumachlor, coumafuryl, and coumatetrally may easily be fit into the chiral cavities of the helical DMPC-amylose phase. This may result in better inclusion and lead to stronger interactions among the different functional groups of the solutes and stationary phase. In contrast, the linear structure of the DMPC-cellulose phase may be more suitable for the planar 4-hydroxycoumarin to undergo multiple-site interactions, leading to greater retention.

The effect of stationary phase on chiral selectivity is also compared in Table 3.2. As can be seen from Figure 3.4, the DMPC-amylose phase provides excellent resolution for warfarin, coumachlor, and coumatetralyl, and adequate resolution for coumafuryl. In contrast, DMPC-cellulose provides excellent resolution only for coumatetralyl and adequate resolution for coumachlor (Figure 3.5). Interestingly, warfarin is not resolved in this phase, despite its structural similarity to coumachlor (Figure 2.1). This observation suggests that the chlorine atom attached to the phenyl group plays a significant role in the interaction of each enantiomer with the DMPC-cellulose phase. The chlorine

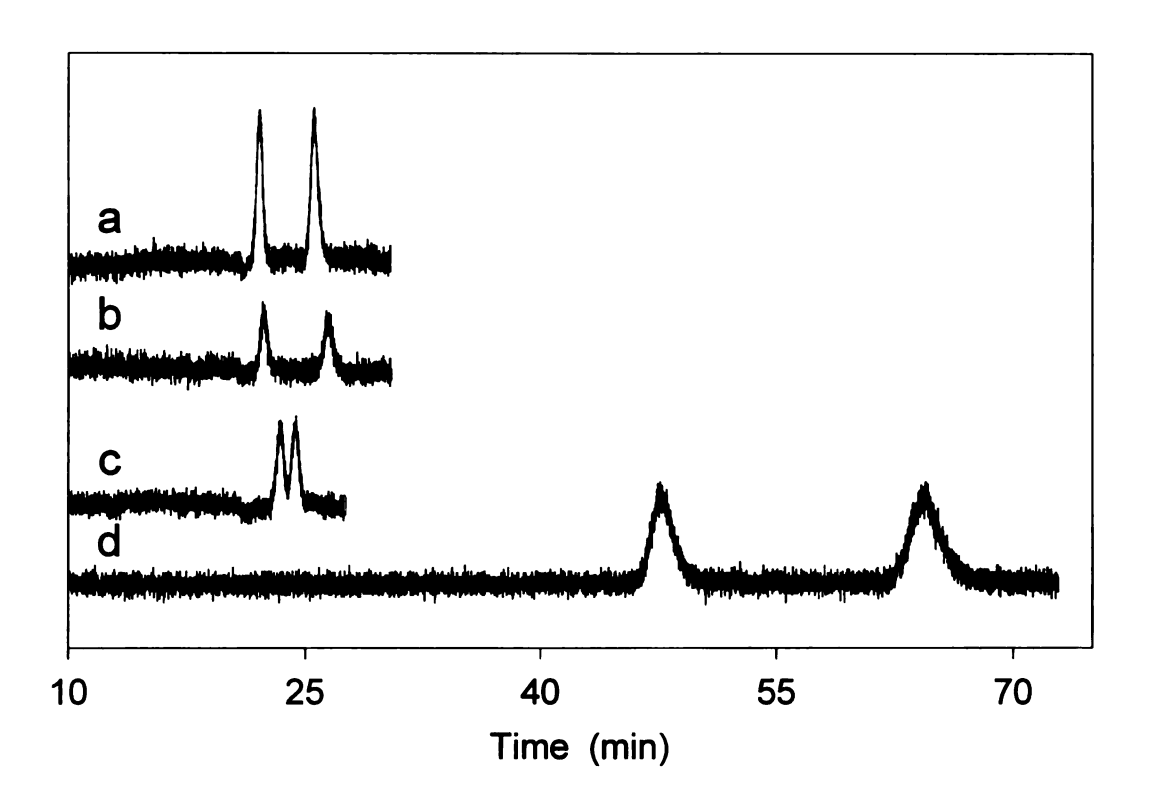


Figure 3.4. Separation of coumarins using DMPC-amylose phase and acetonitrile mobile phase that contains 0.1 % acetic acid and 0.2 % triethylamine. Solutes: a) warfarin; b) coumachlor; c) coumafuryl; d) coumatetralyl.

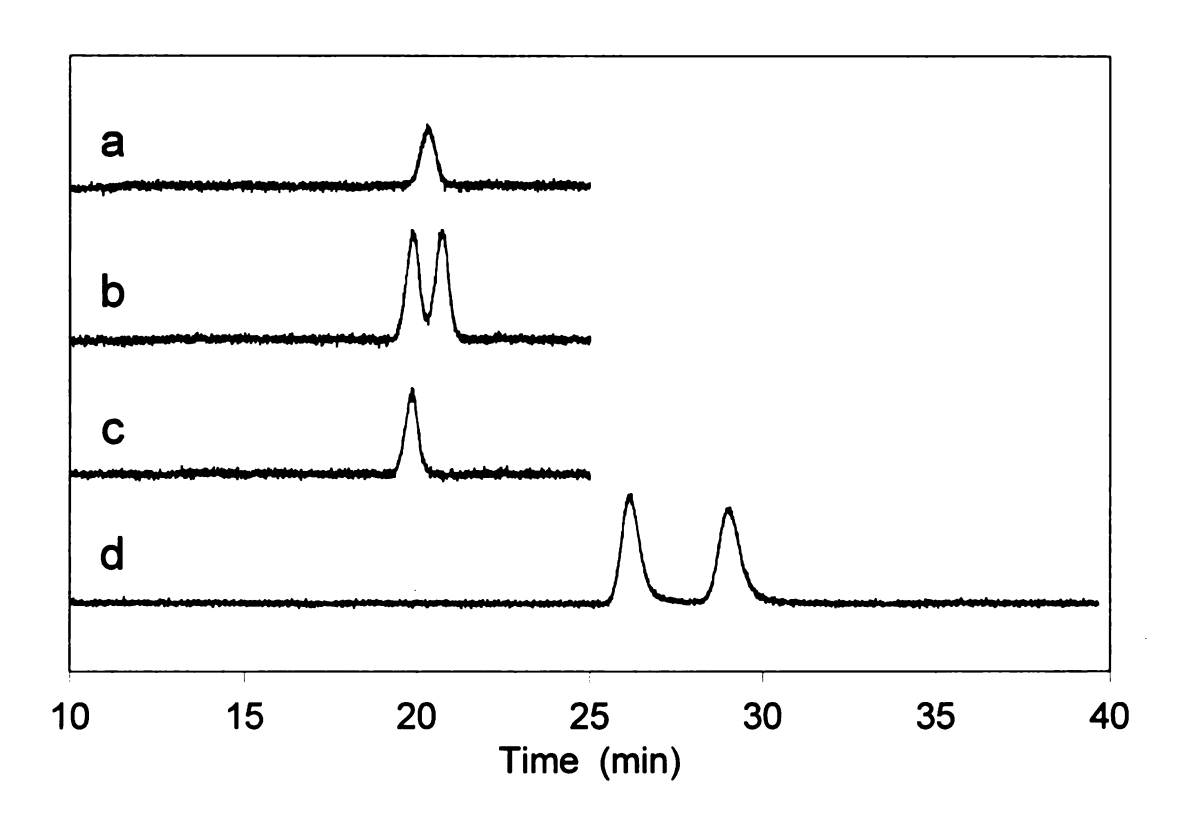


Figure 3.5. Separation of coumarins using DMPC-cellulose phase and acetonitrile mobile phase that contains 0.1 % acetic acid and 0.2 % triethylamine. Solutes: a) warfarin; b) coumachlor; c) coumafuryl; d) coumatetralyl.

atom can inductively withdraw electron density from the benzene ring to make it a π -acidic group. This π -acidic group can easily undergo interaction with the π -basic 3,5-dimethylphenyl group of the carbamate derivatizing agent. This interaction, together with other weak forces such as hydrogen bonding, might be responsible for the resolution of coumachlor. The main chiral adsorption sites in both phases are probably the polar carbamate groups and residual hydroxyl groups. But, by virtue of its helical structure, the amylose phase may also have inclusion interactions that enhance chiral selectivity. On the basis of the separation of the coumarins, we can conclude that these two stationary phases have different chiral recognition mechanisms.

3.3.3. Effect of modifiers

The effect of organic modifiers is investigated by adding methanol, acetone, and tetrahydrofuran to the bulk acetonitrile mobile phase. The magnitudes of the thermodynamic quantities (retention and selectivity) are compared with those in bulk acetonitrile on the DMPC-amylose phase (Table 3.3). When 5 % methanol is added, the retention factors of all coumarins decrease. The second-eluted enantiomer is affected to a greater extent than the first enantiomer, leading to an overall reduction in chiral selectivity. This is most evident for the coumatetralyl enantiomers, where the retention factors (k₁ and k₂) decrease by 48 % and 56 %, respectively, and the selectivity decreases by 13.8 %. When the concentration of methanol in the mobile phase is increased to

Table 3.3. Effect of modifier concentration on the separation of coumarins using DMPC-amylose phase. Mobile phase contains acetonitrile with 0.1 % acetic acid and 0.2 % triethylamine and varying concentrations of organic modifier (%). Standard deviations in k and α are \pm 0.01.

Modifier	%		Warfarin		S	Coumachlor		0	Coumafuryl		ŏ	Coumatetralyl	yl
	2	Кſ	k2	ø	К₁	k ₂	b	k	k ₂	ø	k ₁	k2	α
None	% 0	1.08	1.40	1.30	1.10	1.50	1.36	1.21	1.29	1.07	3.32	4.82	1.45
7	2 %	0.95	1.06	1.12	0.98	1.12	1.14	1.01	1.01	1.00	1.71	2.13	1.25
E 0	10 %	0.89	96'0	1.07	0.93	1.00	1.08	0.92	0.92	1.00	1.27	1.46	1.15
400	2%	96.0	1.18	1.22	66.0	1.23	1.24	1.05	1.10	1.05	2.60	3.73	1.43
	10 %	96.0	1.20	1.22	1.01	1.25	1.24	1.07	1.13	1.06	2.65	3.84	1.45
F	2%	1.00	1.30	1.30	1.03	1.37	1.33	1.09	1.21	1.10	2.93	4.67	1.60
Ė	10 %	96.0	1.27	1.29	1.00	1.31	1.31	1.02	1.16	1.14	2.28	4.07	1.78

10 %, retention and selectivity decrease slightly for warfarin, coumachlor, and coumafuryl, and more significantly for coumatetralyl. Because the second enantiomer is, in all cases, affected more greatly than the first enantiomer, we may infer that methanol has a more significant impact on the chiral retention sites than the achiral sites. Methanol can act as a proton donor or acceptor (Bronsted acid/base). Consequently, it can compete with or displace the coumarins by forming hydrogen bonds with the carbamate group of the derivatized polysaccharide phase and/or the residual hydroxyl groups. Both of these groups are adjacent to the chiral carbons of the D-glucose rings. This competition or displacement reduces the chiral interaction of the stationary phase with the coumarins, thereby decreasing the retention factor and selectivity.

When 5 % acetone is added, the retention factors of all coumarins decrease. The second-eluted enantiomer is affected more greatly than the first enantiomer, however, the effect of acetone is not as great as that of methanol. As a consequence, the selectivity is reduced very slightly. For coumatetralyl, the retention factors (k₁ and k₂) decrease by 22 % and 23 %, respectively, and the selectivity decreases by only 1 %. When the concentration of acetone is increased to 10 %, the retention and selectivity are statistically indistinguishable from the values in 5 % acetone. This suggests that acetone may interact with chiral and/or achiral sites that are easily saturated. Acetone can act as an electron-pair donor (Lewis base), with particular affinity for trace metals. It could also potentially interact with hydroxyl groups in the stationary phase or coumarin ring.

When 5 % THF is added, there is a slight decrease in the retention factors of the coumarins. However, unlike the effect of methanol and acetone, THF decreases the retention factors (k₁ and k₂) of coumatetralyl by only 11 % and 3 %, respectively. It is noteworthy that THF affects the retention of the second enantiomer of coumatetralyl very slightly compared to the first enantiomer. Consequently, the chiral selectivity increases by about 10 %. An increase in the concentration to 10 % THF leads to a further decrease in the retention time of all coumarins. Chiral selectivity remains essentially the same for warfarin, but decreases slightly for coumachlor. In contrast, it increases by 6 % and 22 % for coumafuryl and coumatetralyl, respectively. Because the first enantiomer is, in most cases, affected more greatly than the second enantiomer, we may infer that THF has a more significant impact on the achiral retention sites than the chiral sites. THF can act as an electron-pair donor (Lewis base). Consequently, it can interact with the acidic OH group of the coumarin ring, which is distant from the chiral center (Figure 2.1). This interaction reduces achiral interaction of the coumarins with the stationary phase, thereby decreasing the retention factor but increasing the selectivity.

For the DMPC-cellulose phase, the addition of methanol decreases both the retention factor and selectivity for coumachlor and coumatetralyl (other coumarins are not resolved). The addition of acetone does not cause any significant change in retention and selectivity. On the other hand, THF causes a decrease in retention for all coumarins, while selectivity remains essentially the

same. From these results, we can conclude that the organic modifiers have little influence in improving the separation of the coumarin enantiomers.

3.3.4. Kinetics

Under most conditions, narrow symmetric peaks are observed for warfarin, coumachlor, and coumafuryl in both stationary phases. This suggests that the isotherms are linear and that the kinetics of sorption/desorption are relatively fast. In contrast, broader asymmetric peaks are observed for coumatetralyl and 4-hydroxycoumarin. This behavior may result from slow mass transfer in the stationary phase.

Taking this into consideration, the kinetics of separation on both stationary phases are compared by using coumatetralyl as a model solute. First, the rate constants for sorption (k_{sm}) and desorption (k_{ms}) are evaluated with bulk acetonitrile as mobile phase (Table 3.4, 0 %). The rate constants for sorption are uniformly greater than those for desorption for both enantiomers in both stationary phases. This indicates that the rate-limiting step in all cases is release from the stationary phase. The rates of sorption and desorption are generally higher on DMPC-amylose than on DMPC-cellulose for both enantiomers. This is somewhat surprising, given that the retention factors and, therefore, the time spent in the stationary phase by both enantiomers are much greater on the amylose phase (Table 3.2).

Next, the rate constants are evaluated with THF modifier in the bulk acetonitrile mobile phase (Table 3.4, 5 % and 10 %). For the first-eluted enantiomer, the rate of sorption increases as the concentration of THF increases for both stationary phases. On the DMPC-amylose phase, this rate constant increases substantially by 28 % and 510 % for 5 % and 10 % THF, respectively. On the DMPC-cellulose phase, this rate constant increases more moderately by 135 % and 200 % for 5 % and 10 % THF, respectively. For the second-eluted enantiomer, the rate of sorption decreases on DMPC-amylose, but increases on DMPC-cellulose as the concentration of THF increases. On the DMPC-amylose phase, this rate constant decreases substantially by 91 % and 99.6 % for 5 % and 10 % THF, respectively. In contrast, on the DMPC-cellulose phase, this rate constant increases moderately by 150 % and 160 % for 5 % and 10 % THF, respectively.

In general, similar trends are observed for desorption. For the first-eluted enantiomer, the rate of desorption increases as the concentration of THF increases for both stationary phases. On the DMPC-amylose phase, this rate constant increases substantially by 45 % and 790 % for 5 % and 10 % THF, respectively. On the DMPC-cellulose phase, this rate constant increases more moderately by 160 % and 270 % for 5 % and 10 % THF, respectively. For the second-eluted enantiomer, the rate of desorption decreases on DMPC-amylose, but increases on DMPC-cellulose as the concentration of THF increases. On the DMPC-amylose phase, this rate constant decreases substantially by 91 % and

Table 3.4. Comparison of sorption (k_{sm}) and desorption (k_{ms}) rate constants of coumatetralyl enantiomers using DMPC-amylose and DMPC-cellulose phases. Mobile phase contains acetonitrile with 0.1 % acetic acid and 0.2 % triethylamine and varying concentrations of THF (%).

Rate Constant	DI	MPC-Amyl	ose	DMPC-Cellulose			
(s ⁻¹)	0 %	5 %	10 %	0 %	5 %	10 %	
(k _{sm}) ₁ ^a	23.0	29.5	140	18.8	44.1	56.5	
(k _{sm}) ₂ ^a	87.5	8.00	0.34	16.9	41.9	43.7	
(k _{ms}) ₁	7.08	10.3	63.2	12.3	31.9	45.0	
(k _{ms}) ₂	18.5	1.73	0.08	9.36	25.8	31.8	

^aSubscripts denote the first (1) and second (2) eluted enantiomers.

99.6 % for 5 % and 10 % THF, respectively. In contrast, on the DMPC-cellulose phase, this rate constant increases moderately by 180 % and 240 % for 5 % and 10 % THF, respectively. The behavior of the coumatetralyl enantiomers on the DMPC-amylose phase is interesting and somewhat surprising. As shown in Figure 3.6, both enantiomers become less retained as the concentration of THF modifier increases. However, the first-eluted enantiomer maintains a narrow symmetric peak shape, whereas the second-eluted enantiomer becomes extremely broad and asymmetric. As the concentration of THF increases, the rates of sorption and desorption increase for the first enantiomer, but decrease dramatically for the second enantiomer (Table 3.4). For 10 % THF, the first enantiomer is approximately 400 times faster at sorption and 800 times faster at desorption than the second enantiomer. This dramatic change in the kinetics of coumatetralyl is much greater than might be expected for a simple reduction in the number of achiral binding sites, as suggested by the thermodynamic data above. Instead, THF may be affecting the crystallinity or other aspects of the helical structure of the DMPC-amylose phase. This behavior is not observed for the other organic modifiers and, clearly, is worthy of more detailed investigation. In contrast, the behavior of the coumatetralyl enantiomers on the DMPCcellulose phase is more predictable. As shown in Figure 3.7, both enantiomers become less retained as the concentration of THF modifier increases. Both enantiomers maintain a narrow symmetric peak shape, which is indicative of fast kinetics. As the concentration of THF increases, the rates of sorption and

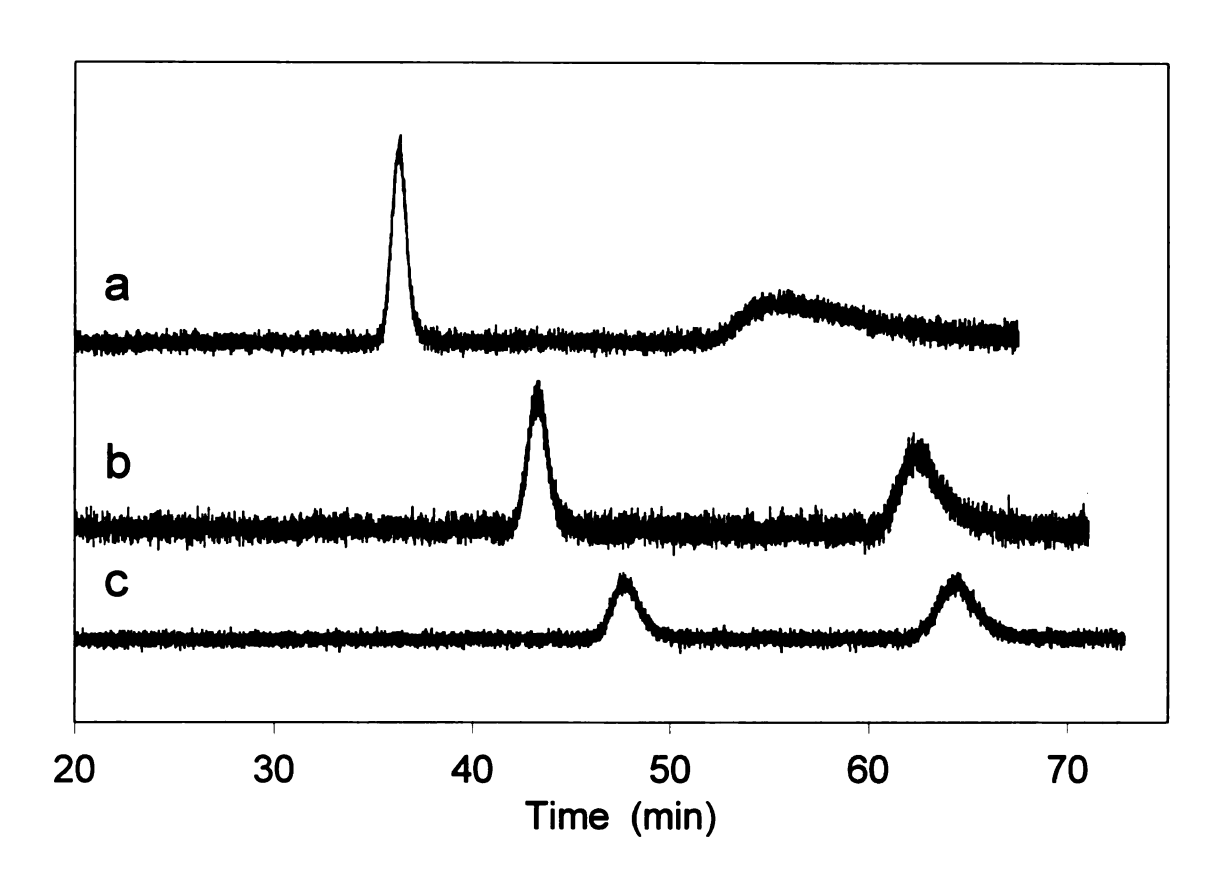


Figure 3.6. Effect of THF on the kinetics of coumatetralyl using DMPC-amylose phase and acetonitrile mobile phase that contains 0.1 % acetic acid and 0.2 % triethylamine with a) 10 % THF; b) 5 % THF; c) 0 % THF.

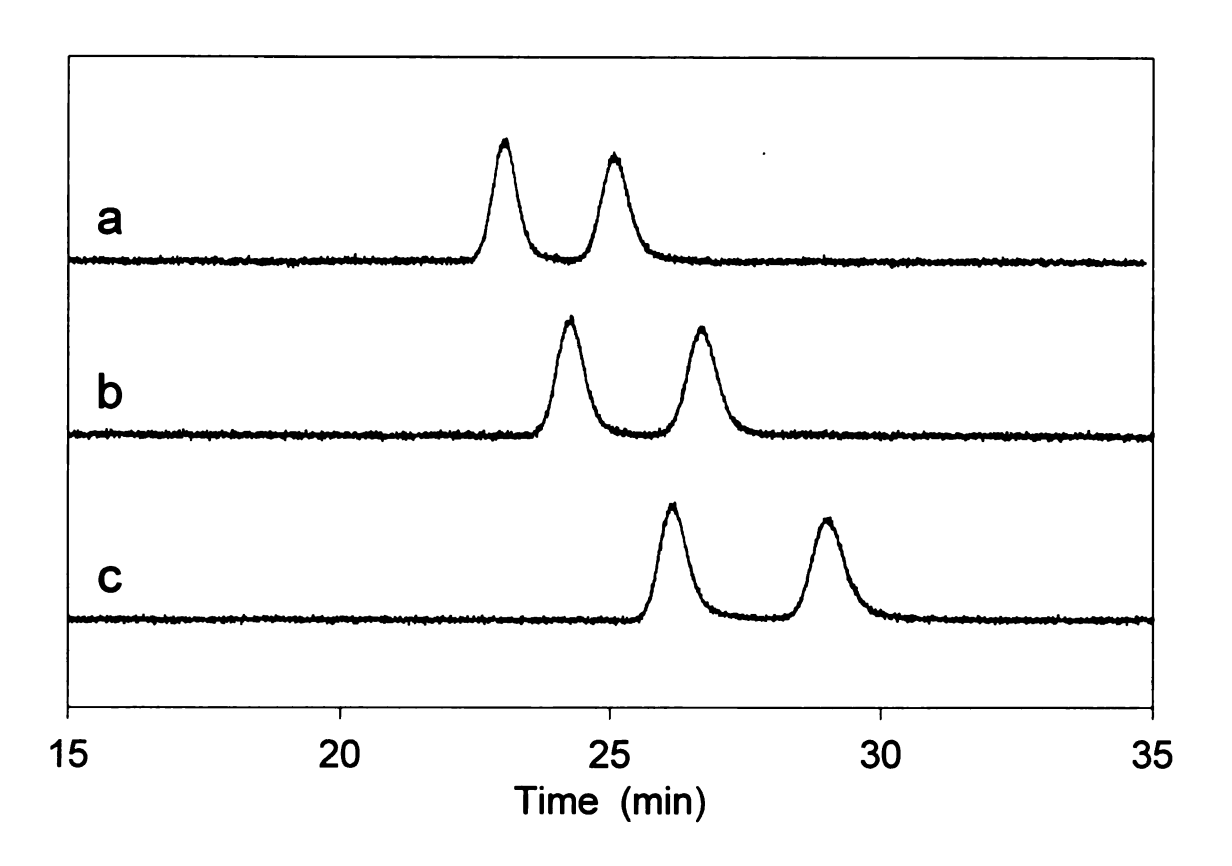


Figure 3.7. Effect of THF on the kinetics of coumatetralyl using DMPC-cellulose phase and acetonitrile mobile phase that contains 0.1 % acetic acid and 0.2 % triethylamine additives with a) 10 % THF; b) 5 % THF; c) 0 % THF.

desorption increase proportionally for both enantiomers (Table 3.4). For 10 % THF, the first enantiomer is only 1.3 times faster at sorption and 1.4 times faster at desorption than the second enantiomer. These results suggest that THF probably acts only as a displacing agent and has little influence upon the linear structure of the DMPC-cellulose phase.

3.4. CONCLUSIONS

The retention and selectivity of the coumarin solutes depend on the higher-order structure of amylose and cellulose stationary phases. These solutes are generally more retained in the helical amylose than in the linear cellulose phase, with the exception of 4-hydroxycoumarin. The DMPC-amylose phase has chiral selectivity that is adequate for coumafuryl and excellent for warfarin, coumachlor, and coumatetralyl. In contrast, the DMPC-cellulose phase has selectivity that is adequate for coumachlor and excellent for coumatetralyl, but not for warfarin and coumafuryl.

Mobile phase modifiers such as methanol, acetone, and tetrahydrofuran affect the thermodynamics and kinetics of the separation of coumarins. Methanol and acetone decrease the retention and selectivity of the coumarins on DMPC-amylose and DMPC-cellulose phases. However, this effect is more pronounced in methanol than in acetone. Tetrahydrofuran decreases the retention of all coumarins, but increases the selectivity of coumafuryl and coumatetralyl on the DMPC-amylose phase. On the DMPC-cellulose phase, retention of the coumarins decreases but selectivity remains unaffected with an increase in

concentration of THF. Investigation of the kinetic parameters reveals that DMPC-amylose and DMPC-cellulose display different behavior for coumatetralyl. For the first-eluted enantiomer, the sorption and desorption rate constants increase with an increase in THF concentration in both stationary phases. For the second-eluted enantiomer, the sorption and desorption rates decrease on DMPC-amylose and increase on DMPC-cellulose as the concentration of THF increases. When 10 % THF is used on DMPC-amylose, the first-eluted enantiomer undergoes very fast kinetics with a desorption rate constant of 63 s⁻¹. In contrast, the second-eluted enantiomer has very sluggish kinetics with a desorption rate constant of 0.08 s⁻¹. On DMPC-cellulose, the first- and secondeluted enantiomers have desorption rate constants of 45 s⁻¹ and 32 s⁻¹, respectively. The above results suggest that DMPC-amylose and DMPCcellulose have different chiral discrimination mechanisms for the coumarin-based anticoagulants.

The thermodynamic and kinetic aspects of the retention mechanism on the DMPC-amylose phase are elucidated in greater detail in chapter 4.

3.5. REFERENCES

- (1) Aboul-Enein, H. Y. J. Chromatogr. A 2001, 906, 185-193.
- (2) Anderson, M. E.; Aslan, D.; Clarke, A.; Roeraade, J.; Hagman, G. *J. Chromatogr. A* **2003**, *1005*, 83-101.
- (3) Okamoto, Y.; Kaida, Y. *J. Chromatogr. A* **1994**, *666*, 403-419.
- (4) Okamoto, Y.; Yashima, E. *Angew. Chem. Int. Ed.* **1998**, *37*, 1020-1043.
- (5) Tachibana, K.; Ohnishi, A. *J. Chromatogr. A* **2001**, *906*, 127-154.
- (6) Yamamoto, C. O., Y. Bull. Chem. Soc. Jpn. 2004, 77, 227-257.
- (7) Yashima, E. J. Chromatogr. A 2001, 906, 105-125.
- (8) Yashima, E.; Okamoto, Y. Bull. Chem. Soc. Jpn. 1995, 68, 3289 3307.
- (9) Yashima, E.; Fukaya, H.; Okamoto, Y. *J. Chromatogr. A* **1994**, 677, 11-19.
- (10) Lynam, K. G.; Stringham, R. W. Chirality 2006, 18, 1-9.
- (11) Ali, I.; Naim, L.; Ghanem, A.; Aboul-Enein, H. Y. *Talanta* **2006**, *69*, 1013-1017.
- (12) Zhang, T.; Kientzy, C.; Franco, P.; Ohnishi, A.; Kagamihara, Y.; Kurosawa, H. *J. Chromatogr. A* **2005**, *1075*, 65-75.
- (13) Zhang, T.; Nguyen, D.; Franco, P.; Murakami, T.; Ohnishi, A.; Kurosawa, H. *Anal. Chim. Acta* **2006**, *557*, 221-228.
- (14) Wang, T.; Wenslow, R. M. J. Chromatogr. A 2003, 1015, 99-110.
- (15) Wenslow, R. M.; Wang, T. Anal. Chem. 2001, 73, 4190-4195.
- (16) Kasat, R. B.; Zvinevich, Y.; Hillhouse, H. W.; Thomson, K. T.; Wang, N. H. L.; Franses, E. I. *J. Phys. Chem. B* **2006**, *110*, 14114-14122.
- (17) Chang, S. C.; Reid, I. G.; Chen, S.; Chang, C. D.; Armstrong, D. W. *Trends Anal. Chem.* **1993**, *12*, 144-153.
- (18) Matthijs, N.; Maftouh, M.; Vander Heyden, Y. *J. Chromatogr. A* **2006**, *1111*, 48-61.
- (19) Miller, L.; Orihuela, C.; Fronek, R.; Murphy, J. *J. Chromatogr. A* **1999**, *865*, 211-226.

- (20) Goossens, J. F.; Foulon, C.; Bailly, C.; Bigg, D. C. H.; Bonte, J. P.; Vaccher, C. *Chromatographia* **2004**, *59*, 305-313.
- (21) Jing, J. Y.; Wonjae, L.; Jung, P. H.; Hag, J.; Jae, R. J. *J. Liq. Chromatogr.* & *Rel. Technol.* **2006**, *29*, 1793-1801.
- (22) Salvatore, C.; Salvatore, B.; Guy, T. C. Chirality 2007, 19, 647-653.
- (23) Wang, T.; Chen, Y. D. W.; Vailaya, A. *J. Chromatogr. A* **2000**, *902*, 345-355.
- (24) Wang, T. C., Y. D. W. J. Chromatogr. A 1999, 855, 411-421.
- (25) Gluckman, J. C.; Hirose, A.; McGuffin, V. L.; Novotny, M. *Chromatographia* **1983**, *17*, 303-309.
- (26) Howerton, S. B.; Lee, C.; McGuffin, V. L. *Anal. Chim. Acta* **2003**, *478*, 99-110.
- (27) Howerton, S. B.; McGuffin, V. L. Anal. Chem. 2003, 75, 3539-3548.
- (28) McGuffin, V. L.; Lee, C. J. Chromatogr. A 2003, 987, 3-15.
- (29) Ye, Y. K.; Stringham, R. J. Chromatogr. A 2001, 927, 53-60.
- (30) Ye, Y. K.; Stringham, R. W. J. Chromatogr. A 2001, 927, 47-52.
- (31) Ye, Y. K.; Stringham, R. W.; Wirth, M. J. J. Chromatogr. A **2004**, 1057, 75-82.
- (32) Li, X. P.; McGuffin, V. L. *J. Liq. Chromatogr. Relat. Technol.* **2007**, *30*, 937-964.
- (33) Valente, E. J.; Lingafelter, E. C.; Porter, W. R.; Trager, W. F. *J. Med. Chem.* **1977**, *20*, 1489-1493.
- (34) Valente, E. J.; Porter, W. R.; Trager, W. F. *J. Med. Chem.* **1978**, *21*, 231-234.
- (35) Heimark, L. D.; Trager, W. F. J. Med. Chem. 1984, 27, 1092-1095.
- (36) Karlsson, B. C. G.; Rosengren, A. M.; Andersson, P. O.; Nicholls, I. A. *J. Phys. Chem. B* **2007**, *111*, 10520-10528.
- (37) Stella, V. J.; Mooney, K. G.; Pipkin, J. D. *J. Pharm. Sci.* **1984**, *73*, 946-948.

CHAPTER 4

THERMODYNAMIC AND KINETIC STUDY OF CHIRAL SEPARATION OF COUMARIN-BASED ANTICOAGULANTS ON DERIVATIZED AMYLOSE STATIONARY PHASE

4.1. INTRODUCTION

Chiral stationary phases based on derivatized polysaccharides have been widely used for the direct separation of enantiomers in both analytical and preparative applications. These derivatives include the tris-(3,5-dimethylphenyl carbamate) of amylose, tris-(3,5-dimethylphenyl carbamate) of cellulose, tris-(S-methylbenzyl carbamate) of amylose, and tris-(ρ -methylbenzoate) of cellulose. ¹⁻³ Among these, amylose derivatized with tris-(3,5-dimethylphenyl carbamate) is the most successful for chiral separations in liquid chromatography. ⁴⁻⁹ This phase has many chiral centers, together with hydrogen bonding and π -electron donor sites. It is commercially available as coated (Chiralpak AD) and chemically immobilized (Chiralpak IA) forms. Unlike the coated form, the immobilized form has greater solvent versatility ¹⁰ and temperature stability.

Due to the complex structure of polysaccharide phases, the exact mechanism of chiral separations is not completely understood. These phases have multiple interaction sites with different affinities for enantiomers. One way to probe their mechanism is to investigate the temperature dependence of retention and chiral selectivity. Insight into understanding retention mechanisms is usually obtained from van't Hoff plots (the natural logarithm of retention factor or chiral selectivity versus the reciprocal of absolute temperature). Linear 12-17

and nonlinear^{16, 18-20} van't Hoff plots have been observed for chiral separations using polysaccharide stationary phases. Linear van't Hoff plots indicate that the separation mechanism is unchanged in the temperature range studied (i.e., ΔH and ΔS are constant with temperature). Nonlinear van't Hoff plots are usually attributed to a change in the retention mechanism as a result of either a change in the conformation of the stationary phase or multiple types of binding sites. 11 Temperature-induced conformational changes of polysaccharide phases have been reported by Wang et al. 16, 20 The van't Hoff plot obtained for the retention factor and selectivity of dihydropyrimidinone (DHP) acid when heating the amylose column from 5 to 50 °C is not superimposable on that obtained upon cooling from 50 to 5 °C. The authors concluded that the thermally induced, pathdependent behavior resulted from slow structural equilibration of the amylose phase. Conformational changes in the stationary phase can affect adsorption and desorption rates. Rizzi²¹ reported two types of binding sites for cellulose triacetate that differ in the rate of adsorption and desorption. According to his model, one type of adsorption site is easily accessible ("quick" site), while the other site is sterically hindered ("slow" site), and they differ in their types of interaction with analytes.

The thermodynamic and kinetic properties of solute transfer can also be affected by the mobile phase composition. The solvent may cause changes in the availability and accessibility of the adsorption sites by modifying the size, crystallinity, and shape of chiral cavities.^{21, 22} Wang et al.²³ utilized solid-state NMR to identify structural changes in a tris-(3,5-dimethylphenyl carbamate)

amylose phase as a function of mobile phase composition. *i*-Propanol modifier displayed more efficient displacement of incorporated hexane and formed relatively more ordered solvent complexes compared to ethanol. Kasat et al.²⁴ used infrared spectroscopy, X-ray diffraction, and solid-state NMR to elucidate the role of solvent in modifying the structure of the amylose phase. The authors concluded that the type of solvent determines the extent of changes of the crystallinity of the polymer. These changes are more substantial for polar and hydrogen bonded solvents such as alcohols and less for nonpolar solvents such as hexane.

In this study, we investigated the detailed thermodynamics and kinetics of the separation of coumarin solutes on tris-(3,5-dimethylphenyl carbamate) amylose as a function of temperature using the polar-organic mode. The polar-organic eluents usually consist of methanol, ethanol, acetonitrile, or their combinations. This mode provides an alternative chiral recognition mechanism by separating enantiomers that cannot be separated by either normal-phase or reversed-phase modes.²⁵ Easy evaporation of the solvents used in this mode is especially attractive in preparative-scale applications.²⁶ This thermodynamic and kinetic study is believed to provide further understanding of this stationary phase and its chiral recognition mechanism.

4.2. EXPERIMENTAL METHODS

4.2.1. Chemicals

Coumarin-based anticoagulants, consisting of warfarin, coumachlor, coumafuryl, coumatetralyl, and 4-hydroxycoumarin, are used as solutes in this study. With the exception of 4-hydroxycoumarin, all of them are chiral. The structures of these solutes are shown as insets in Figure 2.1. The solutes are obtained from Sigma-Aldrich as solids and are dissolved in high-purity acetonitrile (Burdick and Jackson, Honeywell) to yield standard solutions at 10⁻³ M concentration. The polar-organic mobile phases consist of bulk acetonitrile together with organic modifiers and acid/base additives. High-purity methanol (Burdick and Jackson, Honeywell), *i*-butanol, *t*-butanol (ACS reagent grade, Columbus Chemical Industries, Inc.), and tetrahydrofuran (reagent grade, Jade Scientific) are used as modifiers. Acetic acid (0.1 % or 0.18 M, Sigma-Aldrich) and triethylamine (0.2 % or 0.14 M, Sigma-Aldrich) are used as additives to all mobile phase compositions in this study.²⁷

4.2.2. Instrumental system

For this study, liquid chromatography with an optically transparent, fused-silica capillary column (200- μ m i.d., 110 cm length, Polymicro Technologies) is used. Before the column is packed, a detection window (~ 84 cm from inlet) is made by removing the polyimide coating. The column is terminated by using a quartz wool frit. The silica packing (Chiralpak IA, Chiral Technologies) is characterized by a 5 μ m particle size that is immobilized with tris-(3,5-

dimethylphenyl carbamate) amylose. The slurry method is used to pack the stationary phase. 28 This method provides a column with uniform packing along the length and diameter. It involves selection of a solvent that will result in slow settling and minimal aggregation of particles of the stationary phase. From all the solvents tested (methanol, acetonitrile, acetone, ethyl acetate, tetrahydrofuran, and hexane), methanol is the best for packing the Chiralpak IA stationary phase. The resulting column has a plate height of 16 μ m and a reduced plate height of 3.2 determined with a neutral solute (pyrene).

The mobile phase is delivered by a single-piston reciprocating pump (Model 114M, Beckman Instruments), operated in the constant pressure mode at 1500 psi. After injection (Model EC14W1, Valco Instruments), the samples are split between the column and a fused-silica capillary (50-μm i.d., 6 m length, Polymicro Technologies) to prevent excessive broadening and overload of the stationary phase. The injection volume is about 16 nL for a split ratio of 60. To vary the temperature between 5 and 45 °C, the column, injector, and splitter are housed within a cryogenic oven (Model 3300, Varian Associates). Column equilibration is ensured by alternately cycling the temperature between 5 and 50 °C. At each temperature, the column is equilibrated for an hour and coumatetralyl is injected in triplicate. The calculated retention factors are found to be constant (± 0.9 %) for each temperature and for each cycle.

Laser-induced fluorescence is used for on-column detection. A helium-cadmium laser (Model 3074-20M, Melles Griot) provides excitation at 325 nm.

To monitor solute zone profiles along the column, four windows have been

available by removing the polyimide coating. The laser is focused onto UV-grade optical fibers (100 μ m, Polymicro Technologies) and is then transmitted to the four windows along the column. At each window, the fluorescence emission is collected orthogonally by optical fibers (500 μ m, Polymicro Technologies) and is transmitted through a 420-nm interference filter (S10-420-F, Corion) to a photomultiplier tube (Model R760, Hamamatsu). The resulting photocurrent is amplified, converted to the digital domain (Model PCIMIO-16XE-50, National Instruments), and stored by a user-defined program (Labview v5.1, National Instruments).

4.2.3. Data analysis

To extract thermodynamic and kinetic information, statistical moments are used to analyze the data, as they make no assumptions about the shape of the zone profiles or the mechanism of retention. The individual zone profiles are extracted from the chromatogram and fit by using nonlinear regression (Tablecurve v2.02, SYSTAT Software, Inc.), so that the statistical moments can be determined without contributions from noise. Gaussian and asymmetric double sigmoidal (ADS) functions are used for fitting, since these two functions are found to provide good quality of fit (r² > 0.998) and random residuals. The Gaussian function is

$$C(t) = a_0 \exp \left[-0.5 \left(\frac{t - a_1}{a_2} \right)^2 \right]$$
 (1)

where a_0 is the amplitude, a_1 is the peak center, and a_2 is the peak width. Similarly, the ADS function is

$$C(t) = \left[\frac{a_0}{1 + \exp\left[-\left(\frac{t - a_1 + \frac{a_2}{2}}{a_3}\right)\right]}\right] \left[1 - \frac{1}{1 + \exp\left[-\left(\frac{t - a_1 - \frac{a_2}{2}}{a_4}\right)\right]}\right]$$
(2)

where a_0 is the amplitude, a_1 is the peak center, and a_2 , a_3 , and a_4 are peak widths. Using the fitting parameters from both functions, the peaks are regenerated in a spread sheet program (Excel, Microsoft Corporation). The first (M_1) and second (M_2) statistical moments are calculated from the zone profiles as

$$M_1 = \frac{\int C(t)tdt}{\int C(t)dt}$$
 (3)

$$M_2 = \frac{\int C(t)(t - M_1)^2 dt}{\int C(t) dt}$$
(4)

where C(t) is the concentration as a function of time. The integration is performed using a spread sheet program. For this study, the integration limits are taken at 0.1 % of the maximum peak height. This integration limit provides minimum error in the determination of statistical moments.²⁹

The first moment represents the mean retention time (t_r) and is used to determine the retention factor. Since the stationary phase has multiple interaction sites with analytes, it is difficult to find a non-retained marker (t_0) having no interaction with the stationary phase. Based on previous reports in the

nitromethane,³⁰ 1,3,5-tri-(*t*-butyl)benzene,¹⁰ 4-bromomethyl-7literature. methoxycoumarin.³¹ and pyrene are tested as non-retained solutes. However, they are more retained than the least retained solute (warfarin) or are not Consequently, the to marker is determined as follows. At each temperature and mobile phase composition, flow rates are carefully measured before sample injection and after sample elution. The least retained solute, warfarin, is separated in the presence of only 0.2 % triethylamine additive in the acetonitrile mobile phase. In the absence of acetic acid, the warfarin peak elutes very early, and the enantiomers are unresolved and fronting compared to those observed in the presence of both additives.²⁷ Values of t₀ are then taken from the first rising edge of this peak, at each temperature and flow rate, for each mobile phase composition. Then, graphs of t₀ and inverse flow rate (1/F) versus inverse temperature (1/T) are constructed. These plots are found to be linear (r² > 0.999). Consequently, the slope and intercept of a graph of t_0 versus 1/F (t_0 = 655.68/F - 73.49; $r^2 = 0.999$) are used to predict t_0 values for each solute injection depending on the measured flow rate. The retention factor (k) is then calculated as

$$k = \frac{\left(M_1 - t_0\right)}{t_0} \tag{5}$$

Chiral selectivity (α) is calculated as

$$\alpha = \frac{k_2}{k_1} \tag{6}$$

where k_1 and k_2 are the retention factors for the first and second eluted enantiomer, respectively.

The second moment represents the peak variance and is used to determine kinetic rate constants. The second moment is related to the plate height (H) by 32

$$H = \frac{M_2 L}{M_1^2} \tag{7}$$

where L is the column length. From Giddings generalized non-equilibrium theory, 33 the mass transfer term for slow kinetics (C_s) is given by

$$C_s = \frac{2k}{\left(1 + k\right)^2 k_{ms}} \tag{8}$$

Thus, the desorption rate constant (k_{ms}) can be determined as

$$k_{ms} = \frac{2ku}{(1+k)^2 \Delta H} \tag{9}$$

where u is the linear velocity and ΔH is the corrected plate height, which represents slow mass transfer in the stationary phase (C_s). The sorption rate constant (k_{sm}) can then be determined from the expression for k, which relates the thermodynamic and kinetic terms

$$k = \frac{k_{sm}}{k_{ms}} \tag{10}$$

$$k_{sm} = \frac{2k^2u}{(1+k)^2\Delta H}$$
 (11)

The corrected plate height is calculated as

$$\Delta H = H - A - \frac{B}{u} - C_{m}u \tag{12}$$

where H is the total plate height determined for each solute from Equation 7. A, B, and C_m are the individual column contributions to zone broadening from multiple paths, diffusion in the mobile and stationary phases, and resistance to mass transfer in the mobile phase, respectively.³⁴ In this study, the column contributions are determined by injection of 10^{-4} M pyrene. The average plate height is found to be $16 \pm 0.4 \, \mu m$ over the temperature range of 5 to 45 °C. This value is then subtracted from the total plate height measured for each solute. This assumes that all broadening due to axial dispersion and fast mobile phase kinetics is removed, leaving only the slow kinetic contribution from the stationary phase. The use of a nonpolar aromatic hydrocarbon for plate height determination on cellulose triacetate stationary phase was shown by Rizzi.²¹ These compounds, regardless of their size, always showed low plate height values since they were mainly adsorbed onto sites with faster adsorption kinetics.

4.3. RESULTS AND DISCUSSION

4.3.1. Thermodynamic effects

The separation of chiral coumarins (warfarin, coumachlor, coumafuryl, and coumatetralyl) and an achiral coumarin (4-hydroxycoumarin) on Chiralpak IA is shown in Figure 4.1. Values of the retention factor and chiral selectivity at 20 °C are listed in Table 4.1. Comparison of the retention behavior of the first eluted

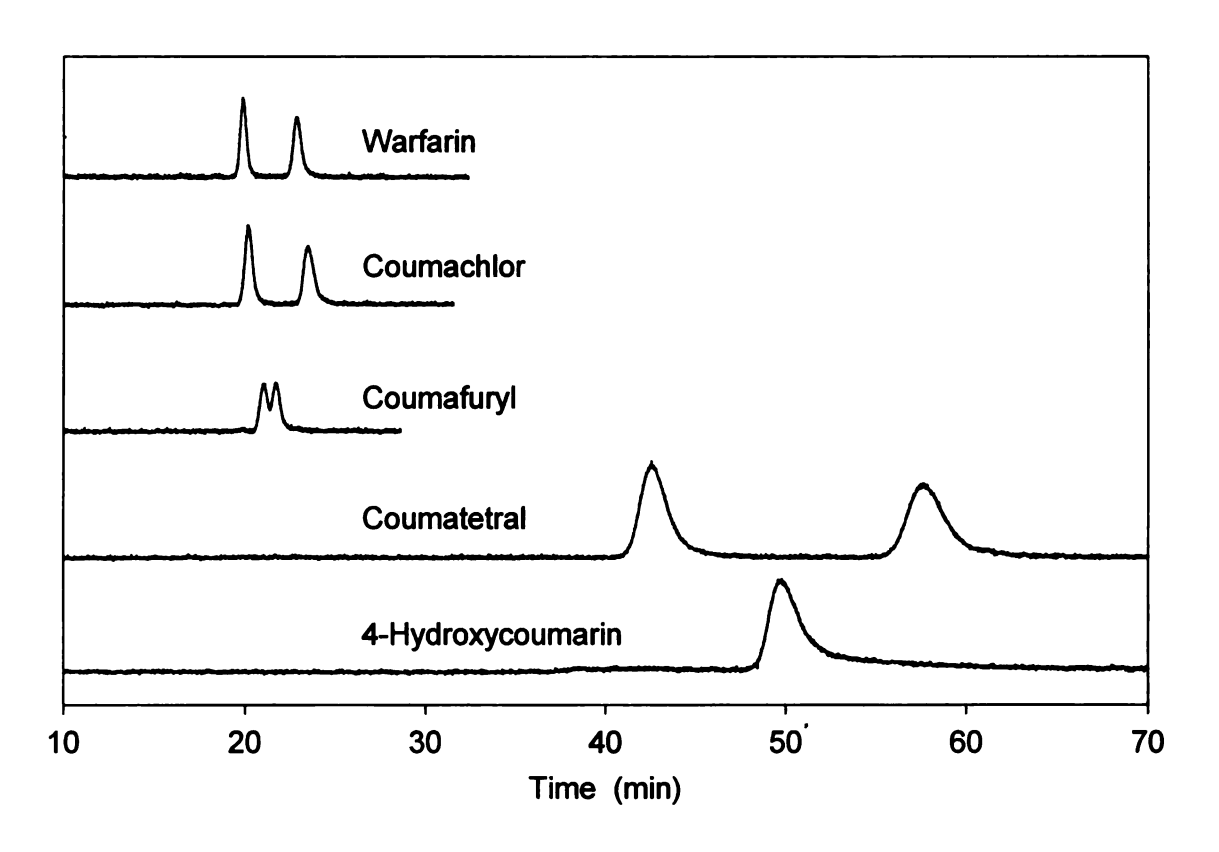


Figure 4.1. Chromatograms and structures of coumarin-based anticoagulants. Column: Chiralpak IA; mobile phase: acetonitrile with 0.1 % acetic acid and 0.2 % triethylamine additives; temperature: 20 °C; flow rate: 1 μ L/min.

Table 4.1. Retention factor (k) and chiral selectivity (α) for the coumarin-based solutes at 20 °C. Column: Chiralpak IA; mobile phase: acetonitrile with 0.1 % acetic acid and 0.2 % triethylamine additives; flow rate: 1 μ L/min.

Solute	k ₁ ^a	k ₂ ^a	α
Warfarin	0.99	1.29	1.30
Coumachlor	1.02	1.35	1.35
Coumafuryl	1.10	1.18	1.07
Coumatetralyl	3.29	4.82	1.46
4-Hydroxycoumarin	4.13	N/A ^b	N/A

^a Subscripts denote the first (1) and second (2) eluted enantiomers.

b Not applicable (N/A).

enantiomer indicates that warfarin, coumachlor and coumafuryl have comparable retention factors, with warfarin being the least retained. The achiral solute, 4-hydroxycoumarin, is the most retained. With no side chain at the 3 position, 4-hydroxycoumarin can have simultaneous interactions of the hydroxyl and carbonyl groups with the DMPC derivatizing group and/or residual hydroxyl or silanol groups of the stationary phase.³⁰ Neverthless, 4-hydroxycoumarin is less retained than the second enantiomer of coumatetralyl. This may be a result of fewer interaction sites for 4-hydroxycoumarin in the derivatized stationary phase or, alternatively, because the chiral sites are conformationally well-suited for the second eluted enantiomer of coumatetralyl.

The chiral solutes, with the exception of coumafuryl, have excellent enantioseparation in the stationary phase. In coumafuryl, the hydroxyl side chain may form intramolecular hydrogen bonds with the oxygen atom of the furan ring, resulting in loss of binding sites that may contribute to chiral recognition.

4.3.1.1. Effect of modifier type and concentration on retention and selectivity

To investigate the effect of organic modifiers on the thermodynamics of the separation on Chiralpak IA, warfarin and coumatetralyl are chosen as probes. The modifiers used for this study are alcohols such as methanol (MeOH), *i*-butanol (*i*-BuOH), *t*-butanol (*t*-BuOH), and tetrahydrofuran (THF). The modifiers have differences in their hydrogen bond donating/accepting abilities

(Table 4.2 35). Alcohols can act as both hydrogen bond donors and acceptors, while tetrahydrofuran is a hydrogen bond acceptor. The modifiers also have differences in molecular size and shape. Methanol is smaller in size, while *i*-BuOH and *t*-BuOH are branched and relatively bulky. THF has size comparable to that of *t*-BuOH. Kasat et al.²⁴ have reported that the size of the cavity formed by intramolecular hydrogen bonds between C=O and N-H groups of the derivatized amylose phase (Figure 1.2) increases as the molecular size of the modifiers increases. Branched alcohols cause twisting of the α -(1,4)-glycosidic linkage of the amylose helix, as evidenced by the reduction in the chemical shift of C₁ and C₄ sites using ¹³C cross polarization and magic angle spinning (CP/MAS) solid-state NMR.^{36, 37}

The retention and selectivity of warfarin enantiomers in varying modifier concentrations are summarized in Table 4.3 and are compared to values in the absence of modifier in Table 4.1. At 5 % modifier concentration, the retention factors of warfarin enantiomers decrease in MeOH and *i*-BuOH, but remain constant or increase in *t*-BuOH and THF. In contrast, the chiral selectivity of warfarin decreases as the hydrogen bond donating ability of the modifiers increases. At 10 % modifier concentration, both the retention factor and selectivity of warfarin further decrease in the alcohol modifiers. In THF, retention factors for the warfarin enantiomers are not significantly affected and, as a result, the chiral selectivity remains almost constant.

The retention and selectivity of coumatetralyl enantiomers in varying modifier concentrations are summarized in Table 4.4 and are compared to values

Table 4.2. Solvatochromic properties of modifiers used in the study³⁵ The α scale represents the ability of a solvent to donate a proton, while the β scale evaluates the ability of a solvent to accept a proton (donate an electron pair) in a solvent-to-solute hydrogen bond.

Modifier	α	β
Methanol (MeOH)	0.93	0.62
<i>i</i> -Butanol (<i>i</i> -BuOH)	N/A ^b	N/A
t-Butanol (t-BuOH)	0.68	1.01
Tetrahydrofuran (THF)	0.00	0.55

^aNot available (N/A)

Table 4.3. Comparison of retention factor (k) and chiral selectivity (α) for warfarin enantiomers at 20 °C. Other experimental conditions as given in Table 4.1.

Modifier	5 %			10 %		
	k ₁ ^a	k ₂ ^a	α	k ₁	k ₂	α
MeOH	0.97	1.10	1.13	0.96	1.03	1.07
<i>i</i> -BuOH	0.93	1.10	1.18	0.89	0.98	1.10
t-BuOH	1.06	1.28	1.21	0.89	1.02	1.14
THF	1.04	1.33	1.28	0.99	1.31	1.32

^aSubscripts denote the first (1) and second (2) eluted enantiomers

Table 4.4. Comparison of retention factor (k) and chiral selectivity (α) for coumatetrally enantiomers at 20 °C. Other experimental conditions as given in Table 4.1.

Modifier	5 %			10 %		
	k ₁ ^a	k ₂ ^a	α	k ₁	k ₂	α
MeOH	1.90	2.35	1.24	1.41	1.61	1.14
<i>i</i> -BuOH	2.03	2.81	1.38	1.44	1.82	1.26
<i>t</i> -BuOH	2.93	4.60	1.57	1.47	2.06	1.40
THF	3.08	4.83	1.57	2.31	4.31	1.87

^aSubscripts denote the first (1) and second (2) eluted enantiomer

in the absence of modifier in Table 4.1. At 5 % modifier concentration, the retention factor of the first eluted enantiomer decreases in all modifiers. For the second eluted enantiomer, retention remains constant in THF, but decreases in the other modifiers. Accordingly, the chiral selectivity of coumatetralyl decreases in MeOH and *i*-BuOH, but increases in *t*-BuOH and THF by about 7.5 %. Despite the different retention behavior of the two enantiomers in *t*-BuOH and THF, the magnitude of the selectivity in both modifiers is identical. At 10 % modifier concentration, the retention factor and selectivity of coumatetralyl enantiomers decrease substantially as the hydrogen bond donating ability of the alcohol modifiers increases. THF causes a decrease in the retention factors of both enantiomers by about 29 % and 12 %, respectively. However, the selectivity increases substantially by about 28 %. This suggests that the second eluted enantiomer of coumatetralyl may have a better conformational fit in the chiral cavity of the stationary phase than the first eluted enantiomer.

4.3.1.2. Effect of temperature on molar enthalpy, entropy, and Gibbs free energy in acetonitrile

To investigate the effect of temperature on retention and chiral selectivity, van't Hoff plots are obtained for the temperature range of 5 to 45 °C. The dependence of retention on temperature is given by

$$\ln k = \frac{-\Delta G}{RT} - \ln \beta = \frac{-\Delta H}{RT} + \frac{\Delta S}{R} - \ln \beta$$
 (13)

where ΔG , ΔH , and ΔS represent the changes in molar Gibbs free energy, enthalpy, and entropy, respectively, R is the gas constant, T is the absolute

temperature, and β is the volumetric ratio of the mobile and stationary phases. Equation 13 indicates that a graph of the natural logarithm of the retention factor versus the inverse of the absolute temperature should be linear with a slope of (– Δ H/R) and an intercept of (Δ S/R – ln β), if Δ H, Δ S, and β are independent of temperature. The dependence of selectivity on temperature is given by

$$\ln \alpha = \frac{-\Delta \Delta G}{RT} = \frac{-\Delta \Delta H}{RT} + \frac{\Delta \Delta S}{R}$$
 (14)

where $\Delta\Delta G$, $\Delta\Delta H$, and $\Delta\Delta S$ represent the differential changes in molar Gibbs free energy, enthalpy, and entropy, respectively, between enantiomers according to Equation 6. A graph of the natural logarithm of selectivity versus inverse temperature will be linear with a slope of ($-\Delta\Delta H/R$) and an intercept of ($\Delta\Delta S/R$), if $\Delta\Delta H$ and $\Delta\Delta S$ are independent of temperature. In chiral separations, only stereoselective interaction with the chiral selector leads to a difference in the retention of enantiomeric pairs.

The van't Hoff plots for the retention factor (ln k versus 1/T) of the coumarins are shown in Figure 4.2a. As can be seen, the plots are linear with correlation coefficients (r^2) ranging from 0.989 to 0.999. Similarly, the van't Hoff plots for the selectivity (ln α versus 1/T) of warfarin, coumachlor, and coumafuryl are also linear (Figure 4.2b). However, this plot is found to be nonlinear (r^2 = 0.897) for coumatetralyl, suggesting that the retention mechanism is not independent of temperature in the range investigated.

The thermodynamic parameters obtained from the van't Hoff plots are

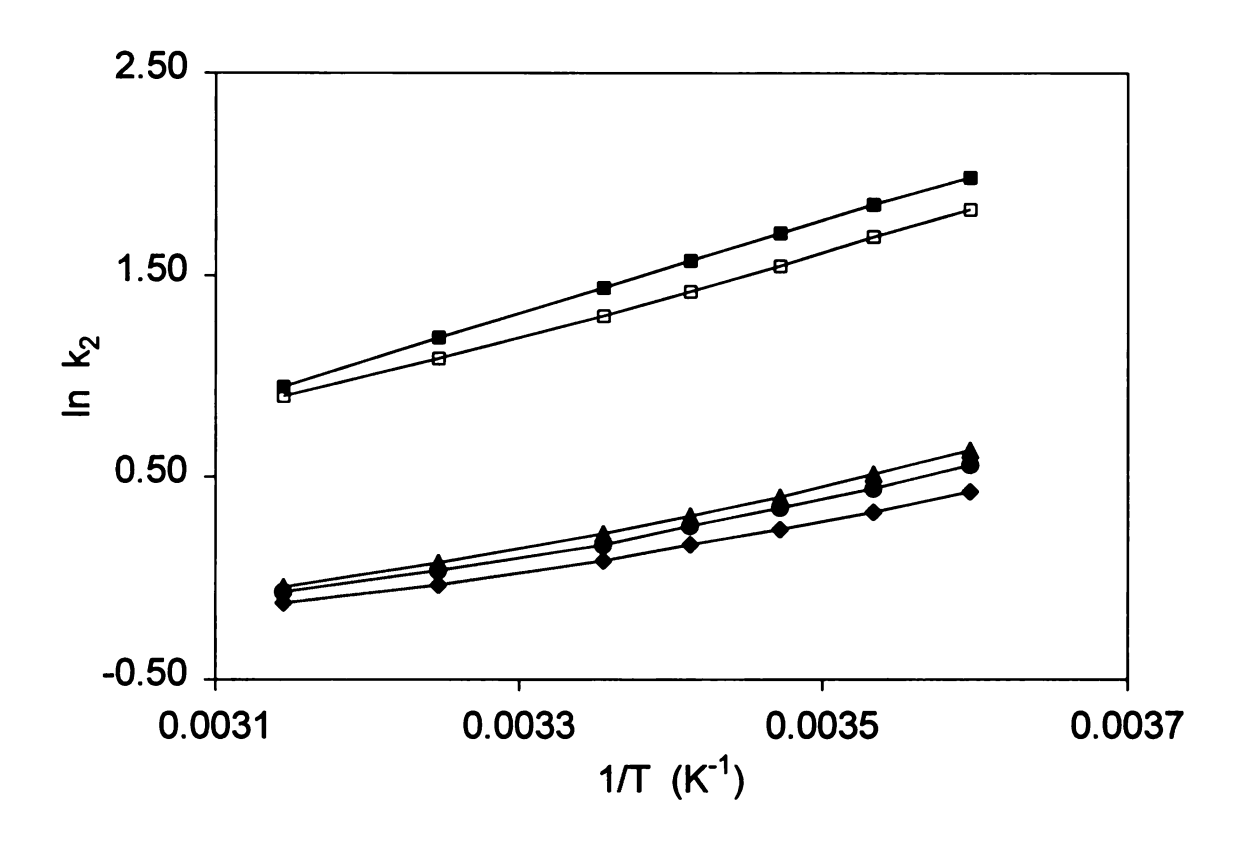


Figure 4.2a. Natural logarithm of the retention factor of the second eluted enantiomer (k_2) versus inverse temperature (1/T) for all coumarins. Warfarin (\bullet) , coumachlor (\blacktriangle) , coumaturyl (\bullet) , coumatetralyl (\blacksquare) , and 4-hydroxycoumarin (\Box) . Other experimental conditions as given in Figure 4.1.

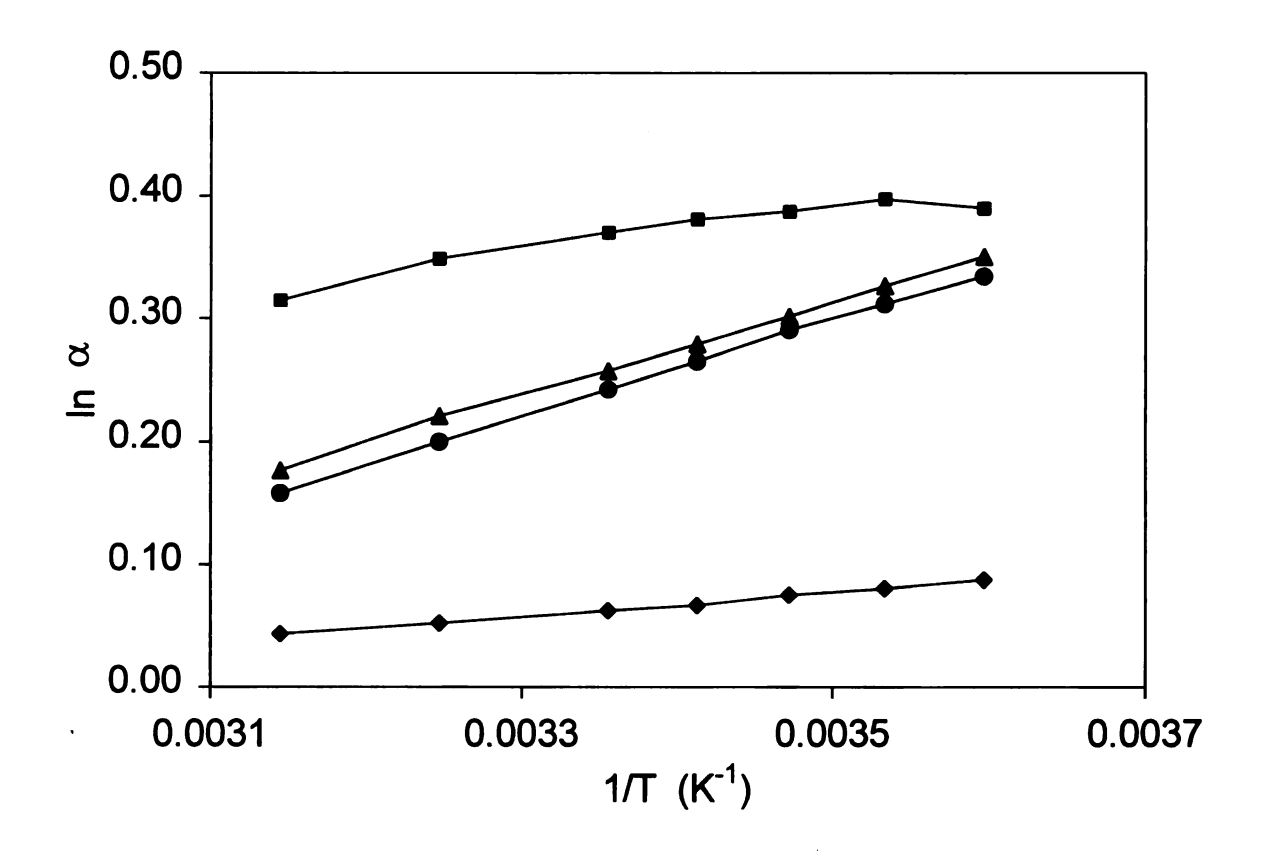


Figure 4.2b. Natural logarithm of selectivity (α) versus 1/T for all coumarins. Warfarin (\bullet) , coumachlor (\blacktriangle) , coumafuryl (\bullet) , and coumatetralyl (\blacksquare) . Other experimental conditions as given in Figure 4.1.

summarized in Table 4.5. The estimated values for ΔH and ΔS for all coumarins The values indicate that solute transfer from the mobile to stationary phase is enthalpically favorable but entropically unfavorable. The magnitude of the change in molar enthalpy for the first eluted enantiomer of coumachlor, coumafuryl, and warfarin is comparable. In contrast, the values for coumatetralyl and 4-hydroxycoumarin are almost twice those for the other coumarins. The enthalpy change is related to the strength of interactions between the enantiomers and the mobile and stationary phases. In the mobile phase, both enantiomers are solvated identically and, hence, have equal molar enthalpy. In the stationary phase, the enthalpy arises mainly from the interactions of each functional group of the enantiomer and stationary phase (heats of adsorption) and/or some additional conformational fitting into cavities. Enantiomeric pairs may have different values for ΔH due to the difference in the orientation of their functional groups relative to the chiral selective sites.

The differential changes in molar enthalpy ($\Delta\Delta H$), entropy ($\Delta\Delta S$), and Gibbs free energy ($\Delta\Delta G$) are also compared in Table 4.5. The magnitude of the differential change in the free energy of enantiomeric pairs represents the extent of chiral selectivity. As can be seen from Table 4.5, warfarin and coumachlor have comparable differential enthalpic and entropic contributions to their differential free energy. As a result, their chiral selectivities are comparable in magnitude (Table 4.1). Coumafuryl has the least negative value for $\Delta\Delta H$ and

Table 4.5. Thermodynamic quantities for coumarins in acetonitrile mobile phase. Other experimental conditions as given in Table 4.1.

Solute	ΔH ₁ ^{a,b} (kJ/mol)	ΔH2 ^{a,b} (kJ/mol)	ΔΔΗ ^c (kJ/mol)	Τ ΔΔS ^C (kJ/mol)	ΔΔG (kJ/mol)
Warfarin	-8.2 ± 0.5	-11.4 ± 0.5	-3.26 ± 0.04	-2.59 ± 0.04	-0.63 ± 0.04
Coumachlor	-9.2 ± 0.5	-12.3 ± 0.5	-3.13 ± 0.04	-2.47 ± 0.04	-0.67 ± 0.04
Coumafuryl	-9.3 ± 0.4	-10.1 ± 0.5	-0.79 ± 0.04	-0.63 ± 0.04	-0.17 ± 0.04
Coumatetralyl	-17.6 ± 0.1	-19.1 ± 0.1	-1.4 ± 0.2	-0.06 ± 0.02	-1.3 ± 0.2
4-Hydroxy- coumarin	-17.0 ± 0.3	N/A ^d	N/A	N/A	N/A

^aSubscripts denote the first (1) and second (2) eluted enantiomers

^bCalculated from the slope of Equation 13

^cCalculated from the slope and intercept of Equation 14 at T_{hm} (294.6 K, 21.6 °C)

^dNot applicable (N/A)

almost equal value for T $\Delta\Delta S$, leading to nearly zero $\Delta\Delta G$. In contrast, coumatetrally has an intermediate contribution to $\Delta\Delta H$, but nearly zero contribution to T $\Delta\Delta S$. This solute has a bulky non-aromatic side chain that isconformationally flexible (Figure 4.1). Its transfer from the mobile to stationary phase may also be accompanied by the expulsion of a large number of solvent molecules from the stationary phase. This desolvation process and/or conformational flexibility may account for the relatively higher entropic contribution. Accordingly, coumatetrally has the greatest negative value of $\Delta\Delta G$ and, hence, the greatest chiral selectivity.

4.3.1.3. Effect of temperature and modifiers on molar enthalpy, entropy, and Gibbs free energy

To investigate the effect of modifier type and concentration on the thermodynamic parameters of warfarin and coumatetralyl, temperature was varied from 5 to 45 °C. The van't Hoff plots for the retention factor of warfarin enantiomers in the presence of 5 % modifiers are shown in Figure 4.3a. The plots of ln k versus 1/T obtained in MeOH, *i*-BuOH, *t*-BuOH, and THF are linear $(r^2 = 0.990 - 0.999)$, suggesting that the change in molar enthalpy is independent of temperature in this range. Similarly, the van't Hoff plots for the chiral selectivity of warfarin enantiomers in the presence of 5 % modifiers are shown in Figure 4.3b. The plots of ln α versus 1/T are linear $(r^2 = 0.996 - 0.999)$ for MeOH, *i*-BuOH, and THF, but nonlinear $(r^2 = 0.965)$ for *t*-BuOH. It is interesting

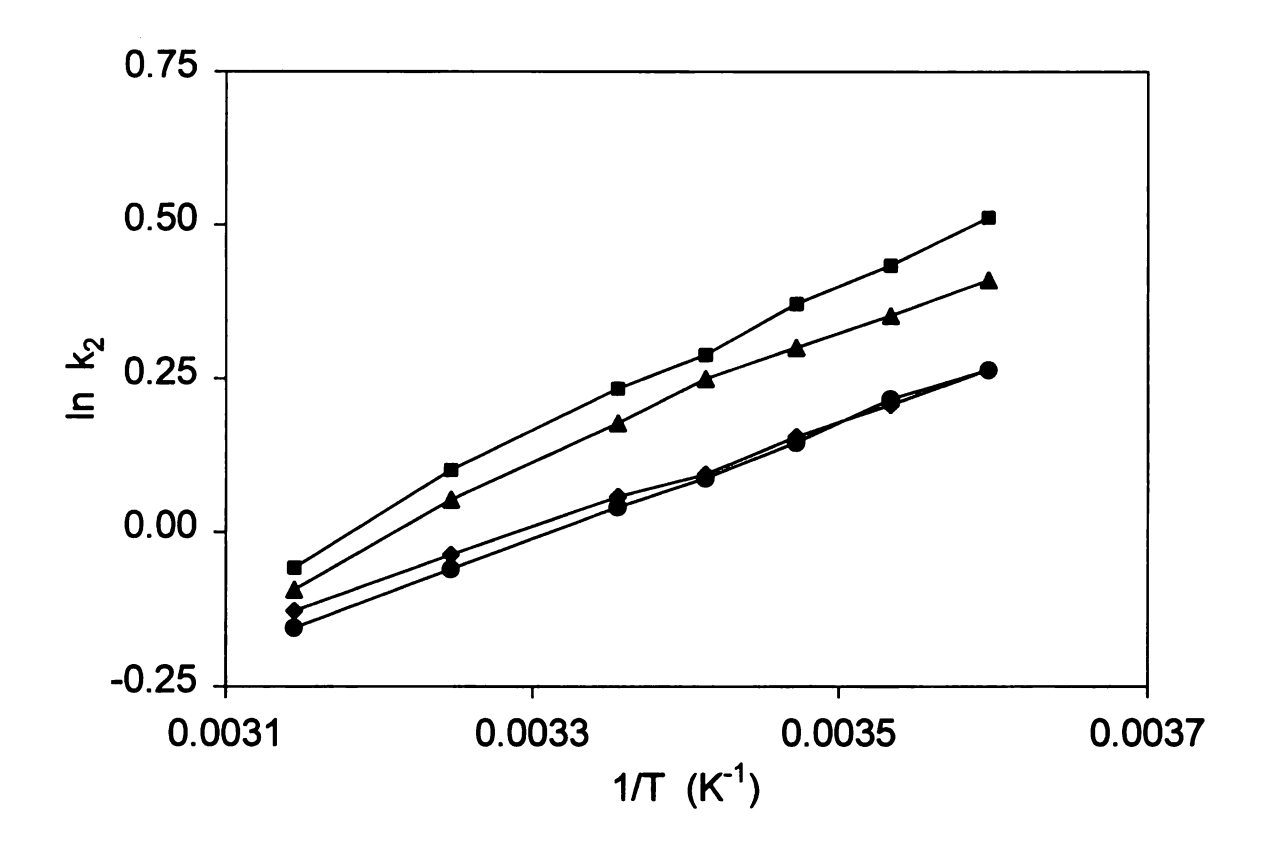


Figure 4.3a. Natural logarithm of the retention factor of the second eluted enantiomer (k_2) versus inverse temperature (1/T) for warfarin enantiomers in the presence of 5 % modifiers. MeOH (\bullet) , *i*-BuOH (\diamond) , *t*-BuOH (\blacktriangle) , and THF (\blacksquare) . Other experimental conditions as given in Figure 4.1.

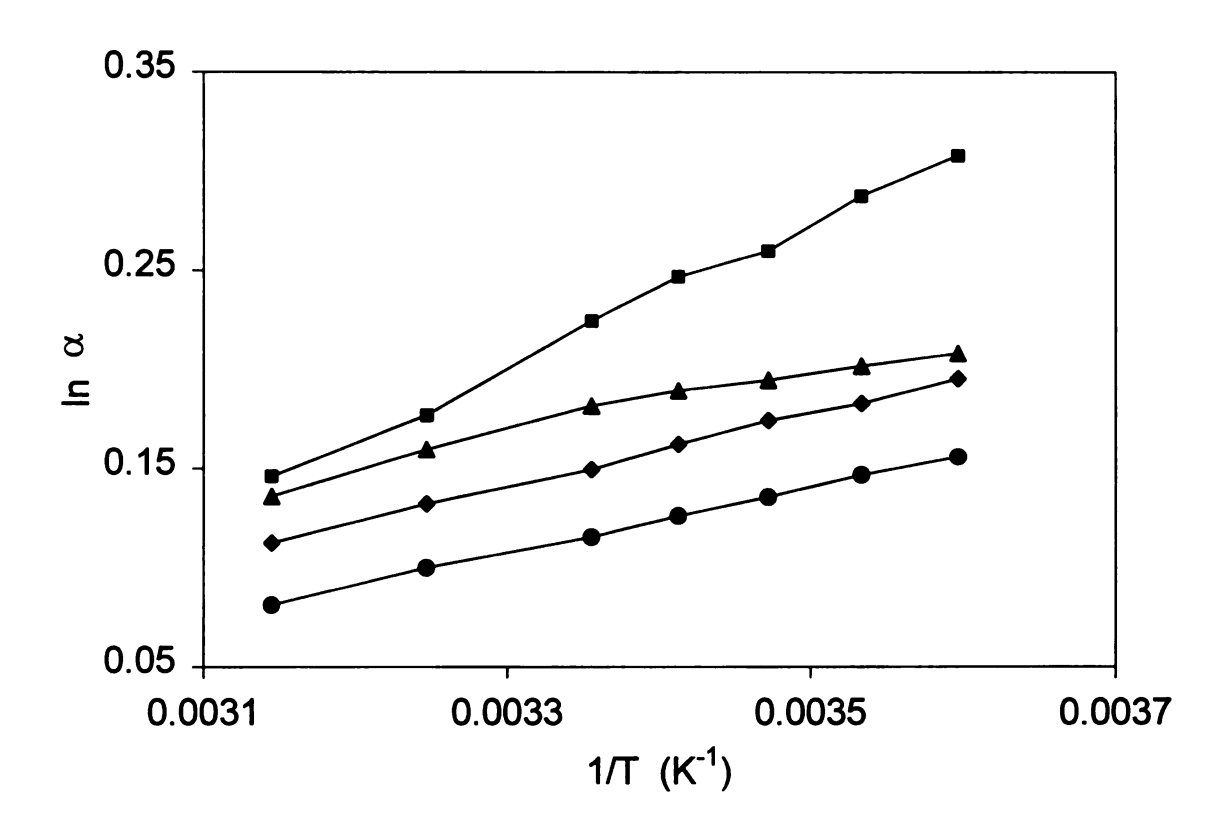


Figure 4.3b. Natural logarithm of selectivity (α) versus 1/T for warfarin enantiomers in the presence of 5 % modifiers. MeOH (\bullet), *i*-BuOH (\bullet), *t*-BuOH (Δ), and THF (Δ). Other experimental conditions as given in Figure 4.1.

to note that the slope of the nonlinear van't Hoff plot for t-BuOH changes around room temperature. In fact, better correlations ($r^2 > 0.99$) are obtained when the plots are taken in the low (5 – 20 °C) and high (25 – 45 °C) temperature regions separately.

The van't Hoff plots for the retention factor of coumatetralyl enantiomers with 5 % modifiers are shown in Figure 4.4a. The plots of ln k versus 1/T are linear ($r^2 = 0.997 - 0.999$) for MeOH, *i*-BuOH, and THF. For *t*-BuOH, the plot has a slightly different trend for the low (5 – 20 °C) and high temperature (25 – 45 °C) regions and, hence, is considered to be nonlinear despite an acceptable value of the correlation coefficient ($r^2 = 0.989$). However, the plots are linear ($r^2 = 0.999$) when data for the low and high temperature regions are plotted separately. Similarly, the van't Hoff plots for the chiral selectivity of coumatetralyl enantiomers with 5 % modifiers are shown in Figure 4.4b. The plots of ln α versus 1/T are linear ($r^2 = 0.996$) in *i*-BuOH, but nonlinear in MeOH, *t*-BuOH, and THF modifiers. In the low temperature region, these plots are linear for MeOH and *t*-BuOH, while in the high temperature region, the plots are linear for *t*-BuOH and THF.

Nonlinear van't Hoff plots are usually attributed to changes in the retention mechanism or conformation of the stationary phase^{11, 18-20}. When such changes are observed, the thermodynamic parameters are no longer independent of

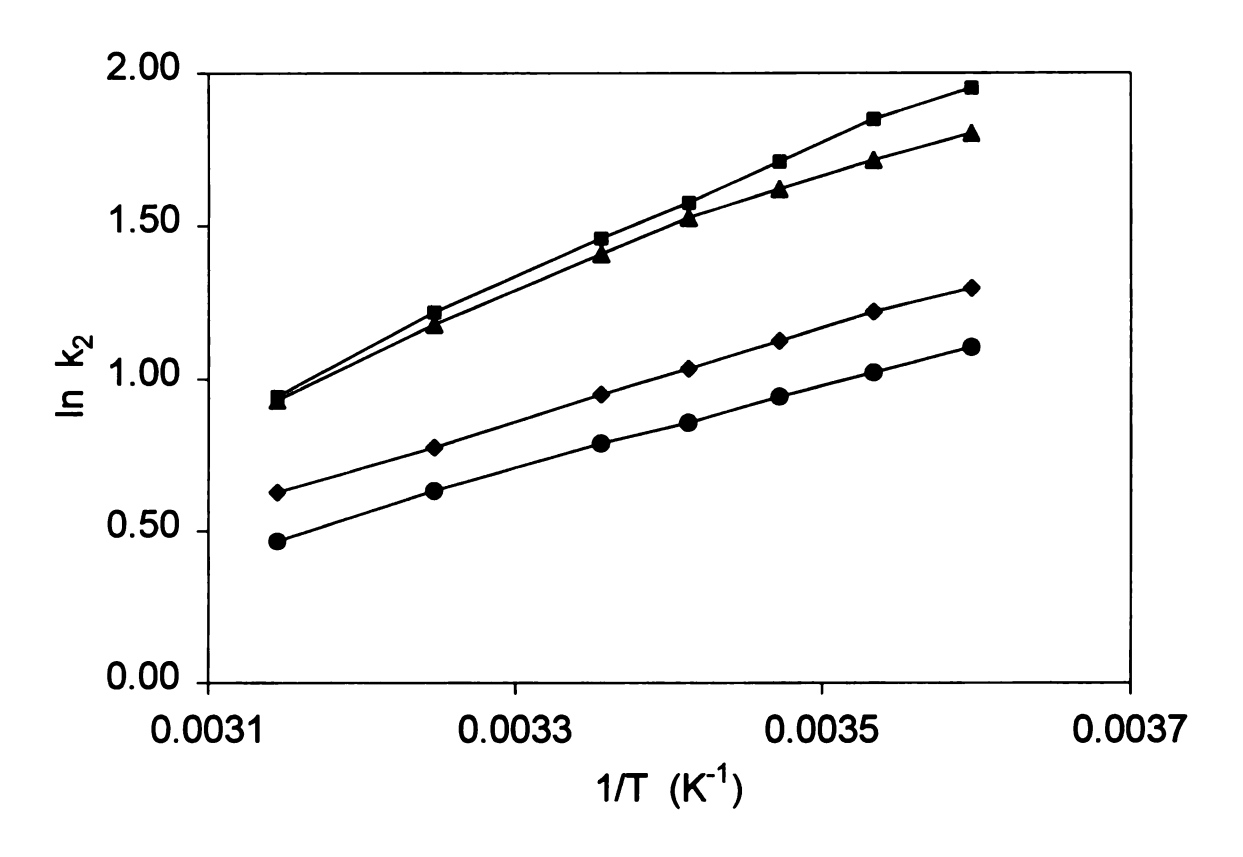


Figure 4.4a. Natural logarithm of the retention factor of the second eluted enantiomer (k_2) versus inverse temperature (1/T) for coumatetrally enantiomers in the presence of 5 % modifiers. MeOH (\bullet) , *i*-BuOH (\bullet) , *t*-BuOH (\blacktriangle) , and THF (\blacksquare) . Other experimental conditions as given in Figure 4.1.

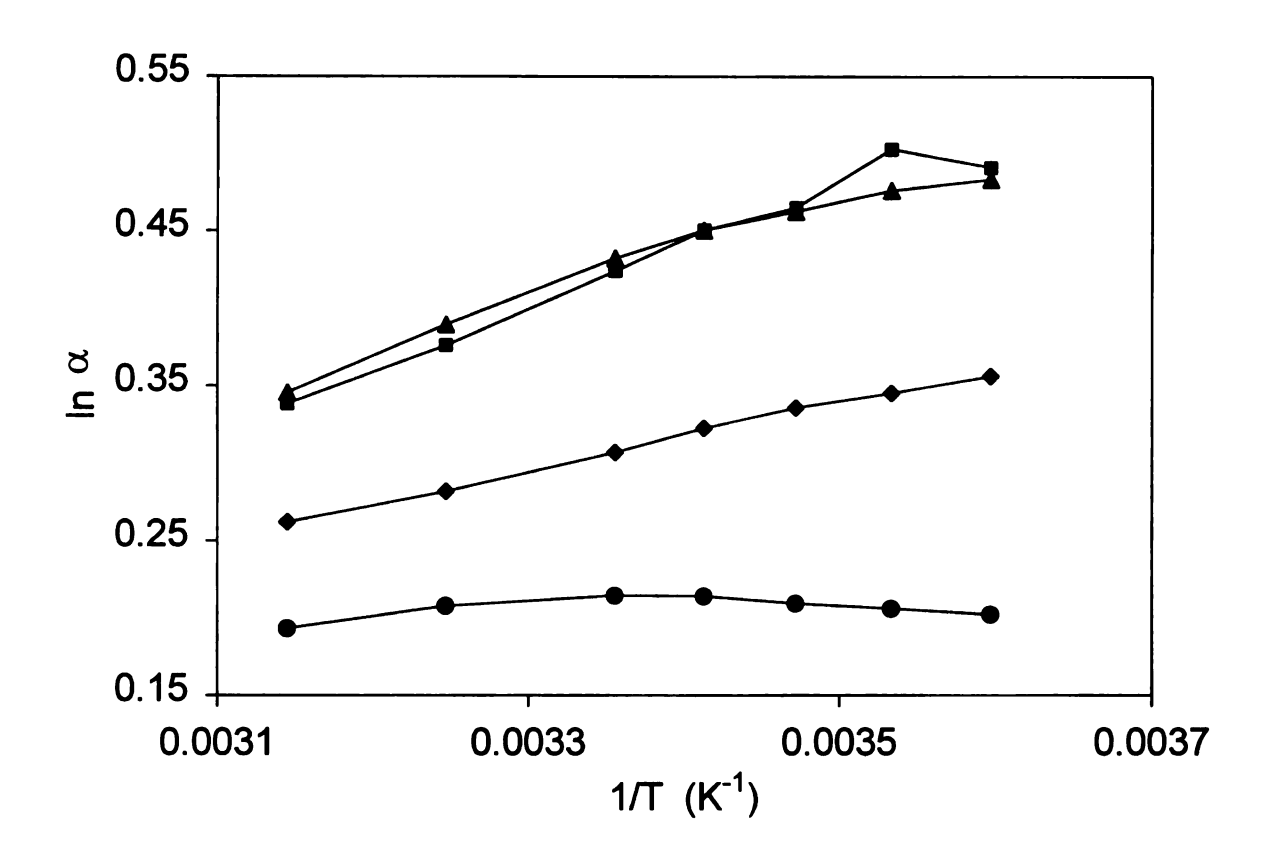


Figure 4.4b. Natural logarithm of selectivity (α) versus 1/T for coumatetralyl enantiomers in the presence of 5 % modifiers. MeOH (\bullet), *i*-BuOH (\bullet), *t*-BuOH (Δ), and THF (Δ). Other experimental conditions as given in Figure 4.1.

temperature. For nonlinear plots of ln α , $\Delta\Delta H$ values are estimated from the differences of ΔH_2 and ΔH_1 , and $\Delta\Delta S$ values are estimated from the corresponding intercepts.

The thermodynamic parameters obtained from the slopes of the van't Hoff plots for the warfarin enantiomers are shown in Table 4.6. The change in molar enthalpy for both enantiomers becomes more negative (favorable) as the proton donating ability of the alcohol modifiers decreases. However, the $\Delta\Delta H$ and T $\Delta\Delta S$ values between the enantiomers are statistically comparable in the alcohol modifiers. In THF, the second enantiomer has much stronger interaction with the stationary phase, as evidenced by its greater negative change in molar enthalpy. The $\Delta\Delta H$ contribution to the free energy is consequently the most favorable in THF, but the T $\Delta\Delta S$ contribution is the least favorable. This might suggest that the extent of solvation of the warfarin enantiomers by THF in the stationary phase is comparable.

The thermodynamic parameters obtained for the coumatetralyl enantiomers are shown in Table 4.7. Some of the trends observed with the modifiers are similar to those noted above for warfarin. For example, the change in molar enthalpy generally becomes more negative for the coumatetralyl enantiomers as the proton donating ability of the alcohol modifiers decreases. Again, the most negative values are observed in THF, a proton acceptor. However, some trends are notably different. For example, the differential changes in molar enthalpy, entropy, and free energy become increasingly more

Table 4.6. Thermodynamic parameters for warfarin in different modifiers. Other experimental conditions as given in Table 4.1.

Modifier (5%)	ΔH ₁ ^{a,b} (kJ/mol)	ΔH ₂ ^{a,b} (kJ/mol)	ΔΔΗ ^c (kJ/mol)	Τ ΔΔS ^C (kJ/mol)	∆∆G (kJ/mol)
MeOH	-5.77± 0.08	-7.11 ± 0.08	-1.37 ± 0.02	-1.04 ± 0.02	-0.33 ± 0.04
<i>i</i> -BuOH	-6.2 ± 0.1	-7.7 ± 0.1	-1.50 ± 0.04	-1.13 ± 0.04	-0.38 ± 0.04
t-BuOH	-7.9 ± 0.3	-9.2 ± 0.4	-1.3 ± 0.5 ^d	-0.9 ± 0.1 ^e	-0.4 ± 0.5
THF	-7.2 ± 0.3	-10.3 ± 0.3	-3.01 ± 0.08	-2.42 ± 0.08	-0.58 ± 0.12

^aSubscripts denote the first (1) and second (2) eluted enantiomers

^bCalculated from the slope of Equation 13

^cCalculated from the slope and intercept of Equation 14 at T_{hm} (294.6 K, 21.6 °C), except as noted

^dNonlinear van't Hoff plot, calculated as $\Delta H_2 - \Delta H_1$

^eNonlinear van't Hoff plot, calculated as T [(Δ S/R – In β)₂ – (Δ S/R – In β)₁] at T_{hm}

Table 4.7. Thermodynamic parameters for coumatetralyl in different modifiers. Other experimental conditions as given in Table 4.1.

Modifier (5%)	ΔH ₁ ^{a,b} (kJ/mol)	ΔH2 ^{a,b} (kJ/mol)	ΔΔΗ ^C (kJ/mol)	Τ ΔΔS ^C (kJ/mol)	ΔΔG (kJ/mol)
MeOH	-11.5 ± 0.1	-11.6 ± 0.2	-0.1 ± 0.2 ^d	0.4 ± 0.3 ^e	-0.5 ± 0.4
<i>i</i> -BuOH	-10.7 ± 0.1	-12.4 ± 0.2	-1.80 ± 0.04	-1.00 ± 0.04	-0.75 ± 0.08
t-BuOH	-13.4 ± 0.5	-16.0 ± 0.7	-2.55 ± 0.21 ^d	-1.50 ± 0.21	-1.04 ± 0.29
THF	-15.4 ± 0.4	-18.5 ± 0.5	-3.09 ± 0.6^{d}	-2.01 ± 0.6 ^e	-1.08 ± 0.8

^a Subscripts denote the first (1) and second (2) eluted enantiomers

^b Calculated from the slope of Equation 13

^c Calculated from the slope and intercept of Equation14 at T_{hm} (294.6 K, 21.6

[°]C), except as noted

d Nonlinear van't Hoff plot, calculated as $\Delta H_2 - \Delta H_1$

^e Nonlinear van't Hoff plot, calculated as T [$(\Delta S/R - \ln \beta)_2 - (\Delta S/R - \ln \beta)_1$] at T_{hm}

negative in the alcohols, but are statistically comparable for t-BuOH and THF. Both t-BuOH and THF have different solvent properties (Table 4.2), but their size is comparable. The fact that $\Delta\Delta$ H and T $\Delta\Delta$ S have comparable magnitude in these two modifiers suggests that bulky size of the modifiers may play an important role in the separation of coumatetrallyl enantiomers.

The effect of increasing the modifier concentration to 10 % is also investigated. When 10 % of each of the modifiers is used, van't Hoff plots for the retention factor of warfarin enantiomers are linear ($r^2 = 0.992 - 0.998$) in the alcohol modifiers, but nonlinear ($r^2 = 0.968$) for the more strongly retained enantiomer in THF (Figure 4.5a). In contrast, the van't Hoff plots for the chiral selectivity are linear only in MeOH, where the solute is least retained (Figure 4.5b). Similarly, the van't Hoff plots for the retention factor of coumatetralyl enantiomers are linear ($r^2 = 0.983 - 0.997$) in the alcohol modifiers, but nonlinear $(r^2 = 0.965)$ for the more strongly retained enantiomer in THF (Figure 4.6a). However, the van't Hoff plots for the chiral selectivity are nonlinear for all modifiers (Figure 4.6b). Taken together, these results suggest that the stationary phase undergoes a conformational change that occurs between 20 and 25 °C. This change is readily evident at 5 % concentration for bulky modifiers such as t-BuOH and THF, and for all modifiers at 10 % concentration. Such conformational changes have implications for the reproducibility of chiral separations and may influence chiral method development and validation.

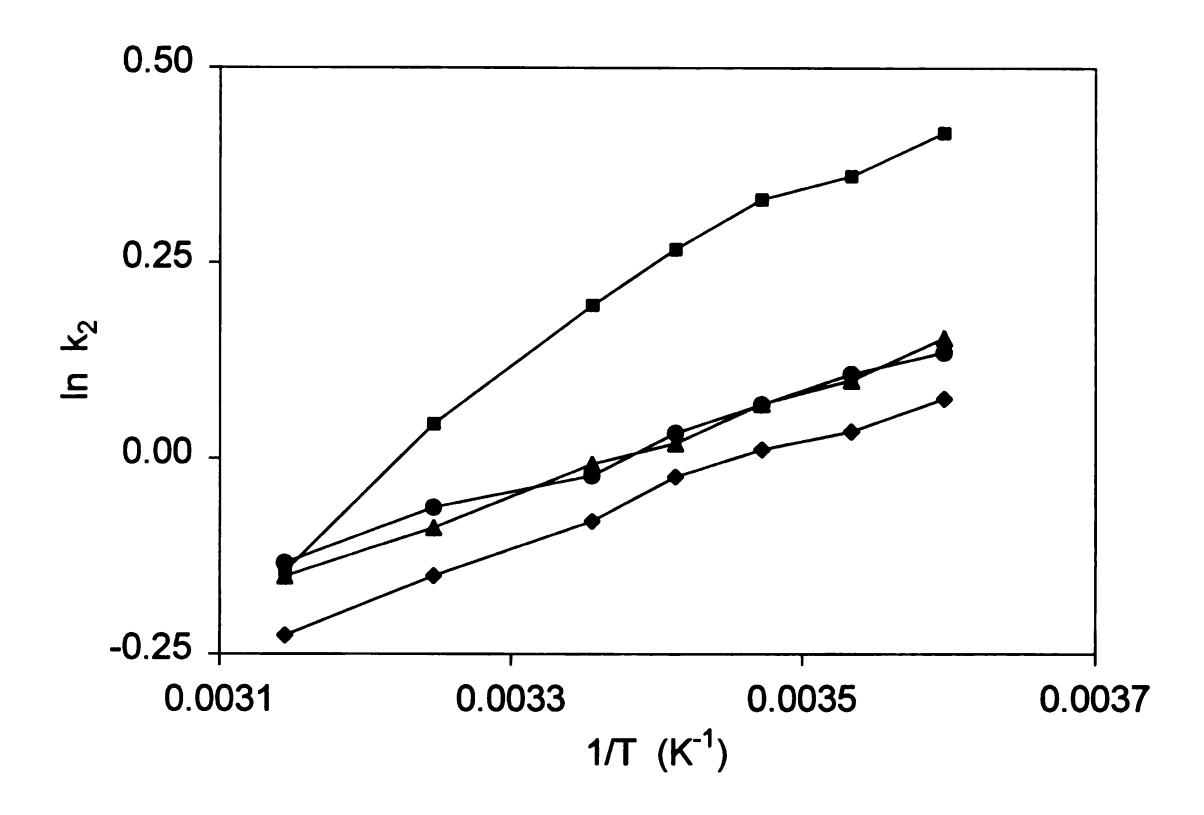


Figure 4.5a. Natural logarithm of the retention factor of the second eluted enantiomer (k_2) versus inverse temperature (1/T) for warfarin enantiomers in the presence of 10 % modifiers. MeOH (\bullet) , *i*-BuOH (\bullet) , *t*-BuOH (\blacktriangle) , and THF (\blacksquare) . Other experimental conditions as given in Figure 4.1.

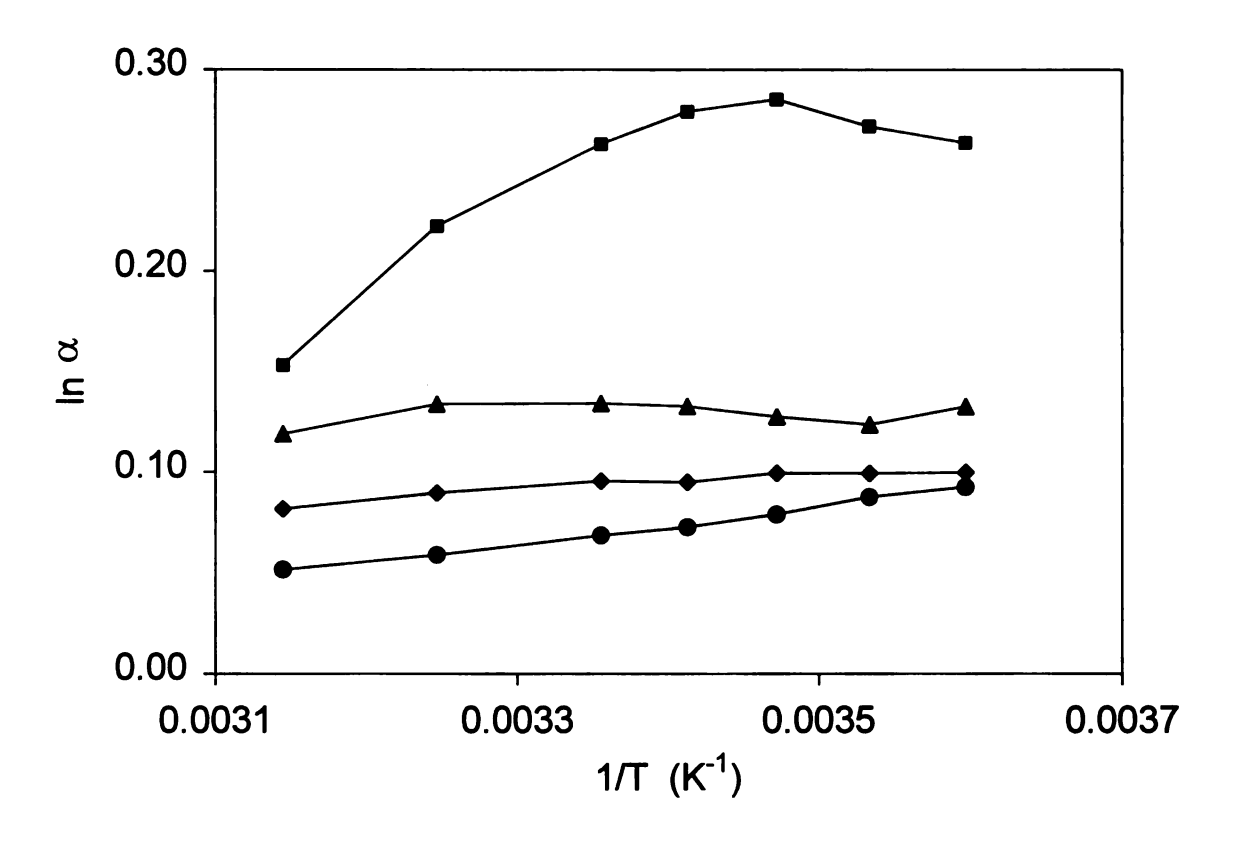


Figure 4.5b. Natural logarithm of selectivity (α) versus 1/T for warfarin enantiomers in the presence of 10 % modifiers. MeOH (\bullet), *i*-BuOH (\bullet), *t*-BuOH (\bullet), and THF (\blacksquare). Other experimental conditions as given in Figure 4.1.

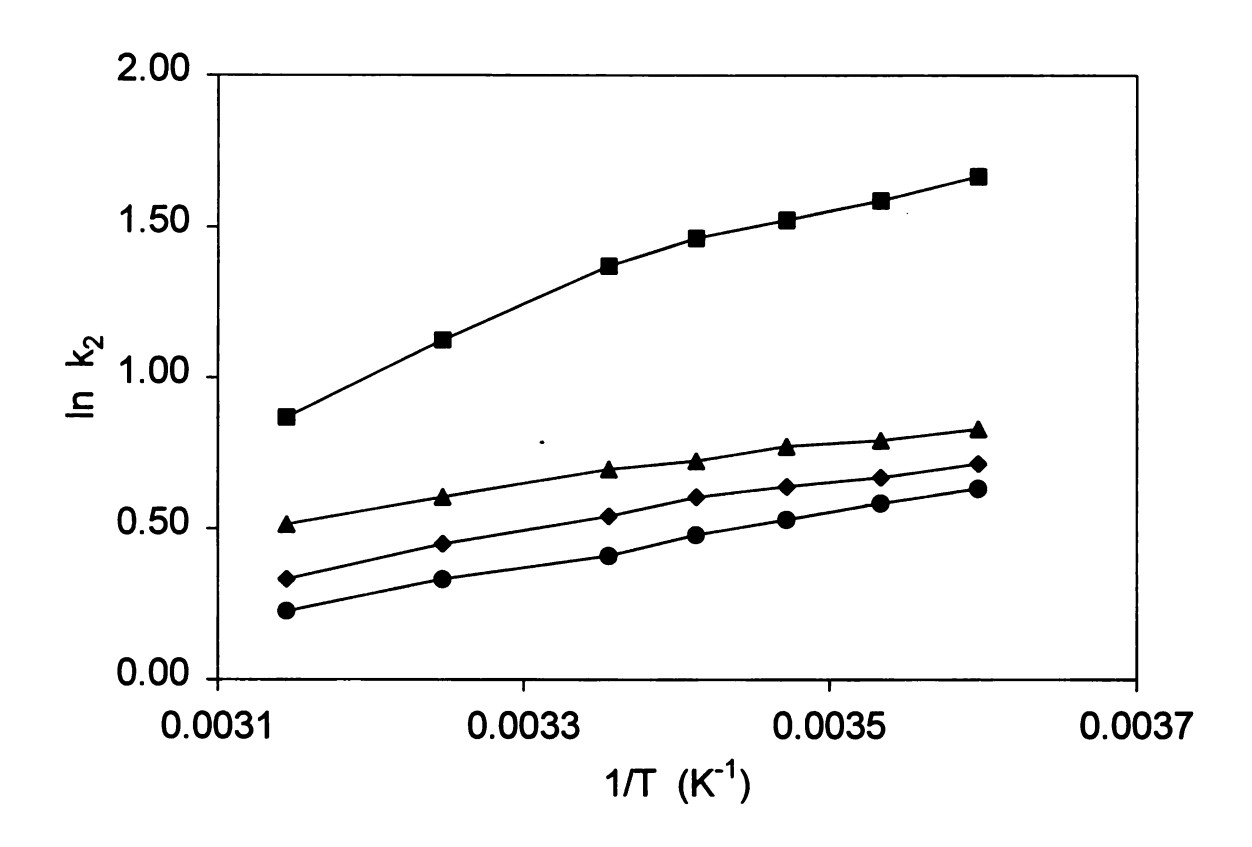


Figure 4.6a. Natural logarithm of the retention factor of the second eluted enantiomer (k_2) versus inverse temperature (1/T) for coumatetrally enantiomers in the presence of 10% modifiers. MeOH (\bullet) , *i*-BuOH (\bullet) , *t*-BuOH (Δ) , and THF (\blacksquare) . Other experimental conditions as given in Figure 4.1.

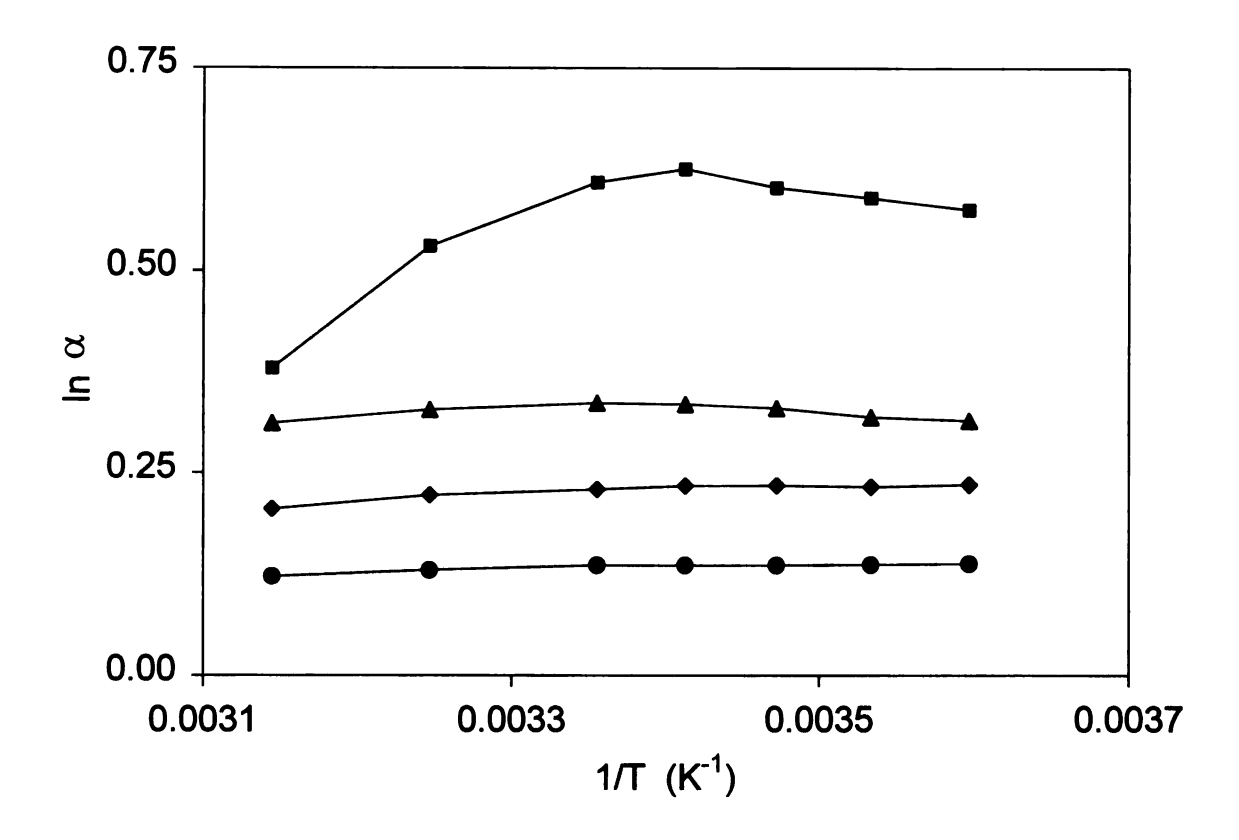


Figure 4.6b. Natural logarithm of selectivity (α) versus 1/T for coumatetralyl enantiomers in the presence of 10 % modifiers. MeOH (\bullet), *i*-BuOH (\bullet), *t*-BuOH (\bullet), and THF (\blacksquare). Other experimental conditions as given in Figure 4.1.

4.3.1.4. Enthalpy—entropy compensation (EEC)

Enthalpy–entropy compensation is usually expressed as the linear correlation between enthalpy (ΔH) and entropy (ΔS) for a series of related processes. ^{38–40}

$$\Delta H = T_C \Delta S + \Delta G_{T_C}$$
 (15)

where T_c is the compensation temperature and represents the temperature at which ΔH and ΔS are completely compensated, i.e., the temperature at which there is no chiral selectivity. Krug et al.^{38, 39} have shown that linear plots of enthalpy—entropy data may arise by propagation of measurement errors rather than a real EEC effect. When real EEC exists, plots of ΔG versus ΔH must provide a linear plot. These linear plots are usually indicative of compensation resulting from similar interactions between the solute and stationary phase.⁴⁰ When Equation 15 is substituted into the definition of Gibbs free energy ($\Delta G = \Delta H - T\Delta S$),

$$\Delta G = \Delta H \left[1 - \frac{T}{T_C} \right] + \frac{T \Delta G_{T_C}}{T_C}$$
 (16)

Upon substituting Equation 16 into the relationship between Gibbs free energy and retention factor in Equation 13,

$$\ln k = \frac{-\Delta H}{R} \left[\frac{1}{T_{hm}} - \frac{1}{T_C} \right] - \frac{\Delta G_{T_C}}{RT_C} + \ln \beta$$
 (17)

where T_{hm} is the harmonic mean of the absolute temperature (<1/T>-1) for the experimental data. Equation 17 shows that if compensation occurs, a plot of ln k versus $-\Delta H$ will be linear, and the slope of the line contains information to

determine the compensation temperature. If the compensation temperature is sufficiently higher than the ambient temperature, the separation is usually considered to be enthalpy dominated.⁴¹ In contrast, if the compensation temperature is lower than the ambient temperature, the separation is entropy dominated.⁴¹ At values close to the compensation temperature, enantioseparations cannot be obtained.

To compare the mechanism of separation of all coumarin solutes in Chiralpak IA, an enthalpy–entropy compensation plot is shown in Figure 4.7. The plot of ln k versus $-\Delta H$ is linear ($r^2 = 0.971$), which suggests that the coumarin enantiomers may have a similar retention mechanism in acetonitrile mobile phase. From the slope of this graph, the compensation temperature is 176 °C, indicating that the separation is enthalpy dominated. This confirms the thermodynamic results in Table 4.5.

The effect of modifiers on the separation of warfarin and coumatetralyl enantiomers is demonstrated by the enthalpy-entropy compensation plot in Figure 4.8. As can be seen, this graph is nonlinear ($r^2 = 0.889$) and no clear compensation is observed for warfarin or coumatetralyl. When the first and second eluted enantiomers are graphed separately, linear plots of ln k versus – ΔH are observed only for the second eluted enantiomers. The correlation coefficients for the first and second enantiomers of warfarin are found to be 0.632 and 0.948, respectively. Similarly, the correlation coefficients for the first and second enantiomers of coumatetralyl are 0.863 and 0.939, respectively. The

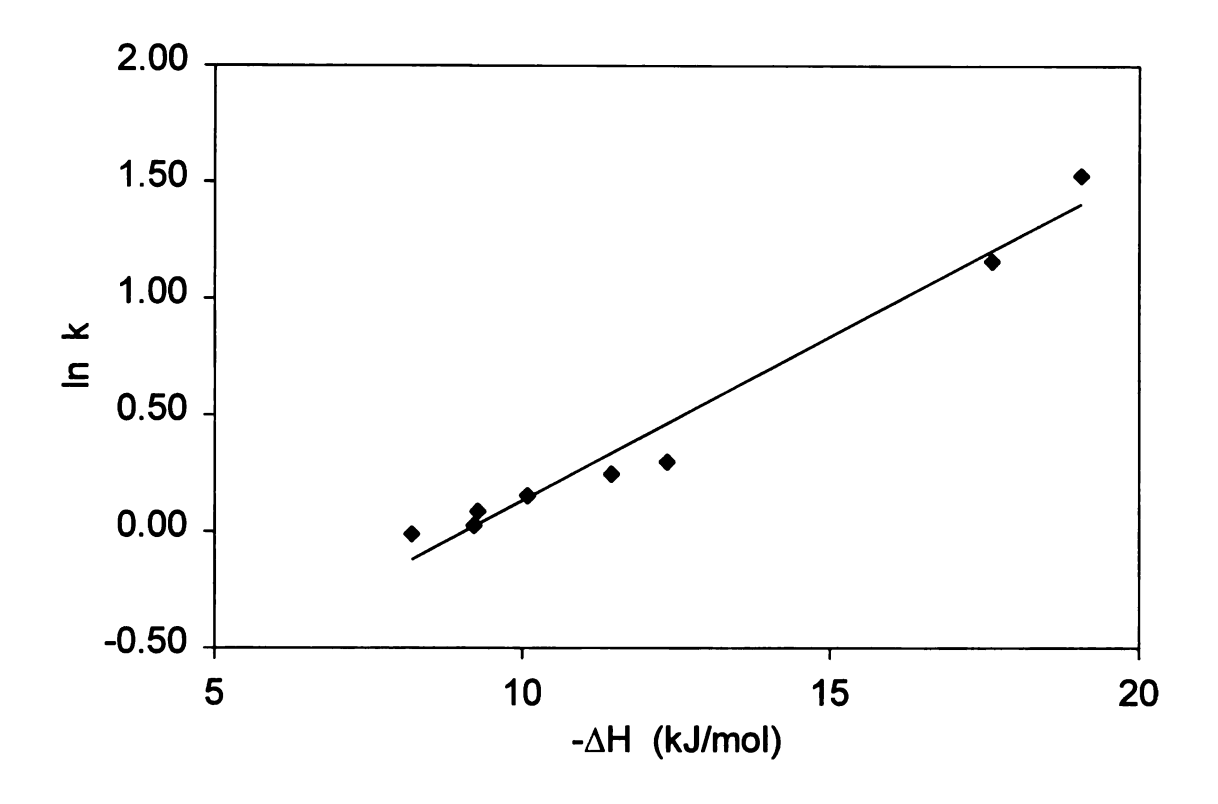


Figure 4.7. Enthalpy—entropy compensation plot of the natural logarithm of the retention factor (k) versus change in molar enthalpy $(-\Delta H)$ for all coumarin enantiomers in Figure 4.1. The equation of the line is $y = 1x10^{-4} x - 1.2719$ ($r^2 = 0.971$). Other experimental conditions as given in Figure 4.1.

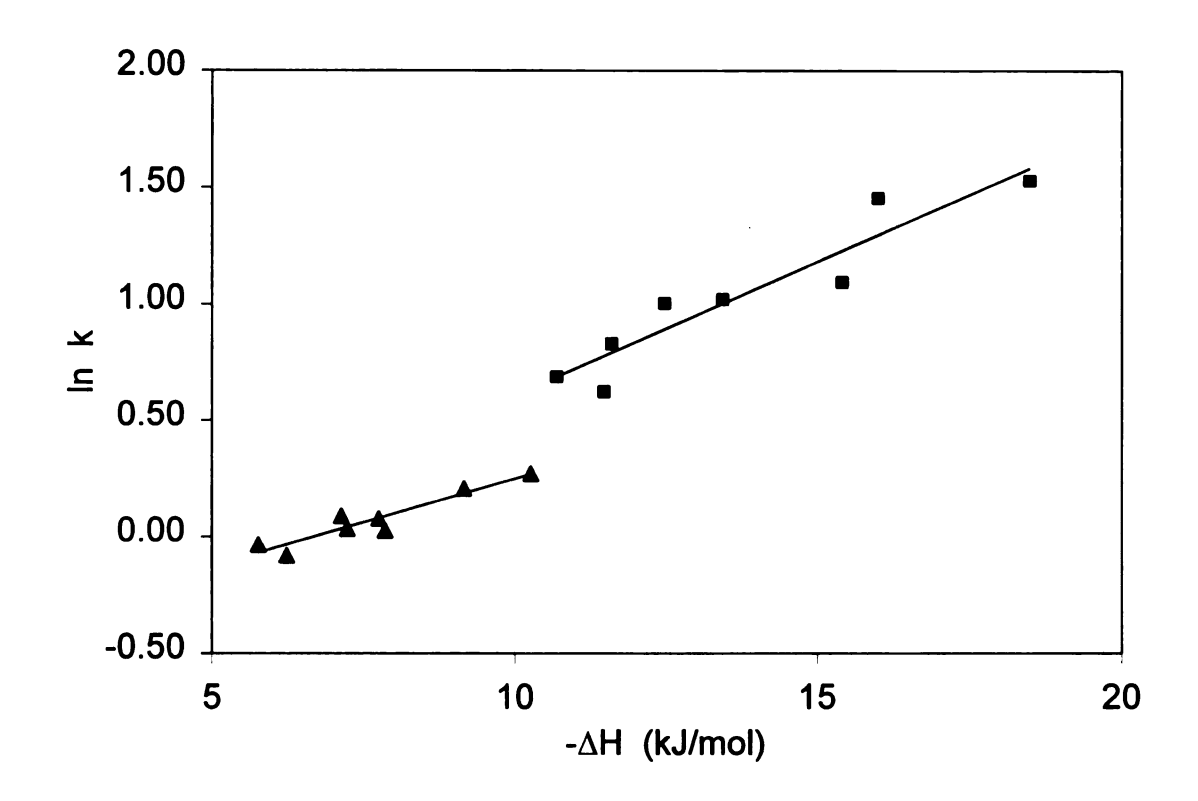


Figure 4.8. Enthalpy—entropy compensation plot of the natural logarithm of the retention factor (k) versus change in molar enthalpy ($-\Delta H$) for warfarin (\blacktriangle) and coumatetralyl enantiomers (\blacksquare) with 5 % of MeOH, *i*-BuOH, *t*-BuOH, and THF. The equation of the lines are: $y = 7x10^{-5} x - 0.503$ ($r^2 = 0.889$) for warfarin and $y = 1x10^{-4} x - 0.538$ ($r^2 = 0.889$) for coumatetralyl. Other experimental conditions as given in Figure 4.1.

compensation temperatures for the second eluted enantiomers are 77 °C for warfarin and 121 °C for coumatetralyl. These results suggest that the second eluted enantiomer of each solute has a similar retention mechanism in the presence of all organic modifiers (MeOH, *i*-BuOH, *t*-BuOH, THF), whereas thefirst eluted enantiomer does not. The second eluted enantiomers, necessarily, have greater interaction with the chiral interaction sites. Hence, these modifiers may have similar ability to displace or compete with the solutes at the chiral interaction sites.

4.3.2. KINETIC EFFECTS

The rate at which solute molecules undergo transfer between mobile and stationary phases is described by

$$X_{m} \xrightarrow{k_{sm}} X_{s} \tag{18}$$

where k_{sm} is the rate constant for transfer from mobile to stationary phase (sorption) and k_{ms} is the rate constant for transfer from stationary to mobile phase (desorption). The rate constants for sorption and desorption of chiral coumarins (warfarin, coumachlor, coumafuryl, and coumatetralyl) and an achiral coumarin (4-hydroxycoumarin) on Chiralpak IA using acetonitrile mobile phase are summarized in Table 4.8. In general, the rate constant for sorption is greater than that for desorption. For the first eluted enantiomer, the rates of sorption and desorption are fastest for coumafuryl and slowest for coumachlor. For the

Table 4.8. Sorption (k_{sm}) and desorption (k_{ms}) rate constants for coumarin enantiomers at 10 °C. Other experimental conditions as given in Table 4.1.

Solute	(k _{sm}) ₁ ^a (s ⁻¹)	(k _{ms}) ₁ (s ⁻¹)	(k _{sm}) ₂ ^a (s ⁻¹)	(k _{ms}) ₂ (s ⁻¹)
Warfarin	3.9	3.4	2.7	1.7
Coumachlor	0.9	0.8	1.6	1.0
Coumafuryl	11.0	8.6	2.5	1.8
Coumatetralyl	1.4	0.3	1.5	0.2
4-Hydroxycoumarin	0.2	0.04	N/A ^b	N/A
^a Subscripts denote the first (1) and second (2) eluted enantiomers ^b Not applicable				

first eluted enantiomer, the rates of sorption and desorption are fastest for coumafuryl and slowest for coumachlor. For the second eluted enantiomer, the rates are fastest and comparable for coumafuryl and warfarin, but slowest and comparable for coumachlor and coumatetralyl. The rate constants for the achiral solute, 4-hydroxycoumarin, are substantially smaller than those for the chiral coumarins. As noted in Section 4.3.1 above, 4-hydroxycoumarin does not have a substituent at the 3-position and, hence, can have simultaneous interactions of the hydroxyl and carbonyl groups with the stationary phase. This concerted adsorption may have slower kinetics than the isolated interactions of these groups in the chiral coumarins.

4.3.2.1. Effect of modifier type and concentration on rate constants

To investigate the effect of organic modifiers on the kinetics of the separation on Chiralpak IA, warfarin and coumatetralyl are chosen as probes. The desorption rate constants for warfarin enantiomers in varying modifier concentrations are summarized in Table 4.9 and are compared to values in the absence of modifier in Table 4.8. At 5 % modifier concentration, the desorption rate constants for both enantiomers are increased in all modifiers. This behavior is expected for modifiers that serve as better displacing or competing agents than acetonitrile for active sites on the derivatized amylose phase. For the first eluted enantiomer, the desorption rate constant is increased slightly in *i*-BuOH and *t*-BuOH and more substantially in MeOH and THF. Interestingly, the desorption

Table 4.9. Effect of concentration of modifier on desorption rate constants (k_{ms}) of warfarin enantiomers at 10 °C. Other experimental conditions as given in Table 4.1.

Modifier	5 %		10 %	
Modifier	(k _{ms}) ₁ ^a (s ⁻¹)	$(k_{ms})_2^a (s^{-1})$	$(k_{ms})_1^a (s^{-1})$	(k _{ms}) ₂ ^a (s ⁻¹)
MeOH	8.3	13.0	14.8	31.1
<i>i</i> -BuOH	4.5	10.5	10.5	14.2
t-BuOH	5.7	3.0	11.3	0.6
THF	7.2	2.5	1.6	1.4

^a Subscripts denote the first (1) and second (2) eluted enantiomers

rate constant for the first eluted enantiomer is faster than that for the second eluted enantiomer in *t*-BuOH and THF. For the second eluted enantiomer, the desorption rate constant is increased significantly in MeOH and *i*-BuOH, but decreased in *t*-BuOH and THF. The rate of mass transfer for the second eluted enantiomer increases with an increase in the hydrogen bonding ability of the modifiers. However, the same trend is not observed for the first eluted enantiomer. As the concentration of the modifier increases to 10 %, the desorption rate constant for the first enantiomer is found to increase further in the alcohol modifiers. In contrast, the desorption rate constant is decreased significantly in THF. For the second eluted enantiomer, the desorption rate constant is increased significantly in MeOH and *i*-BuOH, but decreased in *t*-BuOH and THF.

The desorption rate constants for coumatetralyl enantiomers in varying modifier concentrations are summarized in Table 4.10 and are compared to values in the absence of modifier in Table 4.8. At 5 % modifier concentration, the desorption rate constants for both enantiomers is increased substantially in all modifiers. The rate constants are comparable for the first and second eluted enantiomers for most modifiers, but somewhat smaller for the second eluted enantiomer in THF. As the concentration of the modifier increases to 10 %, the desorption rate constant of the first eluted enantiomer increases significantly. For the second eluted enantiomer, the desorption rate constant increases significantly in MeOH, *i*-BuOH, and *t*-BuOH, but decreases significantly in THF. It

Table 4.10. Effect of concentration of modifier on desorption rate constants (k_{ms}) of coumatetralyl enantiomers at 10 °C. Other experimental conditions as given in Table 4.1.

Modifier	5 %		10 %	
Modifier	$(k_{ms})_1^a (s^{-1})$	$(k_{ms})_2^a (s^{-1})$	$(k_{ms})_1^a (s^{-1})$	(k _{ms}) ₂ ^a (s ⁻¹)
MeOH	1.0	0.8	4.0	2.7
<i>i</i> -BuOH	1.3	1.0	2.6	2.9
t-BuOH	0.7	0.6	2.6	0.8
THF	1.2	0.6	3.2	0.09

^aSubscripts denote the first (1) and second (2) eluted enantiomer.

is interesting to note that the desorption rate constant of the second eluted enantiomer is reduced by 85 % as the concentration of THF increased from 5 to 10 %. Consequently, the desorption rate constant of the first eluted enantiomer is about 36 times faster than that for the second eluted enantiomer in 10 % THF. This observation might explain why the selectivity of coumatetralyl enantiomers increases from 1.46 in bulk acetonitrile to 1.87 in 10 % THF.

4.3.2.2. Effect of temperature on the rate constants and activation energy

When the solute is transferred between the mobile and stationary phases, it passes through a short-lived, high-energy transition state (‡) that uniquely characterizes the path-dependent aspects of the retention mechanism. The kinetic rate constant is related to the activation energy by means of the Arrhenius equation, ⁴²

$$lnk_{sm} = lnA_{\ddagger m} - \frac{\Delta E_{\ddagger m}}{RT}$$
 (19)

where $A_{\pm m}$ is the pre-exponential factor and $\Delta E_{\pm m}$ is the activation energy arising from the transition from mobile phase to transition state. The activation energy for the sorption process ($\Delta E_{\pm m}$) can be determined from the slope of ln k_{sm} versus 1/T, if $A_{\pm m}$ and $\Delta E_{\pm m}$ are independent of temperature. Likewise, the activation energy for the desorption process ($\Delta E_{\pm s}$) can be determined from the slope of ln k_{ms} versus 1/T, if $A_{\pm s}$ and $\Delta E_{\pm s}$ are independent of temperature. When one of these transitions is slow with respect to the mobile phase velocity, it will be

manifested chromatographically in the symmetric and asymmetric broadening of the solute zone. ³³

The Arrhenius plots for the desorption rate constant (ln k_{ms} versus 1/T) for the coumarin enantiomers in acetonitrile are shown in Figure 4.9. For all coumarins, the rates of desorption increase with an increase in temperature. The highest desorption rate is observed for coumafuryl, while the lowest is for 4hydroxycoumarin. A representative Arrhenius plot for the coumatetralyl enantiomers in the presence of 5% modifiers is illustrated in Figure 4.10 and corresponding values for the activation energy are summarized in Table 4.11. Figure 4.10 indicates a general trend of decrease in the activation energy with an increase in temperature. This result is consistent with the thermodynamic observation where changes in the slope are observed around room temperature. In all modifiers, the activation energy for sorption is lower than that for desorption for both enantiomers (Table 4.11). However, because of the uncertainty in these measurements, both enantiomers have statistically equivalent activation energies for sorption and, similarly, statistically equivalent activation energies for desorption. Moreover, with the exception of i-BuOH, the activation energies for sorption are comparable in all modifiers and, similarly, the activation energies for desorption are comparable in all modifiers. These results suggest that the rate of mass transfer in the chirally selective sites is comparable for both enantiomers.

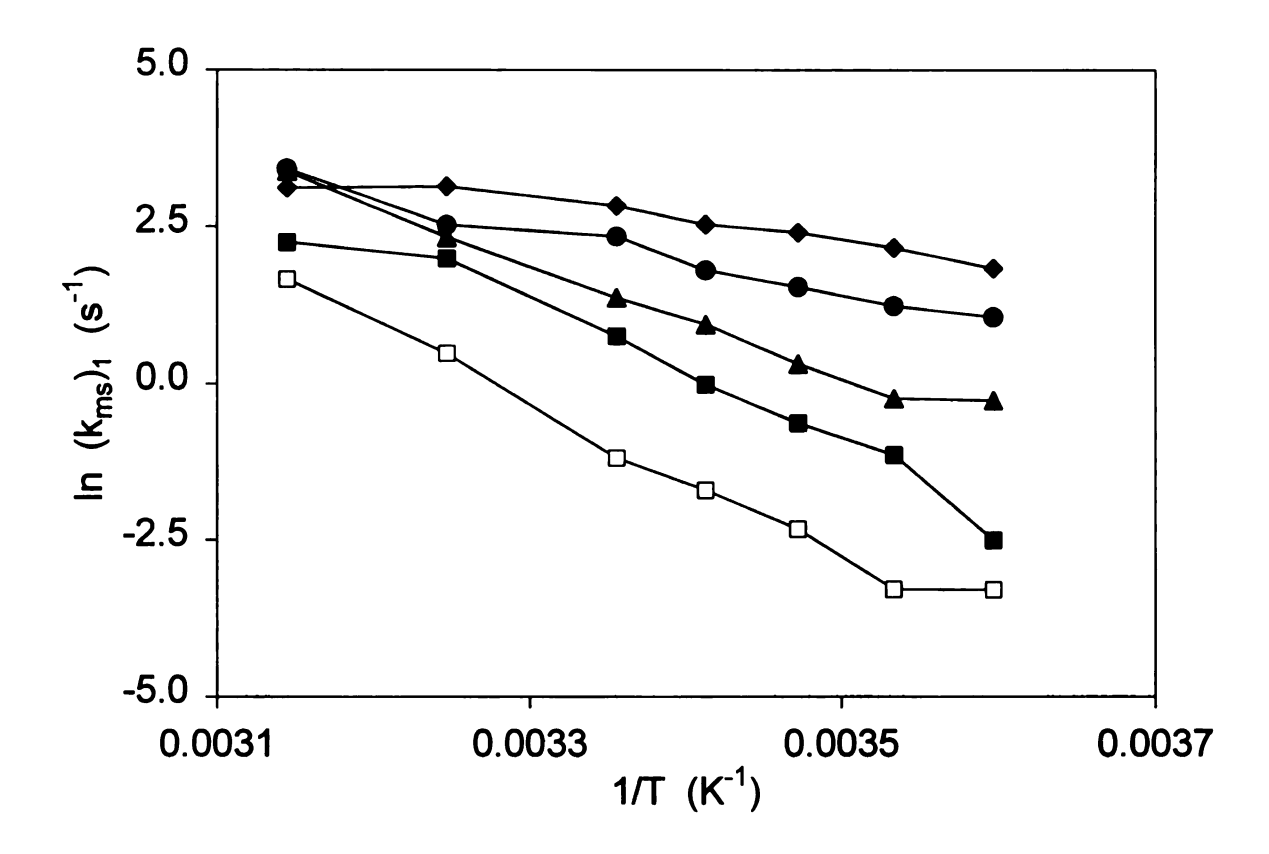


Figure 4.9 Natural logarithm of the desorption rate constant of the first eluted enantiomer (k_{ms1}) versus inverse temperature (1/T). Warfarin (\bullet), coumachlor (\blacktriangle), coumafuryl (\bullet), coumatetralyl (\blacksquare), and 4-hydroxycoumarin (\square). Other experimental conditions as given in Figure 4.1.

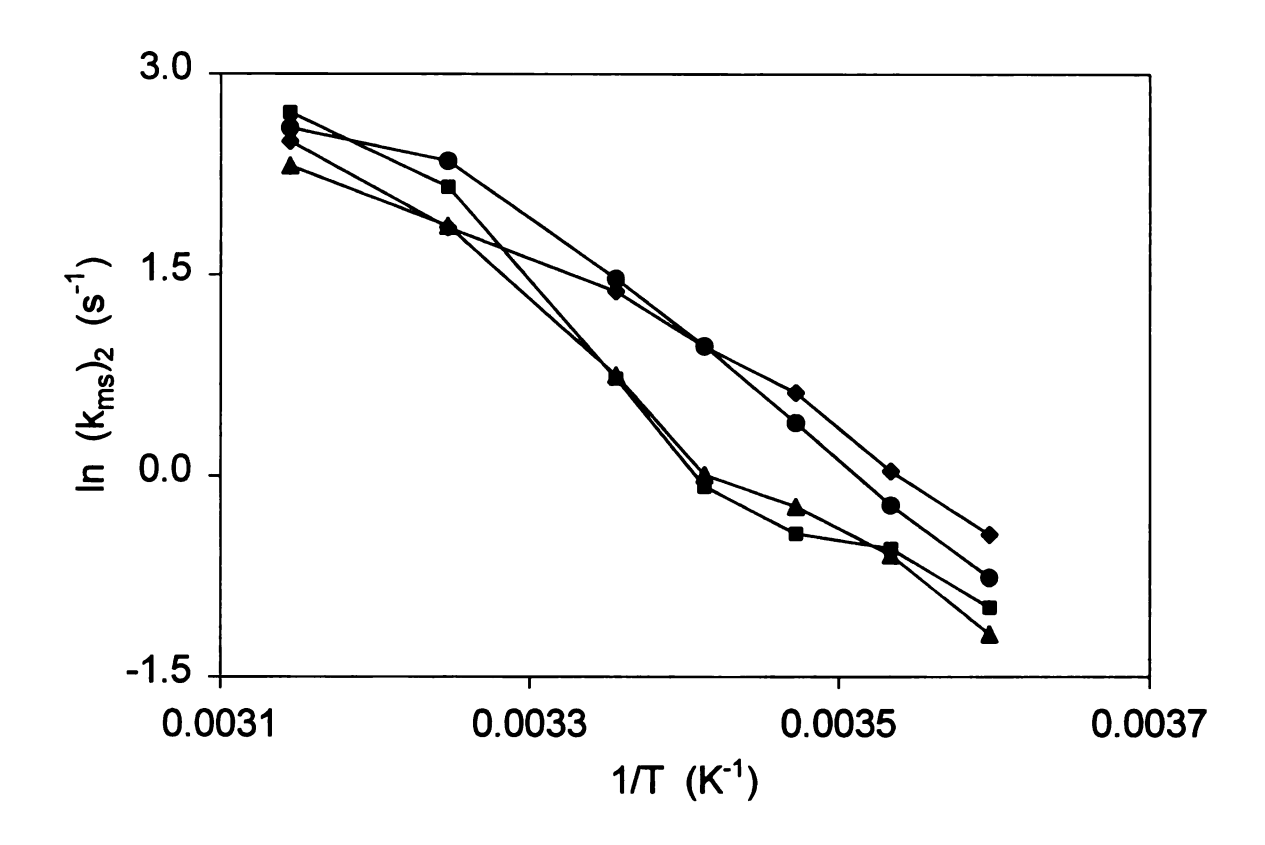


Figure 4.10. Arrhenius plots for coumatetralyl: natural logarithm of the desorption rate constant of the second eluted enantiomer (k_{ms2}) versus inverse temperature (1/T) in the presence of 5 % modifiers. MeOH (\bullet) , *i*-BuOH (\bullet) , *i*-BuOH (\bullet) , and THF (\blacksquare) . Other experimental conditions as given in Figure 4.1.

Table. 11. Comparison of activation energy for sorption ($\Delta E_{\ddagger m}$) and desorption ($\Delta E_{\ddagger s}$) processes of coumatetralyl enantiomers. Other experimental conditions as given in Table 4.1.

Modifier (5%)	(ΔE _{‡m}) ₁ ^{a,b} (kJ/mol)	(∆E _{‡s}) ₁ (kJ/mol)	(ΔE _{‡m})2 ^{a,b} (kJ/mol)	(∆E _{‡s}) ₂ (kJ/mol)
Acetonitrile	70 ± 8	87 ± 8	43 ± 4	63 ± 4
MeOH	50 ± 5	62 ± 5	53 ± 5	65 ± 5
<i>i</i> -BuOH	26 ± 3	35 ± 4	40 ± 3	53 ± 3
t-BuOH	49 ± 2	62 ± 2	51 ± 4	67 ± 4
THF	53 ± 5	68 ± 5	54 ± 7	73 ± 7

^a Subscripts denote the first (1) and second (2) eluted enantiomers
^b Calculated from the slope of Equation 19.

4.4. CONCLUSIONS

The effect of temperature and modifiers on the enantioseparation of coumarin-based solutes on Chiralpak IA stationary phase is studied for the coumarins in bulk acetonitrile indicate that coumatetralyl enantiomers have the most exothermic enthalpies and least exothermic entropies. The change in molar enthalpy and entropy induced by each mobile phase modifier varies greatly. Values of enthalpy in the presence of MeOH and *i*-BuOH are smaller than those in *t*-BuOH and THF. In general, retention and selectivity decrease as concentration and hydrogen bond donating ability of the alcohol modifier increases. As the concentration of THF increases, retention and chiral selectivity remain constant or increases for warfarin. On the other hand, retention decreases, while chiral selectivity increases for coumatetralyl enantiomers.

Temperature affects the thermodynamics and kinetics of the separation. Both retention and selectivity of coumarins decrease as the temperature increases. The thermodynamic values, estimated from van't Hoff plots, show linear and nonlinear behaviors. The nonlinear plots are attributed to conformational changes in the stationary phase and are observed between 20 and 25 °C. Enthalpy-entropy compensation plots obtained for coumarins in bulk acetonitrile mobile phase suggest that the separation mechanism may be similar. On the other hand, no compensation is observed for warfarin and coumatetralyl enantiomers separated in the presence of modifiers. This suggests that the mechanism of each warfarin and each coumatetralyl enantiomers are not identical.

The kinetic data demonstrate that the rate of sorption is always greater than the rate of desorption for all mobile phase compositions. An increase in the concentration of alcohol modifiers causes an increase in the rate of desorption suggesting that the alcohols are serving as displacing agents. In contrast, the rate of desorption decreases as the concentration of THF increases. Consequently, the rate of desorption of the second eluted enantiomer of coumatetralyl is decreased by about 55 % in 10 % THF. These thermodynamic and kinetic data provide some insight into the mechanism of chiral separations in Chiralpak IA.

4.5. REFERENCES

- (1) Okamoto, Y.; Kawashima, M.; Yamamoto, K.; Hatada, K. Chem. Lett. 1984, 739-742.
- (2) Okamoto, Y.; Aburatani, R.; Fukumoto, T.; Hatada, K. *Chem. Lett.* **1987**, 1857-1860.
- (3) Okamoto, Y.; Kawashima, M.; Hatada, K. *J. Am. Chem. Soc.* **1984**, *106*, 5357-5359.
- (4) Lynam, K. G.; Stringham, R. W. Chirality 2006, 18, 1-9.
- (5) Mangelings, D.; Maftouh, M.; Vander Heyden, Y. *J. Sep. Sci.* **2005**, *28*, 691-709.
- (6) Okamoto, Y.; Kaida, Y. *J. Chromatogr. A* **1994**, *666*, 403-419.
- (7) Okamoto, Y.; Yashima, E. *Angew. Chem. Int. Ed.* **1998**, *37*, 1020-1043.
- (8) Yashima, E. J. Chromatogr. A 2001, 906, 105-125.
- (9) Yashima, E.; Okamoto, Y. Bull. Chem. Soc. Jpn. 1995, 68, 3289 3307.
- (10) Zhang, T.; Kientzy, C.; Franco, P.; Ohnishi, A.; Kagamihara, Y.; Kurosawa, H. *J. Chromatogr. A* **2005**, *1075*, 65-75.
- (11) Pirkle, W. H. J. Chromatogr. 1991, 558, 1-6.
- (12) Booth, T. D.; Wainer, I. W. *J. Chromatogr. A* **1996**, *741*, 205-211.
- (13) Ming, Y. F.; Zhao, L.; Zhang, H. L.; Shi, Y. P.; Li, Y. M. *Chromatographia* **2006**, *64*, 273-280.
- (14) Smith, R. J.; Taylor, D. R.; Wilkins, S. M. *J. Chromatogr. A* **1995**, *697*, 591-596.
- (15) Weng, W.; Guo, H. X.; Zhan, F. P.; Fang, H. L.; Wang, Q. X.; Yao, B. X.; Li, S. X. *J. Chromatogr. A* **2008**, *1210*, 178-184.
- (16) Wang, F.; Yeung, D.; Han, J.; Semin, D.; McElvain, J. S.; Cheetham, J. Journal of Separation Science 2008, 31, 604-614.
- (17) Cirilli, R.; Del Giudice, M. R.; Ferretti, R.; La Torre, F. *J. Chromatogr. A* **2001**, 923, 27-36.
- (18) Kazusaki, M.; Kawabata, H.; Matsukura, H. *J. Liq. Chromatogr. & Rel. Technol.* **2000**, *23*, 2937-2946.

- (19) O'Brien, T.; Crocker, L.; Thompson, R.; Thompson, K.; Toma, P. H.; Conlon, D. A.; Feibush, B.; Moeder, C.; Bicker, G.; Grinberg, N. *Anal. Chem.* **1997**, *69*, 1999-2007.
- (20) Wang, F.; O'Brien, T.; Dowling, T.; Bicker, G.; Wyvratt, J. *J. Chromatogr. A* **2002**, *958*, 69-77.
- (21) Rizzi, A. M. J. Chromatogr. 1989, 478, 71-86.
- (22) Wenslow, R. M.; Wang, T. Anal. Chem. 2001, 73, 4190-4195.
- (23) Wang, F.; Wenslow, R. M.; Dowling, T. M.; Mueller, K. T.; Santos, I.; Wyvratt, J. M. *Anal. Chem.* **2003**, *75*, 5877-5885.
- (24) Kasat, R. B.; Zvinevich, Y.; Hillhouse, H. W.; Thomson, K. T.; Wang, N. H. L.; Franses, E. I. *J. Phys. Chem. B* **2006**, *110*, 14114-14122.
- (25) Chang, S. C.; Reid, I. G.; Chen, S.; Chang, C. D.; Armstrong, D. W. *Trends Anal. Chem.* **1993**, *12*, 144-153.
- (26) Chankvetadze, B.; Kartozia, I.; Yamamoto, C.; Okamoto, Y. J. Pharm. Biomed. Anal. 2002, 27, 467-478.
- (27) Gebreyohannes, K. G.; McGuffin, V. L. Submitted to J. Liq. Chromatogr. & Rel. Technol. 2010, 949, 41-51.
- (28) Gluckman, J. C.; Hirose, A.; McGuffin, V. L.; Novotny, M. *Chromatographia* **1983**, *17*, 303-309.
- (29) Howerton, S. B.; Lee, C.; McGuffin, V. L. *Analytica Chimica Acta* **2003**, *478*, 99-110.
- (30) Li, X. P.; McGuffin, V. L. *J. Liq. Chromatogr. Relat. Technol.* **2007**, *30*, 965-985.
- (31) McGuffin, V. L.; Evans, C. E. *Journal of Microcolumn Separations* **1991**, *3*, 513-520.
- (32) Li, X.; Hupp, A. M.; McGuffin, V. L., in: Grushka, E., Grinberg, N. (Eds.) Advances in chromatography, CRC Press, Boca Raton, FL 2007 2007.
- (33) Giddings, J. C. Dynamics of Chromatography, Part I: Principles and Theory, Dekker, Inc., NY 1965.
- (34) Vandeemter, J. J.; Zuiderweg, F. J.; Klinkenberg, A. *Chem. Eng. Sci.* **1956**, *5*, 271-289.
- (35) Kamlet, M. J.; Abboud, J. L. M.; Abraham, M. H.; Taft, R. W. *J. Org. Chem.* **1983**, *48*, 2877-2887.

- (36) Gidley, M. J.; Bociek, S. M. J. Am. Chem. Soc. 1988, 110, 3820-3829.
- (37) Wang, T.; Wenslow, R. M. J. Chromatogr. A 2003, 1015, 99-110.
- (38) Krug, R. R.; Hunter, W. G.; Grieger, R. A. *J. Phys. Chem.* **1976**, *80*, 2335-2341.
- (39) Krug, R. R.; Hunter, W. G.; Grieger, R. A. *J. Phys. Chem.* **1976**, *80*, 2341-2351.
- (40) Li, J. J.; Carr, P. W. J. Chromatogr. A 1994, 670, 105-116.
- (41) Yao, B. X.; Zhan, F. P.; Yu, G. Y.; Chen, Z. F.; Fan, W. J.; Zeng, X. P.; Zeng, Q. L.; Weng, W. J. Chromatogr. A 2009, 1216, 5429-5435.
- (42) Atkins, P. W. Physical Chemistry, 6th ed., W.H. Freeman, New York 1987.

CHAPTER 5

COMPUTATIONAL STUDIES ON SAMPLING OF WARFARIN ENANTIOMERS AND THEIR DOCKING INTERACTION WITH β -CYCLODEXTRIN

5.1. SAMPLING OF WARFARIN ENANTIOMERS

5.1.1. Introduction

Warfarin, the most common coumarin anticoagulant, is a drug used to treat blood clotting.¹ Anticoagulants inhibit the synthesis of calcium binding sites in blood clotting factors such as prothrombin, by blocking the vitamin K cycle that is vital for their biosynthesis.¹⁻⁴ Many studies reported the binding of warfarin to proteins such as human serum albumin (HSA), a principal carrier protein in serum.⁵⁻⁹. Crystallographic and spectroscopic results showed that warfarin binds to HSA, , in its ring opened anionic form (see Figure 3.3).^{7,8} Warfarin also binds at the active site of cytochrome P450 2C9 (CYP2C9), a hydrophobic environment, in its ring closed (hemiketal) form. ^{10, 11} In fact, this enzyme carries out most of the metabolic removal of S-warfarin from the body to its biologically inactive forms.¹⁰

Warfarin enantiomers have different pharmacological and pharmacokinetic behaviors. S-Warfarin is five times more potent as an anticoagulant than R-warfarin and binds more strongly with plasma proteins. 10,12,13 However, the exact reason is not known. Thermodynamic and kinetic studies on the binding of R-and S-warfarin to immobilized HSA as a stationary phase for liquid chromatography showed that the two enantiomers have different equilibrium constants and kinetics for their interactions. 14,15 The R- and S-warfarin

molecules interact with HSA binding sites located on the interior and exterior regions, respectively of subdomain IIA.⁸

The solvent environment also affects the retention properties of warfarin on common chiral stationary phases such as cyclodextrin and other polysaccharide phases. In native β -cyclodextrin stationary phase, S-warfarin is more retained than R-warfarin in an aqueous mobile phase, while the reverse is true in an acetonitrile-based mobile phase. 16,17

Computational studies such as molecular dynamics can provide thermodynamic and kinetic information about the effect of solvent environment on the conformational sampling of warfarin. This study employs a CHARMM (Chemistry at HARvard Macromolecular Mechanics)-style force field to simulate warfarin in water and acetonitrile and provide fundamental information on the effect of protonation state, orientation of phenyl group, and solvent environment on their thermodynamic stability, as well as the possibility of intramolecular hydrogen bonds. These results provide evidence for how R- and S-enantiomers might interact differently with a chiral selector.

5.1.2. Simulated systems and parameters

This simulates R- and S-warfarin enantiomers in three protonation states (4-OH, 2-OH, deprotonated (depr.), see Figure 5.1) in explicit acetonitrile and water solvents. Some of the initial structures of warfarin are taken from their

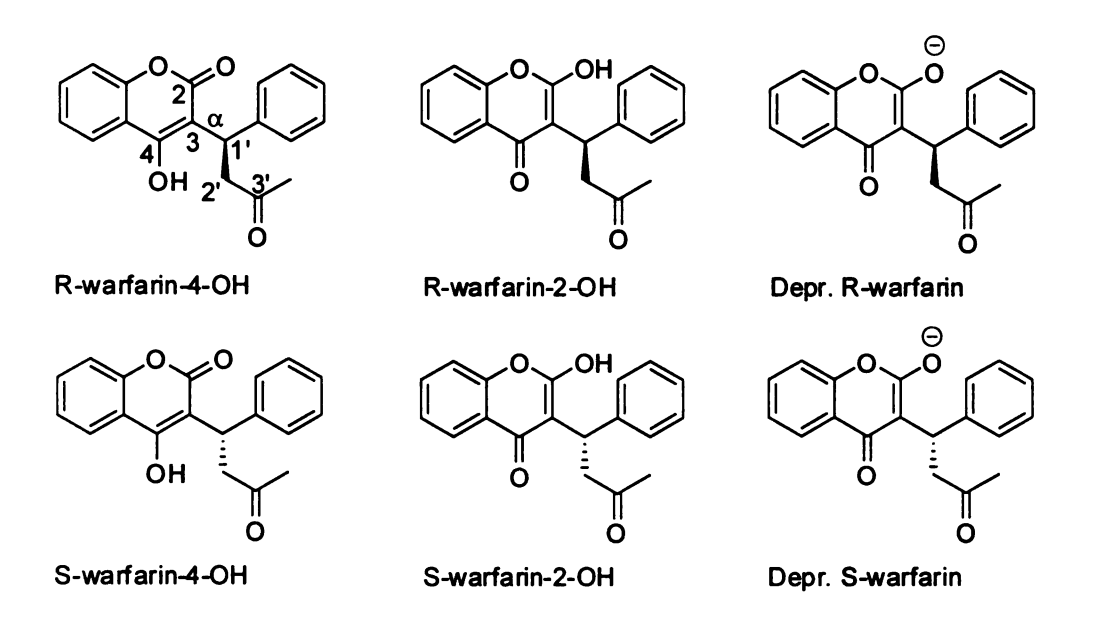


Figure 5.1. Structures of open side chain warfarin conformers

crystallographic data, ¹⁸ while others are constructed manually. Based on the orientation of the phenyl group relative to the plane of the coumarin ring, each warfarin enantiomer is further classified into two states. For state I, the phenyl group is above the plane of the coumarin ring and has a negative value of the torsion angle α (C4-C3-C1'-C2', Figure 5.1), while for state II, the phenyl group is below the coumarin ring and has a positive torsion angle α . All the warfarin forms are then solvated in a cubic box of pre-equilibrated acetonitrile (about 600 molecules) or water (about 1650 molecules). The initial simulation box sizes are about (36-37 Å)³.

Minimization of all simulated systems is carried out using the CHARMM program (version c36a1),¹⁹ together with the Multiscale Modeling Tools for Structural Biology Tool Set (MMTSB).²⁰ An equilibration step (heat up) of 4 ps at temperatures of 50, 100, 150, 200, 250 K and 10 ps at 298 K is performed before the production phase at 298 K. NAnoscale Molecular Dynamics (NAMD, version 2.6)²¹ is used to run the initial equilibration step and production phases. The simulations are performed with a 2 fs time step and at a constant temperature, pressure, and number of particles (NPT). For each warfarin form, the trajectory is then collected every 2 ps over the next 100 ns.

The interaction terms for the bonded and non-bonded (intra- and intermolecular) terms of the force field are described by using a CHARMM-style potential.²² This force field is given by

E_{Van der Waals}

where E is the total energy. The parameters for acetonitrile are obtained from a recently developed six-site model²³ and explicit water is described based on the CHARMM variant of the TIP3P model.^{22,24} For this work, a set of parameters for warfarin enantiomers are newly developed and are described in detail in a recently published article.²⁵

5.1.3. Umbrella sampling simulations

During the course of the unbiased 100 ns simulations, transitions between states I and II are not observed, suggesting that the two states have thermodynamic barriers. The relative free energies between states I and II and the height of their kinetic barriers are determined by running an umbrella sampling along the α dihedral angle (C4-C3-C1'-C2'). For both water and acetonitrile, umbrella sampling simulations are performed for R- and S-warfarin in the three protonation states. For each of the 500 ps simulations, a 10 degree increment is used to cover the entire region of 360 degree, for a total of 37 windows, with an overlap between the first and last windows. For each window, a harmonic biasing potential with a force constant of 10 kcal/mol/rad² is applied to the α dihedral angle. Data analysis is performed by applying the weighted histogram method (WHAM)^{26,27} developed by Grossfield.²⁸

5.1.4. Results and discussions

The flexibility of the torsion angle α (C4-C3-C1'-C2') results in state I (phenyl group above) or state II (phenyl group below) relative to the plane of the

coumarin ring (Figure 5.1). To determine the energy barriers between these two states, umbrella sampling is employed. Figures 5.2 and 5.3 show the resulting potentials of mean force in water and acetonitrile, respectively. It is interesting to see that the two states have comparable free energies but are separated by energy barriers on the orders of 10 kcal/mol, that correspond to kinetic rates in the micro- to millisecond range. The high kinetic barrier accounts for the absence of any transition between these states. Based on Figures 5.2 and 5.3, the relative free energies ($\Delta\Delta$ G) between states I and II in water and acetonitrile are shown in Table 5.1. In both water and acetonitrile, R-warfarin prefers state II over state II. For S-warfarin-4-OH in acetonitrile, state II is slightly more favorable in acetonitrile, but it is possible that the value might be an outlier.

The probability of intramolecular hydrogen bonding between the side chain carbonyl oxygen and the hydroxyl functional group on the coumarin ring (4-OH or 2-OH) is also examined. A hydrogen bond is usually formed when the hydrogen-oxygen distance is less than 3 Å and the angle among the donor atom, the hydrogen, and the acceptor atom is greater than 90 degrees.²⁹ For both R-and S-warfarin, the distance between HO4-O3 and HO2-O3 are analyzed for 4-OH and 2-OH protonation states, respectively (Figure 5.1). The effect of solvent polarity on the extent of hydrogen bonding is evident from Figures 5.4 and 5.5. For R/S-warfarin-2-OH, the potential of mean force for a bond distance of 3.0 Å is about 4.0 and 3.2 kcal/mol in water and acetonitrile, respectively (Figure 5.4).

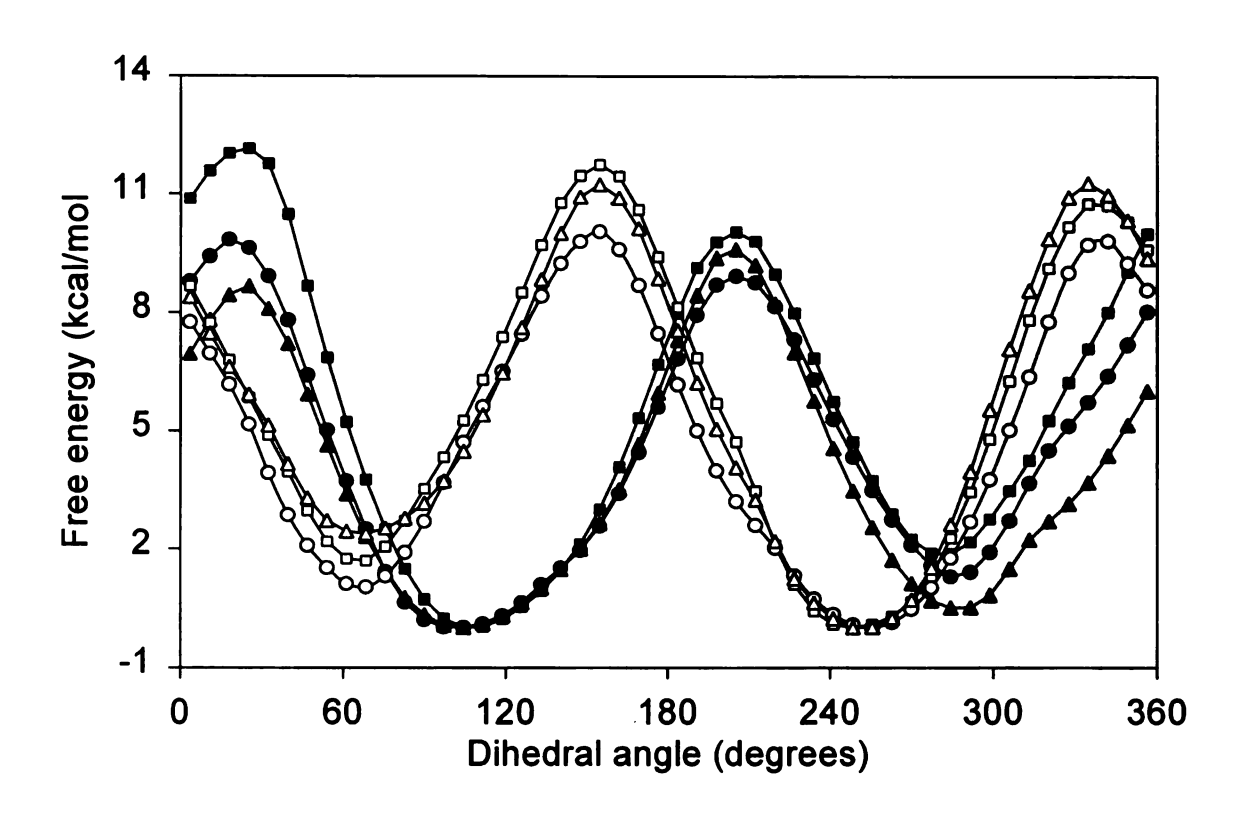


Figure 5.2. Potentials of mean force as a function of dihedral angle α (C4-C3-C1'-C2') from umbrella sampling of R- and S-warfarin in water. R,depr (\blacksquare); R-2OH (\bullet); R-4OH (Δ); S,depr (\square); S-2OH (\circ); S-4OH (Δ).

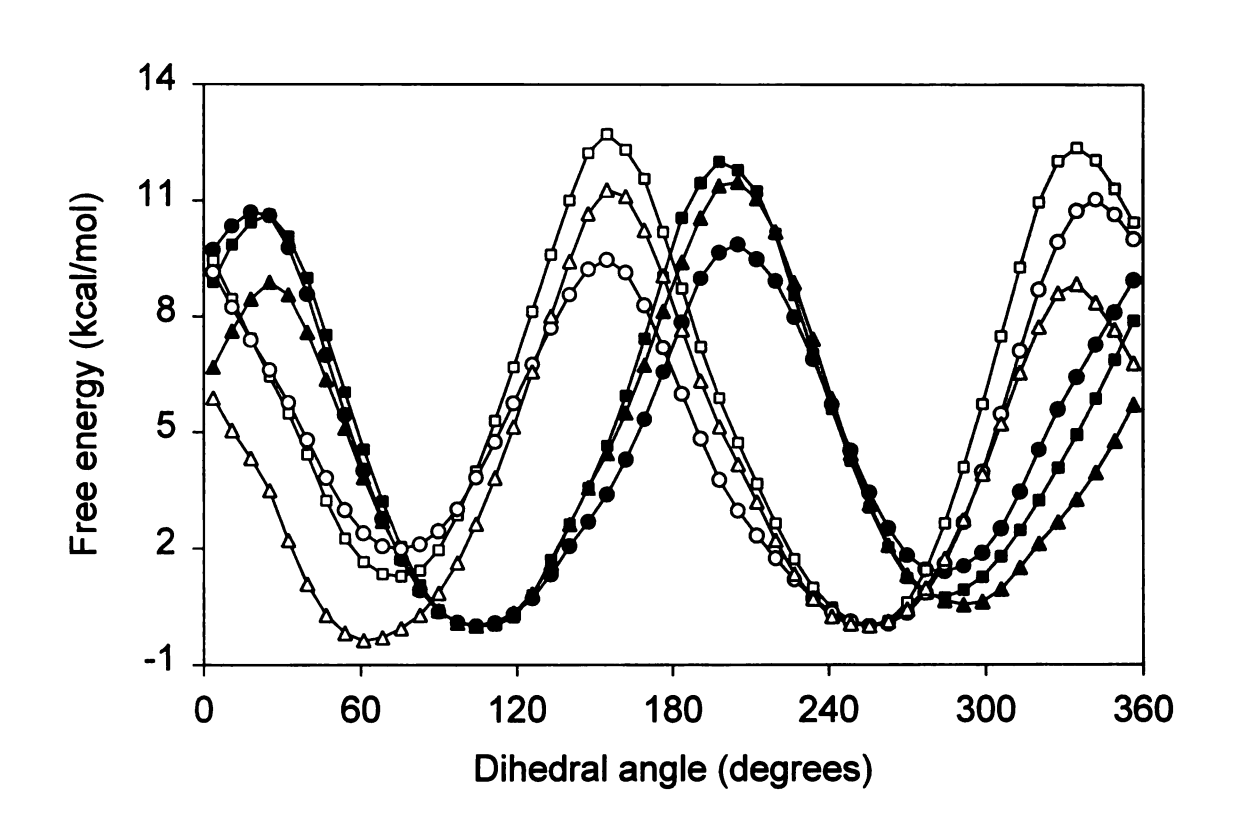


Figure 5.3. Potentials of mean force as a function of dihedral angle α (C4-C3-C1'-C2') from umbrella sampling of R- and S-warfarin in acetonitrile. R,depr (\blacksquare); R-2OH (\bullet); R-4OH (\triangle); S,depr (\square); S-2OH (\circ); S-4OH (\triangle).

Table 5.1. Relative free energies ($\Delta\Delta G$) in kcal/mol between states I and II (ΔG_{II} - ΔG_{I}) obtained from umbrella sampling.

Warfarin	∆∆G (kcal/mol)		
vvariann	Water	Acetonitrile	
R,depr	-1.9	-0.7	
R,2-OH	-1.3	-1.4	
R,4-OH	-0.5	-0.5	
S,depr	1.7	1.3	
S,2-OH	1.0	2.0	
S,4-OH	2.4	-0.4	

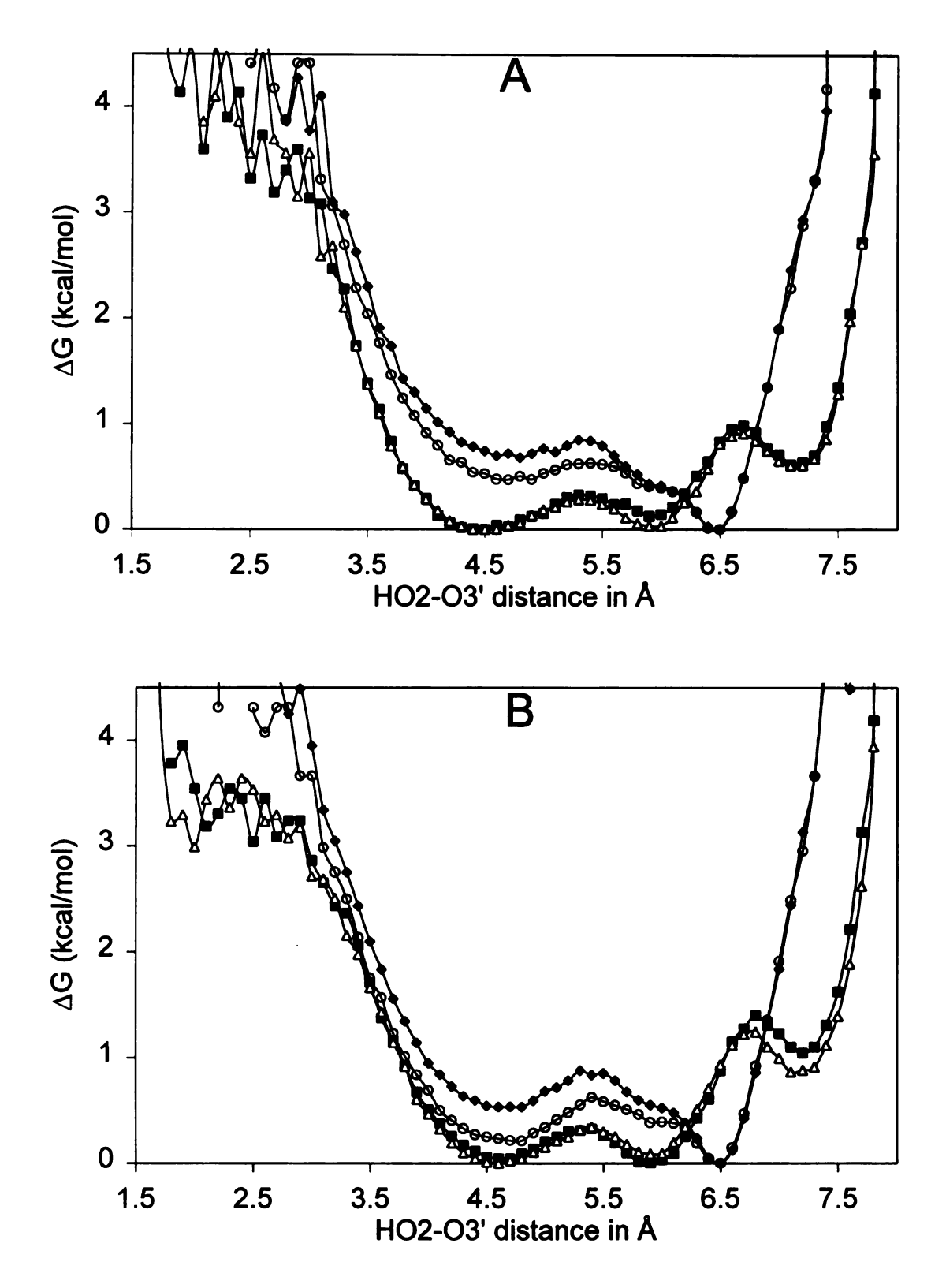


Figure 5.4. Potentials of mean force from probability distributions of HO2-O3 distance in S/R-warfarin-2-OH. (A) in water and (B) in acetonitrile. Sampling for S-warfarin in state I (\diamond) and state II (\bullet); for R-warfarin state I (\triangle) and state II (\circ).

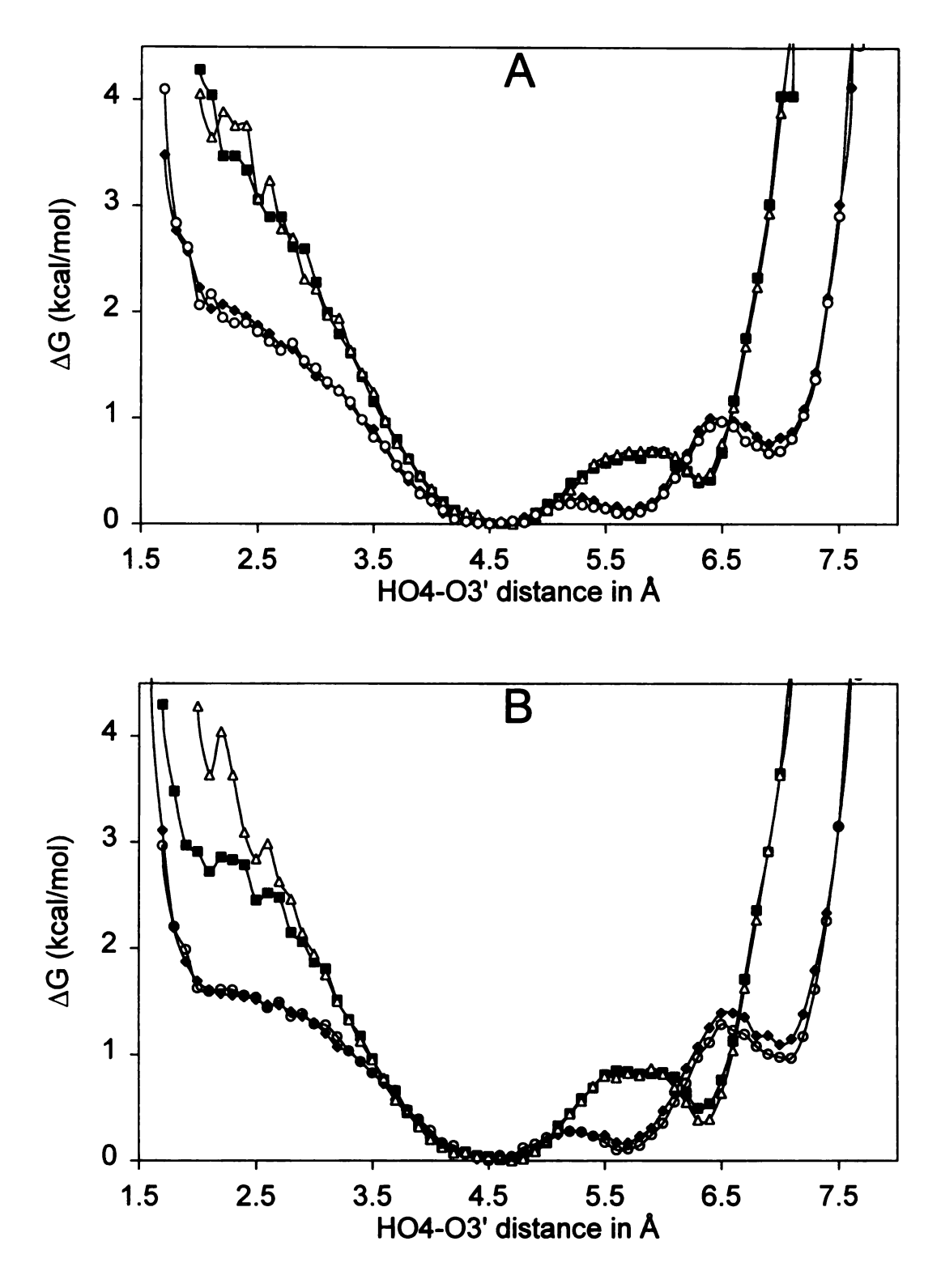


Figure 5.5. Potentials of mean force from probability distributions of HO4-O3 distance in S/R-warfarin-4-OH. (A) in water and (B) in acetonitrile. Sampling for S-warfarin in state I (\diamond) and state II (\bullet); for R-warfarin state I (\triangle) and state II (\circ).

For R/S-warfarin-4-OH, the potential of mean force for a bond distance of about 3 Å is about 1.5 kcal/mol in both solvents (Figure 5.5). Representative hydrogen bonded structures are shown in Figure 5.6. Hence, the probability distribution of hydrogen-bonded conformations is relatively higher in the polar-organic solvent acetonitrile (ϵ = 37) than in water (ϵ = 80). This observation is consistent with their dielectric screening ability. It is interesting to note that the probability distribution of hydrogen-bonded conformations (distances too large for hydrogen bonding) in the 2-OH protonation state is significantly lower in both state I and II. In contrast, a relatively modest probability distribution of hydrogen-bonded conformations is observed for the 4-OH protonation states of R-warfarin in state II and S-warfarin in state I.

As discussed above, R-warfarin predominantly exists in state II, while S-warfarin exists in state I. Experimentally, it is known that complexes of R- and S-warfarin with HSA exist in state I. ^{6,9} Moreover, HSA has a higher binding affinity for S-warfarin than R-warfarin. ^{14,30} These observations may be due to the preference for state I of S-warfarin over state II of R-warfarin. ²⁵

5.1.5. Conclusions

R- and S-warfarin enantiomeric forms in state I and II are found to have comparable free energies but are separated by an energy barrier on the order of 10 kcal/mol. This accounts for the absence of any transition between these states. The larger barrier between states I and II of R- and S-warfarin means that

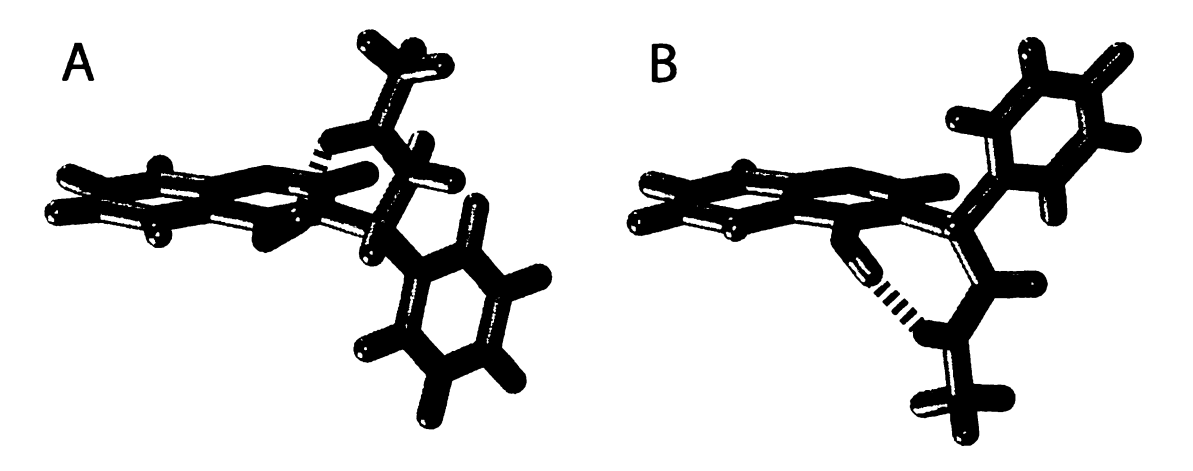


Figure 5.6. Representative structures with hydrogen-bonded conformations. (A) R-warfarin-4-OH in state II and (B) S-warfarin-4-OH in state I.

there will be a kinetic contribution to their interaction with other chiral molecules. In general, R-warfarin prefers state II over state I, while S-warfarin prefers state I over state II in both water and acetonitrile solvents.

5.2. DOCKING OF WARFARIN ENANTIOMERS WITH β-CYCLODEXTRIN

5.2.1. Introduction

β-Cyclodextrin forms a conical "bucket" with its secondary 2- and 3-OH groups lining the larger opening of the cavity and primary 6-OH groups at the smaller opening (Figure 1.1). It can form inclusion complexes with various classes of compounds based partly on the fit of the guest molecule into the cyclodextrin cavity.³¹ Thermodynamic and NMR studies showed that the interior of the cavity is relatively hydrophobic, which aqueous solution permits inclusion of hydrophobic portions of guest molecules leaving the polar part exposed to the bulk solvent.³²⁻³⁶

Computational methods have been widely used to study the structure and dynamics of cyclodextrin molecules.³⁷⁻⁴⁰ The simulation results indicate that the interactions in the cavity are predominantly hydrophobic (van der Waals forces) while the interactions outside the molecule are mostly hydrophilic (dipole-dipole and hydrogen bonds) in nature.

Molecular docking is a computational approach that predicts the relative binding affinity (scoring) and orientation of a ligand when it interacts with a receptor. A successful molecular docking should have a force field (energy function) that can reproduce the X-ray crystallographic structure of the ligand in

the ligand-receptor complex.⁴¹⁻⁴³ A docking function is generally considered successful if the root-mean-square deviation (RMSD) between the top ranking (lowest energy) docked structure and X-ray ligand's position is within 2.0 Å, based on the restrictions of crystal structure resolution.⁴⁴

There are many kinds of docking algorithms, including DOCK, 45-47 FlexX, 48 GOLD, 49 and CDOCKER. 42 Generally, the different docking methods vary essentially based on conformational space exploration and binding affinity estimation (i.e. scoring). In many of the docking methods, the receptor is kept rigid while the ligand is flexible. Docking methods can provide information about possible interaction sites and can estimate affinity of the ligand towards the receptor. The questions this study addresses are: Where do the warfarins tend to bind preferably, the interior or exterior to the cavity? Do they bind close to the primary or secondary hydroxyl groups? Which sites are most discriminatory for R- and S-warfarin?

5.2.1. Methods

The docking procedure is carried out using the CDOCKER protocol implemented in Accelrys Discovery Studio 2.1.^{42,50} A grid-based molecular dynamic (MD) docking algorithm, CDOCKER⁴² (with CHARMM param19 parameter set⁵¹) as the energy function for this docking method. The method uses a sphere-matching algorithm to fit warfarin atoms to a sphere in the cyclodextrin structure, which is assumed as the binding or interaction site. The size of this sphere is chosen as 8 Å. The method uses high temperature

molecular dynamics to generate a set of random warfarin conformations followed by translation into the binding sites. The orientation of each candidate pose is then determined using a series of random rotations that continues until the desired number of low-energy orientations is found. Each orientation is then exposed to CHARMM-based simulated annealing molecular dynamics (MD). Each of the structures from the MD run are then located and fully minimized. The minimized structures are then clustered and ranked according to their CHARMM energy (interaction energy plus ligand strain). The top scoring (lowest energy) poses are then retained. For each warfarin structure, 50 docking simulations or poses are chosen.

β-Cyclodextrin is obtained from molecular dynamics simulations as follows. The parameters are obtained from the CHARMM carbohydrate force field parameters developed for hexopyranose monosaccharides. ⁵² β-Cyclodextrin is then solvated in a cubic box filled with explicit water molecules. All simulations are carried out with CHARMM (version c36a1). ¹⁹ After a 5000 ps minimization step, an equilibration run is performed at 50, 100, 150, 200, 250, and 298 K. The simulations are performed with a 2 fs time step and at a constant temperature, pressure, and number of particles (NPT). The trajectory is then collected every 2 ps over the next 7 ns. After the data are analyzed, the structure with the lowest energy conformation is used as a representative for the docking procedure (Figure 5.7).

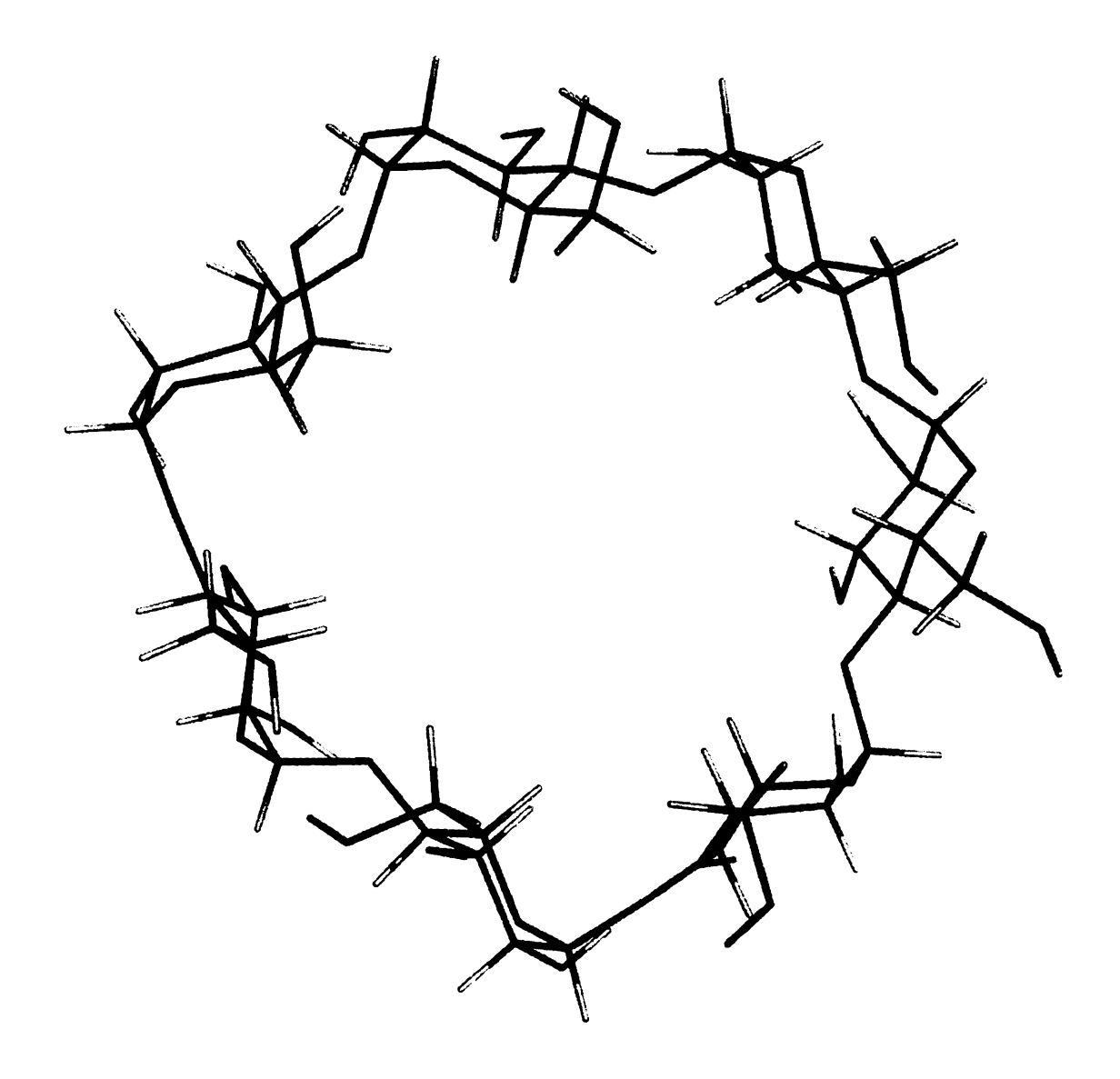


Figure 5.7. Representative lowest energy conformation $\beta\text{-}CD$ obtained from simulation.

5.2.3. Results and discussion

R- and S-warfarin in the 4-OH protonation state (see Figure 5.1) are used as representative models for the docking procedure. These forms are docked with β -cyclodextrin structures obtained from computer simulations. The goal of this docking study is to understand the possible binding modes of R- and S-warfarin and thereby explain why they differ in their binding affinity.

Table 5.2 compares the binding affinity for the energetically most favorable (lowest interaction energy) docked warfarin structures. As can be seen, there is a 1.3 kcal/mol difference in interaction energy between R-warfarin-4-OH in state I and II. Similarly, there is a 0.4 kcal/mol difference between state I and II of S-warfarin-4-OH. In general, R-warfarin-4-OH in state II has the most negative interaction energy, while in state I, the least. R-warfarin-4-OH (state II) has more negative interaction energy compared to S-warfarin-4-OH (state I and II) by about 0.4-0.8 kcal/mol The estimated interaction energies are due to conformational changes or strain of warfarin structures together with van der Waals forces, dipole-dipole interactions, and hydrogen bonds. The interaction energy difference between R- and S-warfarin is less than 1 kcal/mol, which is within the error ranges of the calculations. In chromatography, a 0.11 kcal/mol differential free energy change ($\Delta\Delta G$) between enantiomers is sufficient to give a selectivity (α) of 1.2.⁵³ In this regard, the estimated interaction energy difference between R- and S-warfarin is more than sufficient for chiral selectivity.

Table 5.2. Binding affinity for the energetically most favorable docking pose at 8 $\,$ Å radius from the center of $\,$ β-cyclodextrin cavity.

Structure	CDOCKER energy (kcal/mol)
R, 40H (I)	-15.6
S, 40H (I)	-16.1
R, 4-OH (II)	-16.9
S, 4-OH (II)	-16.5

From the docked structures, two distinct classes are obtained. The first class constitutes a hydroxycoumarin group oriented towards the secondary OH groups or larger opening ("Up", Figure 5.8A), while the second class exhibited an orientation closer to the primary OH groups or smaller opening ("Down", Figure 5.8B). Table 5.3 summarizes the hydroxycoumarin group orientation of docked warfarin structures. As can be seen, 8 % R-warfarin-4-OH (state I) and 16 % of R-warfarin-4-OH (state II) are arranged in the "Up" orientation. Despite the lower number of structures of R-warfarin-4-OH in the "Up" orientation, the average interaction energy in the "Up" and "Down" orientations is statistically similar. This might be due the large negative interaction energy contribution of the structures in the "Up" orientations. In contrast, both state I and II of S-warfarin-4-OH are exclusively docked in the "Up" orientation. This suggests that the most favorable orientation for S-warfarin might involve stronger dipole-dipole or hydrogen bond interaction with the secondary hydroxyl groups on the β-CD with minimum strain in the cavity.

To explain the difference in the binding affinity of R- and S-warfarin forms, the possibility of intermolecular hydrogen bonding with β -CD is investigated. Table 5.4 summarizes the intermolecular hydrogen bond distances observed in the docked warfarin structures. A hydrogen bond is usually formed when the hydrogen-oxygen distance is less than 3 Å. As can be seen, R-warfarin-4-OH (state I and II) shows a single intermolecular hydrogen bond with its carbonyl group of the acetonyl side chain. In contrast, S-warfarin has three and two

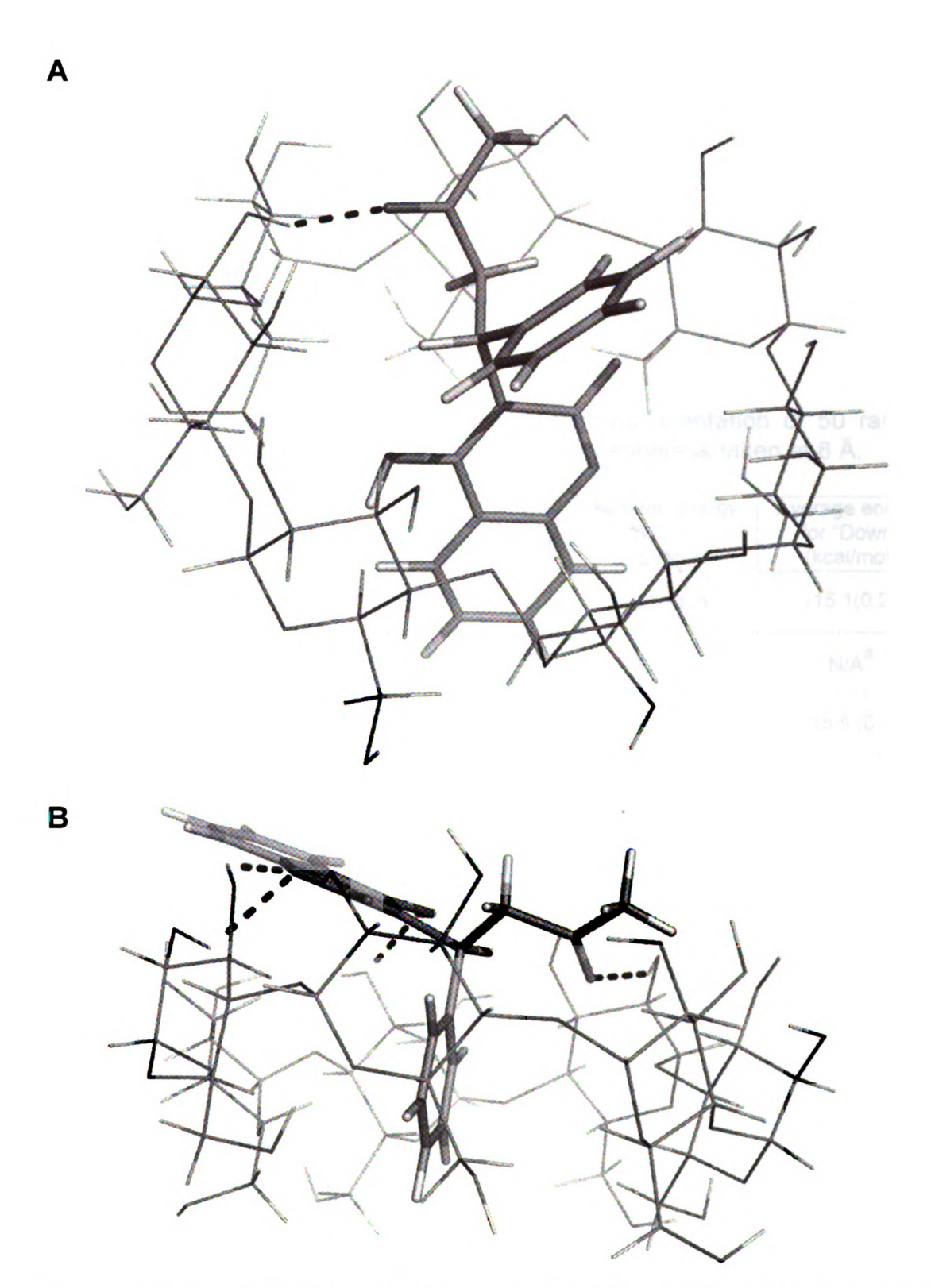


Figure 5.8. Lowest interaction energy docked A) R-warfarin-4-OH (state I) in the "Up" orientation, B) S-warfarin-4-OH (state I) in the "Down" orientation. Radius of sphere from the center of the cavity is 8 Å.

Table 5.3. Comparison of hydroxycoumarin group orientation of 50 randomly generated warfarin structures in β -CD. Radius of sphere is taken at 8 Å.

Warfarin	Hydroxy- coumarin "Up"	Hydroxy- coumarin "Down"	Average energy for "Up" (kcal/mol)	Average energy for "Down" (kcal/mol)
R, 40H (I)	4	46	-15.2 (0.2) ^b	-15.1(0.2)
S, 40H (I)	50	0	-15.5 (0.2)	N/A ^a
R, 40H (II)	8	42	-16.1 (0.6)	-15.5 (0.1)
S, 40H (II)	50	0	-16.0 (0.2)	N/A

^aN/A, not applicable

bValues in bracket are standard deviations

Table 5.4. Intermolecular hydrogen bond distance (Å) between docked warfarin functional groups and the secondary hydroxyl groups of β -CD. Radius of sphere used is 8 Å.

Warfarin	Bond distance (Å)			
VValialiii	C=OH	O-HO	OHO ^a	
R,40H (I)	1.94	N/H ^b	N/H	
S,4OH (I)	1.99	2.12	2.22	
R,4OH (II)	2.11	N/H	N/H	
S,4OH (II)	1.95	N/H	2.08	

aHydrogen bond distance between ester oxygen on warfarin and hydrogen on β-CD

^bN/H, Hydrogen bond greater than cutoff value

intermolecular hydrogen bonds for state I and II, respectively. Despite the greater number of hydrogen bonds for S-warfarin compared to that for R-warfarin, the interaction energies are comparable in magnitude (Table 5.3). This suggests that van der Waals and dipole-dipole interactions together with conformational strains may have significant contribution compared to hydrogen bonds. It is interesting to note that both R- and S-warfarin structures undergo intermolecular hydrogen bonds to only the secondary hydroxyl functional groups of the β -CD molecule. This may have an implication for their difference in chiral discrimination, as the secondary OH groups, which are located in a chiral carbon, may be the chirally selective sites on the β -CD molecule.

5.2.4 Conclusions

From the results of these simulations, both R- and S-warfarin tend to undergo inclusion in the β -cyclodextrin cavity through either the phenyl or hydroxycoumarin group or both. R-warfarin-4-OH (state II) has more negative interaction energy compared to S-warfarin-4-OH (state I and II) by about 0.4-0.8 kcal/mol. The most favorable docked structures of both R- and S-warfarin have a preference for the hydroxycoumarin group to be arranged closer to the larger opening of the CD cavity ("Up"). Both R- and S-warfarin show evidence for intermolecular hydrogen bonds with only the secondary OH functional groups on the β -CD molecule. This docking procedure gives some insight into understanding possible modes of interactions, but it does not include any solvent effect. As a result, it does not provide a complete picture of molecular

interactions. Hence, it is hard to conclude the exact origin of chiral selectivity from this simple method. Extensive computer simulations in the presence of solvent may give a better understanding of chiral discrimination at the molecular level.

5.3. REFERENCES

- (1) Li, T.; Chang, C. Y.; Jin, D. Y.; Lin, P. J.; Khvorova, A.; Stafford, D. W. *Nature* **2004**, *427*, 541-544.
- (2) Bell, R. G.; Stark, P. *Biochem. Biophys. Res. Commun.* **1976**, 72, 619-625.
- (3) Dolmella, A.; Gatto, S.; Girardi, E.; Bandoli, G. *J. Mol. Struct.* **1999**, *513*, 177-199.
- (4) Fernlund, P.; Stenflo, J.; Roepstorff, P.; Thomsen, J. *J. Biol. Chem.* **1975**, 250, 6125-6133.
- (5) Ha, C. E.; Petersen, C. E.; Park, D. S.; Harohalli, K.; Bhagavan, N. V. *J. Biomed. Sci.* **2000**, *7*, 114-121.
- (6) Il'ichev, Y. V.; Perry, J. L.; Simon, J. D. *J. Phys. Chem. B* **2002**, *106*, 460-465.
- (7) He, X. M.; Carter, D. C. *Nature* **1992**, 358, 209-215.
- (8) Kasai-Morita, S. H., T.; Awazu, S. *Biochim. Biophys. Acta* **1987**, *915*, 277-283.
- (9) Petitpas, I.; Bhattacharya, A. A.; Twine, S.; East, M.; Curry, S. *J. Biol. Chem.* **2001**, *276*, 22804-22809.
- (10) He, M. X.; Korzekwa, K. R.; Jones, J. P.; Rettie, A. E.; Trager, W. F. *Arch. Biochem. Biophys.* **1999**, *372*, 16-28.
- (11) Heimark, L. D.; Trager, W. F. J. Med. Chem. 1984, 27, 1092-1095.
- (12) Pisklak, M.; Maciejewska, D.; Herold, F.; Wawer, I. *J. Mol. Struct.* **2003**, *649*, 169-176.
- (13) Lewis, R. J.; Trager, W. F.; Chan, K. K.; Breckenr.A; Orme, M.; Roland, M.; Schary, W. J. Clin. Invest. 1974, 53, 1607-1617.
- (14) Loun, B.; Hage, D. S. Anal. Chem. 1994, 66, 3814-3822.
- (15) Loun, B.; Hage, D. S. Anal. Chem. 1996, 68, 1218-1225.
- (16) Guillaume, M.; Jaulmes, A.; Sebille, B.; Thuaud, N.; Vidal-Madjar, C. *J. Chromatogr. B* **2001**, 753, 131-138.
- (17) Ring, P. R.; Bostick, J. M. J. Pharm. Biomed. Anal. 2000, 22, 573-581.

- (18) Sheth, A. R.; Young, V. R.; Grant, D. J. W. *Acta Crystallogr.* **2002**, *E58*, m197-m199.
- (19) Brooks, B. R.; Brooks, C. L.; Mackerell, A. D.; Nilsson, L.; Petrella, R. J.; Roux, B.; Won, Y.; Archontis, G.; Bartels, C.; Boresch, S.; Caflisch, A.; Caves, L.; Cui, Q.; Dinner, A. R.; Feig, M.; Fischer, S.; Gao, J.; Hodoscek, M.; Im, W.; Kuczera, K.; Lazaridis, T.; Ma, J.; Ovchinnikov, V.; Paci, E.; Pastor, R. W.; Post, C. B.; Pu, J. Z.; Schaefer, M.; Tidor, B.; Venable, R. M.; Woodcock, H. L.; Wu, X.; Yang, W.; York, D. M.; Karplus, M. J. Comput. Chem. 2009, 30, 1545-1614.
- (20) Feig, M.; Karanicolas, J.; Brooks, C. L. *J. Mol. Graph. & Model.* **2004**, *22*, 377-395.
- (21) Phillips, J. C.; Braun, R.; Wang, W.; Gumbart, J.; Tajkhorshid, E.; Villa, E.; Chipot, C.; Skeel, R. D.; Kale, L.; Schulten, K. *J. Comput. Chem.* **2005**, 26. 1781-1802.
- (22) MacKerell, A. D.; Bashford, D.; Bellott, M.; Dunbrack, R. L.; Evanseck, J. D.; Field, M. J.; Fischer, S.; Gao, J.; Guo, H.; Ha, S.; Joseph-McCarthy, D.; Kuchnir, L.; Kuczera, K.; Lau, F. T. K.; Mattos, C.; Michnick, S.; Ngo, T.; Nguyen, D. T.; Prodhom, B.; Reiher, W. E.; Roux, B.; Schlenkrich, M.; Smith, J. C.; Stote, R.; Straub, J.; Watanabe, M.; Wiorkiewicz-Kuczera, J.; Yin, D.; Karplus, M. J. Phys. Chem. B 1998, 102, 3586-3616.
- (23) Nikitin, A. M.; Lyubartsev, A. P. J. Comput. Chem. 2007, 28, 2020-2026.
- (24) Jorgensen, W. L.; Chandrasekhar, J.; Madura, J. D.; Impey, R. W.; Klein, M. L. J. Chem. Phys. 1983, 79, 926-935.
- (25) Feig, M.; Gebreyohannes, K. G.; McGuffin, V. L. *J. Mol. Struct. Theochem* **2010**, *949*, 41-51.
- (26) Roux, B. Comput. Phys. Commun. 1995, 91, 275-282.
- (27) Ferrenberg, A. M.; Swendsen, R. H. *Phys. Rev. Lett.* **1989**, *63*, 1195-1198.
- (28) Grossfield, A. WHAM 2.0.1. University of Rochester, 2008.
- (29) Ye, Y. K.; Bai, S.; Vyas, S.; Wirth, M. J. *J. Phys. Chem. B* **2007**, *111*, 1189-1198.
- (30) Zou, H.; Wang, H.; Zhang, Y. J. Liq. Chromatogr. & Relat. Technol. 1998, 21, 2663-2674.
- (31) Saenger, W. Angew. Chem. Int. Ed. 1980, 19, 344-362.

- (32) Rekharsky, M. V.; Inoue, Y. Chem. Rev. 1998, 98, 1875-1917.
- (33) Matsui, Y.; Mochida, K. Bull. Chem. Soc. Jpn. 1979, 52, 2808-2814.
- (34) Inoue, Y.; Hakushi, T.; Liu, Y.; Tong, L. H.; Shen, B. J.; Jin, D. S. *J. Am. Chem. Soc.* **1993**, *115*, 475-481.
- (35) Rekharsky, M. V.; Schwarz, F. P.; Tewari, Y. B.; Goldberg, R. N.; Tanaka, M.; Yamashoji, Y. *J. Phys. Chem.* **1994**, *98*, 4098-4103.
- (36) Connors, K. A. Chem. Rev. 1997, 97, 1325-1357.
- (37) Lipkowitz, K. B. Chem. Rev. 1998, 98, 1829-1873.
- (38) Heine, T.; Santos, H. F.; Patchkovskii, S.; Duarte, H. A. *J. Phys. Chem. A* **2007**, *111*, 5648-5654.
- (39) Linert, W.; Margl, P.; Renz, F. Chem. Phys. 1992, 161, 327-338.
- (40) Reinhardt, R.; Richter, M.; Mager, P. P. Carbohydr. Res. 1996, 291, 1-9.
- (41) Vieth, M.; Hirst, J. D.; Kolinski, A.; Brooks, C. L. *J. Comput. Chem.* **1998**, *19*, 1612-1622.
- (42) Wu, G. S.; Robertson, D. H.; Brooks, C. L.; Vieth, M. *J. Comput. Chem.* **2003**, *24*, 1549-1562.
- (43) Erickson, J. A.; Jalaie, M.; Robertson, D. H.; Lewis, R. A.; Vieth, M. J. *Med. Chem.* **2004**, *47*, 45-55.
- (44) Gohlke, H.; Hendlich, M.; Klebe, G. J. Mol. Biol. 2000, 295, 337-356.
- (45) Meng, E. C.; Shoichet, B. K.; Kuntz, I. D. *J. Comput. Chem.* **1992**, *13*, 505-524.
- (46) Makino, S.; Kuntz, I. D. *J. Comput. Chem.* **1997**, *18*, 1812-1825.
- (47) Ewing, T. J. A.; Kuntz, I. D. *J. Comput. Chem.* **1997**, *18*, 1175-1189.
- (48) Rarey, M.; Kramer, B.; Lengauer, T.; Klebe, G. *J. Mol. Biol.* **1996**, *261*, 470-489.
- (49) Jones, G.; Willett, P.; Glen, R. C.; Leach, A. R.; Taylor, R. *J. Mol. Biol.* **1997**, *267*, 727-748.
- (50) Inc., A. S. Accelrys Discovery Studio 2.1, San Diego 2008.
- (51) Brooks, B. R.; Bruccoleri, R. E.; Olafson, B. D.; States, D. J.; Swaminathan, S.; Karplus, M. *J. Comput. Chem.* **1983**, *4*, 187-217.

- (52) Guvench, O.; Greene, S. N.; Kamath, G.; Brady, J. W.; Venable, R. M.; Pastor, R. W.; Mackerell, A. D. *J. Comput. Chem.* **2008**, *29*, 2543-2564.
- (53) Okamoto, Y.; Yashima, E. *Angew. Chem. Int. Ed.* **1998**, **37**, 1020-1043.

CHAPTER 6

CONCLUSIONS AND FUTURE DIRECTIONS

6.1. INTRODUCTION

In the last twenty five years, the pharmaceutical industry has shown great interest in the separation and development of racemic drugs. To this end, chiral stationary phases play a pivotal role. Still, their chiral recognition mechanism is not clearly understood. Although there are more than 100 commercially available chiral stationary phases, none of them have universal application. As a result, selection of the appropriate stationary phase for specific compounds or predicting the magnitude of chiral selectivity is a challenging task. One way to obtain insight into chiral discrimination mechanisms is to investigate the thermodynamics and kinetics of the separation.

This dissertation investigated the effect of mobile phase on derivatized β -cyclodextrin (CD) phases and derivatized amylose and cellulose phases. Detailed thermodynamic and kinetic investigation of derivatized amylose phase are also demonstrated. In addition, computer simulations on sampling of warfarin structures and their docking studies with β -CD are examined.

6.2. EXPERIMENTAL STUDIES ON DERIVATIZED β -CD, AMYLOSE AND CELLULOSE STATIONARY PHASES

Chapter 2 compares the separation of coumarin-based anticoagulants on 2,6-dinitro-4-trifluoromethyl phenyl ether (DNP) and tris-(3,5-dimethylphenyl carbamates) (DMPC) derivatized β-CD using polar-organic and reversed-phase

eluents. Comparisons are based on retention factors and chiral selectivities in the different mobile phases. The DNP-CD stationary phase has modest chiral recognition for warfarin and coumafuryl in the polar-organic mode, but not for coumachlor. In contrast, the DMPC-CD stationary phase has little retention and no chiral recognition for any of the coumarins using the polar-organic and reversed-phase modes. Derivatization of β -CD can potentially block the chiral selective sites and/or the cavity of the CD from having inclusion interactions.

Chapter 3 summarizes comparison of derivatized amylose and cellulose stationary phases using polar-organic eluents. Successful chiral separation of the coumarins is demonstrated in the amylose phase. However, the cellulose phase has excellent chiral selectivity only for coumatetrally and adequate chiral selectivity for coumachlor. In general, the coumarins are more retained in the helical amylose than in the linear cellulose phase, with the exception of 4-hydroxycoumarin.

The selection of an appropriate mobile phase is a key factor for any separation. The type of mobile phase affects the retention time, chiral selectivity and, in some cases, the elution order of the enantiomers. Mobile phase modifiers with proton donor/acceptor groups such as methanol, acetone, and tetrahydrofuran are used to compare retention, chiral selectivity, and kinetic rate constants. Methanol and acetone decrease the retention and selectivity of the coumarins on DMPC-amylose and DMPC-cellulose phases. Tetrahydrofuran (THF) decreases the retention of all coumarins, but increases the selectivity of coumafuryl and coumatetralyl on the DMPC-amylose phase. On the DMPC-

cellulose phase, retention of the coumarins decreases but selectivity remains unaffected with an increase in concentration of THF.

The kinetics of the separation is also compared using coumatetralyl as a probe and THF as a modifier. For the first-eluted enantiomer, the sorption and desorption rate constants increase with an increase in THF concentration in both stationary phases. For the second-eluted enantiomer, the sorption and desorption rates decrease on DMPC-amylose and increase on DMPC-cellulose. When 10 % THF is used on DMPC-amylose, the first-eluted enantiomer undergoes very fast kinetics. In contrast, the second-eluted enantiomer has very sluggish kinetics. The above results suggest that DMPC-amylose and DMPC-cellulose have different chiral discrimination mechanisms for the coumarin-based anticoagulants.

Chapter 4 summarizes the more detailed thermodynamic and kinetic aspects of the retention mechanism on the DMPC-amylose phase as a function of mobile phase modifiers and temperature. In general, retention and selectivity of warfarin and coumatetralyl decrease as concentration and hydrogen bond donating ability of the alcohol modifier increases. As the concentration of THF increases, retention and chiral selectivity remain constant or increases for warfarin. On the other hand, retention decreases, while chiral selectivity increases for coumatetralyl enantiomers. The changes in molar enthalpy and entropy induced by each mobile phase modifier are examined. Values of enthalpy in the presence of methanol and *i*-butanol are smaller than those in *t*-butanol and THF. The kinetic data demonstrate that the rate of sorption is

always greater than the rate of desorption for all mobile phase compositions. An increase in the concentration of alcohol modifiers causes an increase in the rate constant of desorption, suggesting that the alcohols serve as displacing agents. In contrast, the rate constant of desorption decreases as the concentration of THF increases. Consequently, the rate of desorption of the second eluted enantiomer of coumatetrally decreases by about 85 % as the concentration of THF increases from 5 to 10 %.

The effect of temperature on the thermodynamics and kinetics of the separation is also demonstrated. As temperature increases, retention and selectivity of all coumarins decrease. Both linear and nonlinear van't Hoff plots are observed. The nonlinear plots are attributed to conformational changes in the stationary phase and are observed between 20 and 25 °C. Such conformational changes have implications for the day-to-day or column-to-column reproducibility of chiral separations and may influence chiral method development and validation. In bulk acetonitrile, coumatetrally enantiomers have the most favored enthalpies and least favored entropies compared to other coumarins. Enthalpy-entropy compensation plots are constructed to compare retention mechanisms. The plots obtained for coumarins in bulk acetonitrile mobile phase suggest that the separation mechanism may be similar. On the other hand, no compensation is observed for warfarin and coumatetrallyl enantiomers separated in the presence of modifiers.

The thermodynamic and kinetic data provide some insight into the mechanism of chiral separations in derivatized β -CD, DMPC-amylose, and

DMPC-cellulose. Overall, the observed thermodynamic and kinetic behaviors of these chiral selectors stem mainly from the difference in their secondary structures.

In future work, DMPC-cellulose can be compared with a recently commercialized derivatized cellulose phase (Chiralpak IC) using bulk acetonitrile mobile phase and the same coumarin probes. As compared to DMPC-cellulose, this stationary phase has a π -acidic derivatizing agent, tris-(3,5-dichlorophenyl carbamate). First, the effect of mobile phase modifiers with proton donor/acceptor properties such as methanol, acetone, and tetrahydrofuran can be investigated. To draw some conclusions, these results may be compared to those obtained with DMPC-cellulose stationary phase under similar chromatographic conditions. Next, detailed thermodynamics and kinetics of this stationary phase can be investigated using two of the coumarins with good chiral selectivities. In this study, the effect of temperature and mobile phase modifiers can be examined. The study may provide some insight into understanding the differences in the chiral recognition of the coumarins in this stationary phase versus the DMPC-cellulose.

6.3. COMPUTATIONAL STUDIES ON WARFARIN SAMPLING AND DOCKING

To explore sampling of warfarin enantiomers in different solvent environments and their interaction with β -cyclodextrin, computational studies are used. Chapter 5 details umbrella sampling of warfarin conformers in water and acetonitrile solvents, and docking of warfarin structures in β -cyclodextrin. An

energy barrier between each structure, with phenyl group above and below the plane of the coumarin ring, of R- and S-warfarin is demonstrated. This barrier, which is on the order of 10 kcal/mol, is responsible for the absence of any transition between these structures. This observation might have kinetic implications when the enantiomers interact with other chiral molecules. In general, R-warfarin prefers phenyl group below over above the plane of the coumarin ring in both water and acetonitrile solvents. On the other hand, S-warfarin prefers phenyl group above over below the plane of the coumarin ring.

Binding affinity differences between R- and S-warfarin-4-OH structures with phenyl group above and below the plane of the coumarin ring are also investigated using docking studies with β -cyclodextrin. R-warfarin-4-OH (state II) interacts more strongly than S-warfarin-4-OH by about 0.4-0.8 kcal/mol. R- and S-warfarin docked structures show evidence of intermolecular hydrogen bonds, with the secondary OH functional groups on β -CD. This may have an implication for their difference in chiral discrimination, as the secondary OH groups may be the chirally selective sites. Although the docking procedure gives some insight into understanding possible modes of interactions, it does not give a complete picture of molecular interactions. Hence, it is difficult to explicitly conclude the exact origin of chiral selectivity between R- and S-warfarin from this simple procedure alone.

In future work, computer simulations such as molecular dynamics in explicit solvent environment may be used to explore the interaction of enantiomers with a chiral selector. In this regard, the interaction of warfarin with

 β -CD can be simulated in the presence of water or acetonitrile solvents. The most stable R/S-warfarin structures obtained from sampling in each solvent can be used to start the simulations. From the simulation results, intermolecular distances and interaction energies of each enantiomer can be estimated. Differences in the interaction energy between the two enantiomers are related to chiral selectivity and can be compared to experimental data. The simulation results may be used to explain the origin of chiral selectivity in β -cyclodextrin.

6.4. REFERENCES

- (1) Wang, T.; Wenslow, R. M. *J. Chromatogr. A* **2003**, *1015*, 99-110.
- (2) Lynam, K. G.; Stringham, R. W. Chirality 2006, 18, 1-9.

